UNIVERSITY OF CALIFORNIA, SAN DIEGO

Vacuole biogenesis, function, and size control in *S. cerevisiae*: central roles for membrane trafficking and lipid signaling

A Dissertation submitted in partial satisfaction of the requirements for the degree Doctor of Philosophy

in

Biology

by

Jem A. Efe

Committee in charge:

Professor Randolph Y. Hampton, Chair
Professor Scott D. Emr, Co-chair
Professor Jack E. Dixon
Professor Richard A. Firtel
Professor Michael P. Yaffe

2007

The Dissertation of Jem A. Efe is approved, and it is acceptable in quality and form for publication on microfilm:

_____

_____

_____

_____
Co-chair

_____
Chair

University of California, San Diego

2007

DEDICATION

This work is dedicated to my paternal grandfather İbrahim Efe, who has indirectly – though quite unmistakably – helped shape my love of scientific inquiry and free thought. I only wish I could have gotten to know him before his untimely death.

TABLE OF CONTENTS

LIST OF FIGURES

Page

LIST OF TABLES

Page

ACKNOWLEDGEMENTS

Several people, both in the world of science and in the “real world”, have contributed immeasurably to the completion of this work. While I realize that I am probably still too young to make liberal use of superlatives, I must say that attaining a Ph.D. has been the most challenging project I have ever undertaken. And now that the end is in sight, I finally have the opportunity to thank the individuals who kept me going during this journey of scientific and personal discovery.

To my wife Hande: thank you so much for believing in me – even as my own faith wavered. Thank you for your patience and understanding, as well as your hard work to keep our dreams alive. You truly deserve as much credit as I, not least because you sacrificed so much and gave of yourself so often. I could not have made it without you. My hope is to some day return the favor in one way or another, and I look forward to a lifetime of opportunities to do so.

Next, I would like to thank my advisor Scott Emr. By allowing me to freely pursue my scientific interests while always keeping an eye on my overall progress, he ensured that my graduate years were both intellectually rewarding and productive. Throughout the process, it was a great comfort to know that Scott was always looking out for me, in every sense.

My Ph.D. work provided me the opportunity to work with a number of exceptional scientists. My committee members Randy Hampton, Jack Dixon, Rick Firtel, and Mike Yaffe encouraged and motivated me to become a better researcher. During my initial years, fellow Emr laboratory members Anjon Audhya, Bill Parrish, Simon Rudge, and Chris Stefan were invaluable sources of knowledge, ideas, and constructive criticism. I would also like to thank my co-authors Rob Botelho, Olivier Deloche, Nadim Shohdy, and Howard Shuman for great collaborations. These people have all contributed much to the quality of my research.

Last but not least, I thank my family: my late grandparents Roberta (my favorite teacher) and James Carpenter for making sure that I got a solid, well-rounded education both abroad and in the United States; my parents Jean and Turan for their unflinching approval and support of my academic endeavors; my dear O'tante for being a dependable source of love, laughter, and optimism; "Ronald Kuzen" for making the transition much easier (both personally and academically) when my wife and I moved out west, and for instilling in me a love of Southern California; and my little brother Jon just for being himself: he may not yet realize it, but being looked up to – regardless of whether I am actually worthy – is an empowering and constant form of moral support.

Chapters 1 and 5 include, in part, material as it appears in *Current Opinion in Cell Biology* 17(4):402-8, 2005. Efe, J.A., Botelho, R.J., and S.D. Emr. The Fab1 phosphatidylinositol kinase pathway in the regulation of vacuole morphology. The dissertation author was the primary investigator and author of this paper.

Chapter 2, in full, is a reprint of the material as it appears in *Journal of Cell Science* 118(20):4751-64, 2005. Efe, J.A., Plattner, F., Hulo, N., Kressler, D., Emr, S.D., and O. Deloche. Yeast Mon2p is a highly conserved protein that functions in the cytoplasm-to-vacuole transport pathway and is required for Golgi homeostasis. The dissertation author was the primary investigator and author of this paper.

Chapter 3, in full, is a reprint of the material as it appears in Shohdy, N., Efe, J.A., Emr, S.D., and H.A. Shuman. *Proceedings of the National Academy of Sciences* 102(13):4866-71. Pathogen effector protein screening in yeast identifies Legionella factors that interfere with membrane trafficking. The dissertation author was a co-investigator and co-author of this paper.

Chapter 4, in full, has been submitted for publication of the material as it appears in Molecular Biology of the Cell, 2007. Atg18 regulates organelle morphology and Fab1 kinase activity independent of its membrane recruitment by phosphatidylinositol 3,5-bisphosphate. The dissertation author was the primary investigator and author of this paper.

VITA & PUBLICATIONS

Education/Research Experience

2001-2007 University of California, San Diego
Doctor of Philosophy in Biology
Advisor: Dr. Scott D. Emr
GPA: 3.83

1997-2001 Grinnell College, Grinnell, IA
Bachelor of Arts in Biology, with Honors
GPA: 3.90

Publications

Efe, J.A., Botelho, R.J., and S.D. Emr (2007) Atg18 regulates organelle morphology and Fab1 kinase activity independent of its membrane recruitment by phosphatidylinositol 3,5-bisphosphate*. Mol. Biol. Cell.* In press*.*

Efe, J.A., Botelho, R.J., S.D. Emr. (2005) The Fab1 phosphatidylinositol kinase pathway in the regulation of vacuole morphology. *Curr Opin Cell Biol*. 17(4):402-8

Shohdy, N., Efe, J.A., Emr, S.D., and H.A. Shuman. (2005) Pathogen effector protein screening in yeast identifies Legionella factors that interfere with membrane trafficking. *PNAS* 102(13):4866-71.

Efe, J.A., Plattner, F., Hulo, N., Kressler, D., Emr, S.D., and O. Deloche (2005) Yeast Mon2p is a highly conserved protein that functions in the cytoplasm-to-vacuole transport pathway and is required for Golgi homeostasis. *J Cell Sci* 118(20):4751-64.

Field of Study

Major Field: Biological Sciences

Studies in Cell Biology and Genetics
Professor Scott D. Emr

ABSTRACT OF THE DISSERTATION

Vacuole biogenesis, function, and size control in *S. cerevisiae*: central roles for membrane trafficking and lipid signaling

by

Jem A. Efe

Doctor of Philosophy in Biology

University of California, San Diego, 2007

Professor Randolph Y. Hampton, Chair

Professor Scott D. Emr, Co-chair

The *Saccharomyces cerevisiae* vacuole serves as the main storage compartment for essential amino acids, nutrients and ions, functions in the regulated turnover of macromolecules, and is required for sporulation and

osmotic homeostasis. Rapid changes in size, shape, and number are critical to ensure an immediate response to dramatic fluctuations in nutrient concentrations and extracellular osmolarity. However, even under relatively static external conditions, the vacuole is in a constant state of regulated flux. The multiple membrane transport pathways that converge on the vacuole are kept in balance to maintain the the proper function and morphology of the vacuole.

We have characterized the Golgi protein Mon2 in an effort to elucidate the connections between homeostasis of this organelle and various functions of the vacuole. The highly fragmented vacuoles of the *mon2Δ* mutant underscore the requirement for a stable Golgi appartus in vacuole biogenesis. Furthermore, our finding that Mon2p is required for cytoplasm-to-vacuole transport indicates that the Golgi, aside from being a critical way station along membrane and protein transport pathways culminating at the vacuole, is likely also a membrane source for autophagic process(es).

Further downstream in anterograde membrane traffic, endosomal maturation defects result in various functional and structural anomalies of the vacuole. We show here that bacterial proteins from *Legionella pneumophila*, when overexpressed, can inhibit multivesicular body formation, leading to missorting of the hydrolase Carboxypeptidase Y and to the formation of an aberrant membrane compartment adjacent to the vacuole. A genetic screen

was used to identify such proteins, all of which were subsequently found to be released into the host cytosol upon *Legionella* infection.

At the vacuolar compartment itself, the phosphoinositide PtdIns(3,5)P_2 plays a key role in regulating morphology. Our findings indicate that the first bona fide PtdIns(3,5)P_2 effector, Atg18, is both necessary and sufficient for the fragmentation of the vacuole observed when levels of this phosphoinositide increase. Moreover, Atg18 is a potent inhibitor of the Fab1 kinase, potentially modulating interaction with primary upstream activator, Vac7. Finally, Atg18 also interacts with Vac17p, indicating a possible function in retrograde membrane transport and/or vacuole inheritance.

CHAPTER 1

INTRODUCTION

A central feature in the evolution of eukaryotic cells is a high degree of compartmentalization, enabling them to very precisely regulate myriad intracellular processes both spatially and temporally. Every cell harbors several distinct membrane-bound organelles, the identities of which are established and maintained by their constituent proteins and lipids. Given the constant and highly dynamic nature of membrane exchange between all cellular compartments, proper targeting and retention of proteins as well as strict regulation of the synthesis and turnover of lipid species are critical. Lipids not only have a profound effect on the biophysical properties of membranes, but can also be modified to selectively recruit cytosolic proteins (Burd and Emr, 1998b).

The budding yeast *Saccharomyces cerevisiae* has proven to be an invaluable model organism for the study of membrane trafficking and lipid signaling. Genetic screens were used to first identify a number of genes required for anterograde membrane traffic, two major groups of which encode the Sec (secretory) and Vps (vacuolar protein sorting) proteins (Bankaitis *et al.*, 1986a; Robinson *et al.*, 1988b; Kaiser and Schekman, 1990). Follow-up studies showed that Vps34p, a lipid kinase that generates phosphatidylinositol

3-phosphate (PtdIns3*P*) on endosomes is required for post-Golgi biosynthetic membrane traffic and macroautophagy (Schu *et al.*, 1993b; Kihara *et al.*, 2001). Subsequently, it was discovered that other phosphoinositides play key roles in secretion (PtdIns4*P*), endocytosis (PtdIns[4,5]P_2), and vacuole size control (PtdIns[3,5]P_2) (Odorizzi *et al.*, 2000). At the same time, numerous *SEC* and *VPS* genes were found to encode other key players in membrane trafficking: SNAREs (soluble *N*-ethylmaleimide-sensitive factor attachment protein receptors), small GTPases, and various tethering factors. Although much remains to be elucidated, significant insight has been gained into how these proteins interface with each other and phospholipids to coordinately regulate membrane flow (Behnia and Munro, 2005).

The big picture that has emerged from decades of research is a tightly regulated, multi-directional, and interconnected network of vesicular traffic central to biosynthetic and catabolic processes as well as organelle biogenesis and function. Importantly, most mechanisms of membrane trafficking elucidated by studies in yeast are conserved in higher eukaryotes, including mammals (Odorizzi *et al.*, 2000).

Here we focus on the yeast vacuole – the functional analog of mammalian lysosomes – and examine different aspects of biogenesis, function and morphology. Relationships between the various membrane trafficking pathways that ensure organelle homeostasis are highlighted, with

special emphasis on the role of phosphoinositide signaling in the regulation of vacuole size, shape, and number.

Membrane Trafficking and the Yeast Vacuole

The fungal vacuole is often compared to the lysosome in higher eukaryotes. However, it is functionally more similar to the plant vacuole: its roles are not limited to degradative and autophagic processes, but also include amino acid and ion storage, osmotic buffering of the cytosol, and regulation of intracellular pH levels (Klionsky *et al.*, 1990). As such, yeast cells must ensure that a) functional homeostasis of the vacuole is maintained at all times and b) vacuoles are properly inherited or established *de novo* by daughter cells during budding and cytokinesis.

Although much progress has been made, a complete picture of how yeast regulate vacuole membrane dynamics has not yet emerged. The multiple endocytic and biosynthetic membrane transport pathways that converge on the vacuole as well as autophagic pathways for recycling and degrading membrane constituents (i.e. lipids and proteins) need to be kept in balance to maintain the proper size and shape of the vacuole (Bryant *et al.*, 1998; Odorizzi *et al.*, 1998a). In addition, the cell cycle-dependent process of vacuole inheritance involves significant changes in vacuole morphology and precise regulation (Weisman, 2003).

In terms of biogenesis, the core fusion machinery of biosynthetic sorting pathways, i.e. Vam3p (t-SNARE), the class C vacuolar protein sorting/HOPS complex (tethering), and Ytp7p (Rab GTPase) play a critical role in fusion at the vacuole (Haas *et al.*, 1995; Sato *et al.*, 2000; Wurmser *et al.*, 2000; Peterson and Emr, 2001). Additionally, actin, phosphoinositides, ergosterol, diacylglycerol, V-ATPase activity, and ion regulation also affect fusion (Wickner, 2002; Fratti *et al.*, 2004; Jun *et al.*, 2004; Starai *et al.*, 2005). Nonetheless, the impact these fusion and biogenesis factors have on vacuole size regulation is only part of the story.

Over the past decade, a plethora of studies have implicated phosphoinositides as key determinants of organelle identity and morphology, and the vacuole is no exception: a growing body of genetic and biochemical evidence suggests that the regulated synthesis and turnover of phosphatidylinositol 3,5-bisphosphate [PtdIns(3,5)P_2] underlies many aspects of vacuole function (Weisman, 2003; Peplowska and Ungermann, 2005).

Roles for PtdIns(3,5)P_2 in Vacuole Size Regulation

PtdIns(3,5)P_2 on the vacuole is generated by Fab1p (the mammalian homolog is called PIKfyve), the sole phosphatidylinositol 3-phosphate (PtdIns3P) 5-kinase in yeast. As a substrate, Fab1p utilizes PtdIns3P generated by the PI 3-kinase Vps34p (Cooke *et al.*, 1998; Gary *et al.*, 1998;

Ikonomov *et al.*, 2001). Fab1p is intimately involved in vacuole size regulation, presumably by modulating PtdIns(3,5)P_2 effector activity (Rudge *et al.*, 2004).

A *fab1Δ* strain entirely devoid of PtdIns(3,5)P_2 displays a complex, pleiotropic phenotype consisting of a dramatically enlarged vacuole, a partial defect in multivesicular body (MVB) sorting, failure in vacuolar acidification and osmoregulation, defective inheritance of vacuoles, and temperature-sensitive growth (Fig. 1.1) (Yamamoto *et al.*, 1995; Cooke *et al.*, 1998; Gary *et al.*, 1998; Odorizzi *et al.*, 1998a; Dove *et al.*, 2002). Mutants deleted for *VAC7* or *VAC14*, encoding the two known activators of Fab1p, closely recapitulate most *fab1Δ* defects (Bonangelino *et al.*, 1997; Bonangelino *et al.*, 2002b; Dove *et al.*, 2002; Gary *et al.*, 2002). Individual deletions cause a severe drop in the levels of PtdIns(3,5)P_2, although *vac14Δ* retains a low level of activity (10% of wild-type), sufficient to permit growth at high temperatures (Dove *et al.*, 2002; Gary *et al.*, 2002; Rudge *et al.*, 2004). Thus, Vac7p (a transmembrane protein) and Vac14p are critical components of the Fab1p/PtdIns(3,5)P_2 regulatory system. Turnover of this phospholipid is predominantly mediated by Fig4p, a Sac-related lipid phosphatase specific for PtdIns(3,5)P_2 (Fig. 1.1) (Gary *et al.*, 2002; Rudge *et al.*, 2004).

Fab1p is a very large protein of 2,278 amino acids, comprised of several conserved domains (Fig. 1.1). The N-terminal FYVE domain binds PtdIns3*P*, and is required for recruitment of the protein to the vacuolar limiting

Figure 1.1 The Phosphatidylinositol-3-phosphate 5-kinase, Fab1p.
(A) *Domain composition of Fab1p*. Fab1p harbors three conserved protein domains. Its N-terminus contains a FYVE domain (residues 230-297) that binds to PtdIns3*P*. Residues 819-1550 are related to the GroEL chaperonin, and within this region is another highly conserved region (840-1032) related to the Cpn60/TCP-1 chaperonin family (CCT). Both GroEL and the CCT family are classified as HSP60 chaperonins. The C-terminal region encompassing residues 1597-2278 encodes a lipid kinase domain related to Mss4p. The first two arrows indicate the position of the double glycine to valine mutations (GG/VV; G2042V/G2045V), while the last arrow points to the position of the D2134R (D/R) mutation that fully ablates Fab1 kinase activity.
(B) *The Fab1 pathway.* Fab1p converts PtdIns3*P* into PtdIns(3,5)P_2, a reaction that requires activation by Vac7p and Vac14p and might be negatively regulated by Atg18p. Conversely, PtdIns(3,5)P_2 can be metabolized to PtdIns3*P* by the 5'-phosphatase, Fig4p. PtdIns(3,5)P_2 modulates multiple cellular functions, many of which could directly impact vacuole morphology. PtdIns(3,5)P_2 is required for vacuolar acidification, perhaps by activating the V-ATPase proton pump and/or by modulating ion channels and/or exchangers. Atg18p, a PtdIns(3,5)P_2 effector, is thought to mediate membrane recycling or efflux from the vacuole; however, Atg18p also appears to act as an antagonist of PtdIns(3,5)P_2 synthesis. In addition, Ent3/Ent5 are suggested PtdIns(3,5)P_2 effectors that mediate MVB sorting.
(C) The vacuoles of "wild-type" (wt) and *FAB1*-deleted yeast cells (*fab1Δ*) were labeled with the endocytic tracer, FM4-64 (red). The respective fluorescence and differential interference contrast images were overlaid. "Wild-type" yeast cells predominantly display small, multi-lobed vacuoles. In comparison, the majority of vacuoles in *fab1Δ* cells are swollen and single-lobed. *fab1Δ* cells are also significantly enlarged.

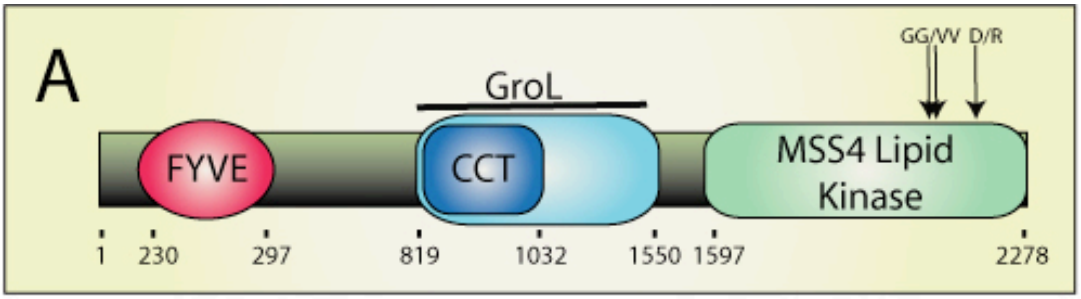
A
GG/VV D/R
GroL
FYVE
CCT
MSS4 Lipid Kinase
1
230
297
819
1032
1550
1597
2278

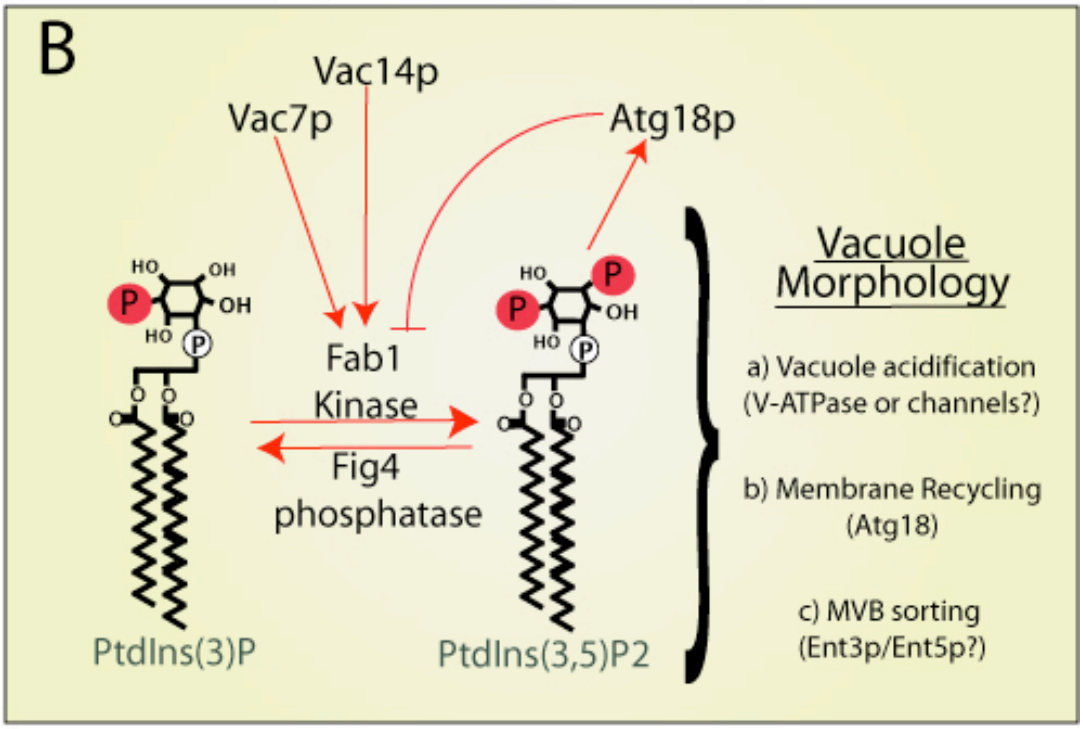
B
Vac14p
Vac7p
Atg18p
Fab1 Kinase
Fig4 phosphatase
PtdIns(3)P
PtdIns(3,5)P2
Vacuole Morphology
a) Vacuole acidification (V-ATPase or channels?)
b) Membrane Recycling (Atg18)
c) MVB sorting (Ent3p/Ent5p?)

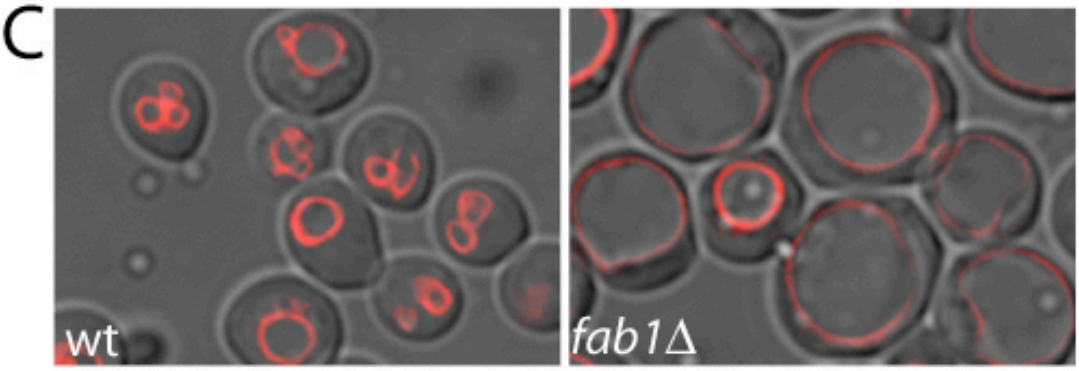
C
wt
fab1Δ

membrane, as Fab1p contains no transmembrane domains. Conversely, the lipid kinase domain is located at the extreme C terminus. Vacuole size control absolutely requires the synthesis of PtdIns(3,5)P_2 by Fab1p. First, expression of a kinase-dead mutant (D2134R) fails to complement any of the defects observed in the *fab1Δ* strain (Gary *et al.*, 1998; Odorizzi *et al.*, 1998a). Second, a Fab1p mutant (G2042V/G2045V) that only synthesizes 10% of the normal levels of PtdIns(3,5)P_2 retains the drastically enlarged vacuoles observed in *fab1Δ* cells, even though they are properly acidified and competent for MVB sorting (Gary *et al.*, 1998; Odorizzi *et al.*, 1998a). Conversely, cells expressing a mutant Fab1p (encoded by *fab1-5*) that displays elevated levels of PtdIns(3,5)P_2 exhibit fragmented or shrunken vacuoles (Gary *et al.*, 2002). These data suggest a simple model in which low levels of PtdIns(3,5)P_2 result in an enlargement of the vacuole and high levels cause the organelle to shrink and fragment. Thus, Fab1p may play a direct role in balancing membrane and ion flux to and from the vacuole. Precisely how the lipid affects changes in vacuole size is unclear, in part because of a paucity of PtdIns(3,5)P_2 effectors identified to date. Currently, three possible mechanisms for the regulation of vacuole size by PtdIns(3,5)P_2 can be envisioned:

a) Regulation of vacuolar ion and solute transport: dysregulation of ion transport across the limiting membrane of the vacuole may create an osmotic

imbalance, causing water from the cytosol to diffuse in and engorge the organelle. In support of such a model, it is striking that in a suppressor screen of *S. pombe Δfab1* mutants, 22 of 66 suppressors consisted of Ca^{2+} transporter homologs (Onishi *et al.*, 2003). Curiously, PtdIns(4,5)P_2 is a regulator of ion channels and exchangers at the plasma membrane (Hilgemann *et al.*, 2001); conceivably, PtdIns(3,5)P_2 might perform a similar role at the vacuole. Alternatively, PtdIns(3,5)P_2 might play a role in keeping the lumen of the vacuole osmotically neutral by controlling the formation of osmotically inactive complexes of ions (e.g. $CaPO_4$) and/or proteins (Fig. 1.2). In fact, electron microscopy imaging of "wild-type" yeast vacuoles shows an electron-dense sub-compartment of the vacuole that appears to be missing in *fab1Δ* cells (Gary *et al.*, 1998).

It is unlikely that vacuolar swelling is a direct consequence of perturbed vacuolar acidification in *fab1Δ,* because these two defects can be dissociated: in *fab1Δ* cells expressing the Fab1p G2042V/G2045V mutant, the vacuoles undergo proper acidification but remain grossly enlarged (Gary *et al.*, 1998).

b) Regulation of vacuolar membrane efflux: PtdIns(3,5)P_2 might modulate a vacuole-to-endosome/Golgi membrane recycling pathway. The vacuole continuously receives membranes via endocytic and biosynthetic membrane trafficking pathways, which do not appear to be blocked in *fab1Δ* cells: carboxypeptidase S (CPS), carboxypeptidase Y (CPY), alkaline

phosphatase (ALP), Phm5p, the pheromone receptor Ste2p, and the endocytic tracer FM4-64 all accumulate steady-state pools at the vacuole (Gary *et al.*, 1998; Odorizzi *et al.*, 1998a; Dove *et al.*, 2002; Rudge *et al.*, 2004). With a continuous proliferation of membrane, a block in retrograde transport would lead to vacuolar enlargement.

Studies of membrane efflux from the vacuole have been precluded by a lack of bona fide recycling cargoes. Nonetheless, Bryant and colleagues have provided evidence for a retrograde transport pathway from the vacuole to the late Golgi compartment by employing an engineered marker, RS-ALP (Bryant *et al.*, 1998). This fusion construct consists of the transmembrane protein ALP modified in its cytosolic tail by insertion of an FXFXD motif from dipeptidyl aminopeptidase (DPAP), which normally permits retrograde traffic from the prevacuolar endosome to the late Golgi. Precursor RS-ALP exits the late Golgi through the ALP (AP3) pathway and is delivered to the vacuole, where it matures by a protease-dependent cleavage. Subsequent appearance of cleaved RS-ALP in the late Golgi is believed to be indicative of recycling from the vacuole (Fig. 1.2). Such recycling is not detected in *vac7Δ* and *vac14Δ* mutants, indicating a requirement for PtdIns(3,5)P_2 (Bryant *et al.*, 1998; Dove *et al.*, 2002).

Interestingly, an *atg18Δ* (*svp1Δ*) strain exhibits the same vacuole-to-Golgi recycling defect, even though Atg18p is not required for PtdIns(3,5)P_2

production (Dove *et al.*, 2004). On the contrary, Atg18p functions downstream of the lipid: it preferentially binds PtdIns(3,5)P_2 *in vitro* (kd=500 nM, about ten times as strong as the affinity of the FYVE domain of Hrs for PtdIns3P) and localizes to the vacuolar limiting membrane in a Fab1p-dependent fashion. The lipid interaction motif lies within a β-propeller fold comprising seven WD40 domains (Dove *et al.*, 2004).

Atg18Δ cells also exhibit single-lobed, swollen vacuoles, albeit not as dramatic as in *fab1Δ* mutants. However, unlike deletion of the kinase or its upstream regulators *VAC7* and *VAC14* (which lowers PtdIns(3,5)P_2 levels dramatically), *atg18Δ* cells exhibit a ten-fold increase in PtdIns(3,5)P_2 compared to wild-type cells (Dove *et al.*, 2004). These observations suggest that Atg18p might function both as an effector of PtdIns(3,5)P_2 – possibly as a component of the vesicle recycling machinery – and in a feedback pathway negatively modulating Fab1p activity (Fig. 1.1). Furthermore, *atg18Δ* vacuoles fail to fragment under hypertonic stress, even though PtdIns(3,5)P_2 levels quickly climb as high as 60 times that of wild-type. This unusual finding raises the possibility that Atg18p is the key effector mediating membrane recycling and partitioning of the vacuole (Fig. 1.2). In further support of such a role, Atg18p has been proposed to also mediate membrane and protein retrieval from pre-autophagosomal structures (PAS) (Reggiori *et al.*, 2004a).

Figure 1.2 Possible mechanisms for vacuole size regulation. PtdIns(3,5)P_2 may govern the activity of vacuolar amino acid transporters, exchangers and ion channels, which would correspondingly affect water flow across the vacuole. We predict that diminishing the levels of PtdIns(3,5)P_2 would enhance net transport into the vacuolar lumen leading to a corresponding increase in water flow and vacuolar swelling. Conversely, elevated levels of PtdIns(3,5)P_2 may induce net exit of vacuolar solutes and water, consequently shrinking the vacuole. Vacuolar size homeostasis may depend on efficient membrane turnover, which requires the inward invagination of membranes to form multivesicular bodies (MVBs). Fusion of MVBs with the vacuole has two consequences: it releases the intraluminar vesicles into the vacuole for degradation and is a replenishing source for the limiting membrane of the vacuole. Therefore, arresting MVB formation and membrane turnover is predicted to augment the amount of membrane input into the limiting membrane of the vacuole. Abrogation of membrane recycling or efflux from the vacuole is predicted to increase membrane surface area, especially if membrane influx remains intact. Evidence for vacuolar recycling is provided by the engineered RS-ALP probe. Immature RS-ALP is targeted to the vacuole via the ALP pathway (also known as the AP-3 pathway) where it undergoes a protease-dependent cleavage producing two fragments: a soluble fragment that remains in the vacuole and a transmembrane-containing (TM-RS-ALP) fragment. The latter portion may recycle to endosomes and Golgi from the vacuole in a manner dependent on PtdIns(3,5)P_2 and its effector, Atg18p.

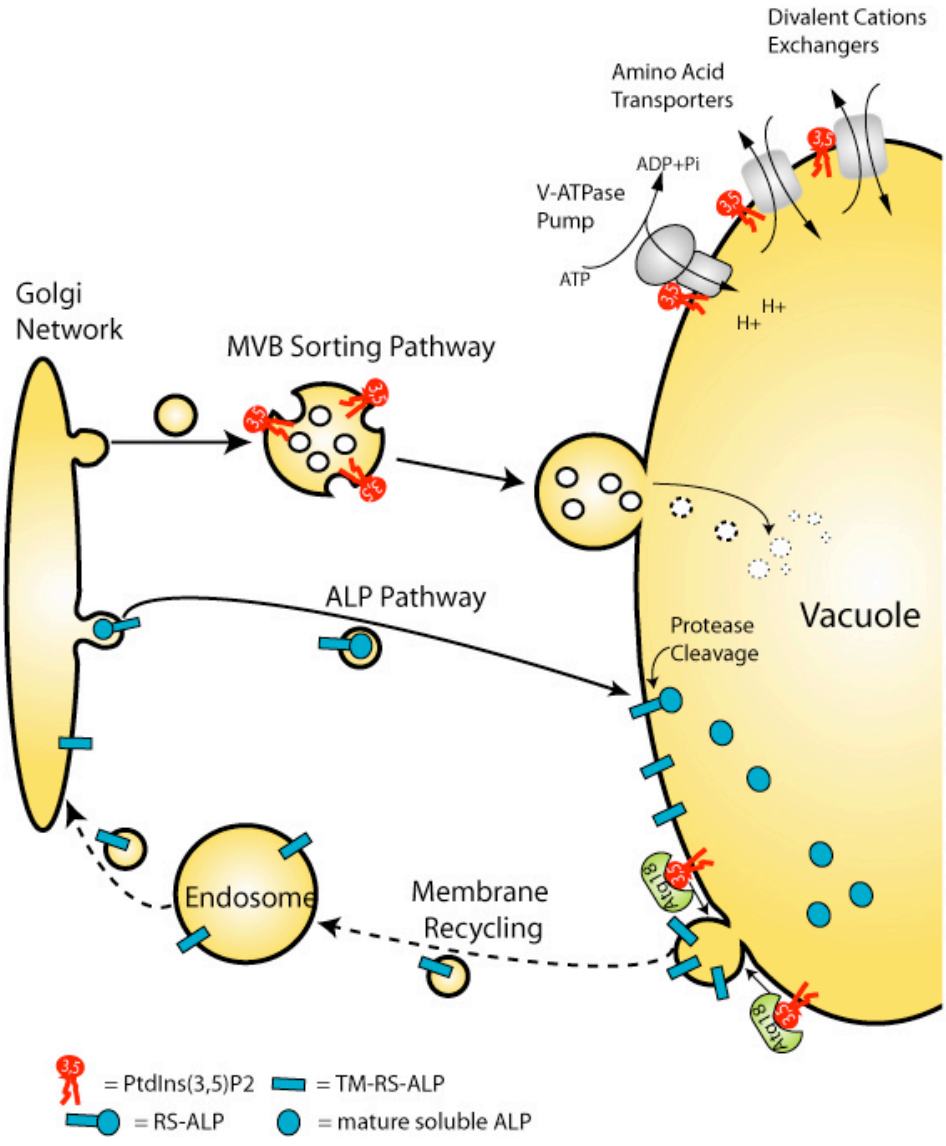
Divalent Cations
Exchangers
Amino Acid
Transporters
ADP+Pi
V-ATPase
Pump
ATP
H+
H+
Golgi
Network
MVB Sorting Pathway
ALP Pathway
Protease
Cleavage
Vacuole
Endosome
Membrane
Recycling
= PtdIns(3,5)P2
= TM-RS-ALP
= RS-ALP
= mature soluble ALP

Like Atg18p, a subset of vacuolar sorting proteins including Vps1p and Vps3p are also involved in the fragmentation of the vacuole, because their deletion mutants exhibit enlarged vacuoles that are entirely unresponsive to hyperosmotic shock (Banta *et al.*, 1988; Peters *et al.*, 2004; Lagrassa and Ungermann, 2005). However, it is highly unlikely that the proteins encoded by these and other class D *VPS* genes have a direct role in membrane recycling/fission, as they are presumably required for either (a) production of normal levels of PtdIns3P, a substrate for Fab1p or (b) transport of cargo and regulatory factors (e.g. Vac7p) to the vacuole. Theoretically, these factors could include an as yet unknown protein partner of Atg18p, as it is not known whether PtdIns(3,5)P_2 alone is sufficient to recruit this protein to the vacuole.

c) Regulation of vacuolar membrane turnover: significant membrane turnover is mediated by the formation of multivesicular bodies. This process occurs at the prevacuolar endosome and is responsible for turnover of membranes and integral membrane proteins (Fig. 1.2) (Katzmann *et al.*, 2002; Gruenberg and Stenmark, 2004). Intralumenal membrane invagination at the MVB may be regulated by PtdIns(3,5)P_2; in *fab1Δ* cells, MVB sorting of biosynthetic cargo (i.e. CPS and Phm5p) is blocked, but the sorting of endocytic cargo (Ste2p) into MVBs remains unperturbed (Odorizzi *et al.*, 1998a; Dove *et al.*, 2002; Katzmann *et al.*, 2004). It is noteworthy that several putative effectors of PtdIns(3,5)P_2 have been implicated in MVB sorting and

biogenesis, including the mammalian ESCRT-III subunit mVps24 and the Ent3 and Ent5 proteins (Friant *et al.*, 2003; Whitley *et al.*, 2003; Eugster *et al.*, 2004). However, these studies were conducted largely *in vitro*, and direct demonstration of a Fab1p-dependent *in vivo* role for Ent3p/Ent5p or mVps24 is still lacking.

Although there is controversy surrounding potential effectors of PtdIns(3,5)P_2 and Fab1p, the relevance of the pathway to metazoan biology is hardly disputable. Homologs of Fab1p (PIKfyve) and Vac14p (hVac14/ArPIKfyve) have been characterized in mammals, and are involved in size control of endomembranes and lysosomes (Ikonomov *et al.*, 2001). More specifically, overexpression of dominant-negative "kinase-dead" point mutants of PIKfyve causes a very dramatic enlargement of late endosomal compartments (Ikonomov *et al.*, 2002).

Finally, microautophagy – the piecemeal uptake of cytosol by inward invagination of the vacuolar limiting membrane – might also help regulate vacuole size by eliminating excess membrane (Muller *et al.*, 2000). However, this process predominantly takes place under starvation conditions and no connection with PtdIns(3,5)P_2 metabolism has been established to date.

Osmoregulation: Separate Roles for Fab1p and Hog1p

To achieve long-term adaptation to hypo- or hyperosmotic stress, *S. cerevisiae* uses the protein kinase C (cell integrity) and HOG-MAP (high osmolarity glycerol mitogen-actived protein) kinase pathways, respectively (Tamas and Hohmann, 2003). It has recently been shown that phosphorylation (and subsequent activation) of plasma membrane channels such as *NHA1* (Na^+/H^+ antiporter) by Hog1p plays a critical role in the immediate response to osmotic shock (Proft and Struhl, 2004). Rapid changes in vacuole size and volume (for uptake or release of water and solutes) plays a key role in balancing cytoplasmic ion concentrations during osmotic stress (Latterich and Watson, 1993). More specifically, the cell must quickly activate the Fab1p and PtdIns(3,5)P_2-dependent size regulation pathway to avoid the fatal consequences of hyperosmotic shock: while Hog1p-mediated accumulation of glycerol takes hours under these conditions, PtdIns(3,5)P_2 levels rise sharply within 10 minutes (Cooke *et al.*, 1998). Accordingly, Fab1-dependent vacuole fragmentation in response to hyperosmotic stress does not require Hog1p activity (Lagrassa and Ungermann, 2005).

Vacuolar Inheritance

Throughout the cell cycle, yeast must transfer their vacuoles in a regulated fashion to ensure proper inheritance by daughter cells. In budding yeast, vacuolar membrane is rapidly transported into a nascent bud via a segregation structure. This membraneous projection mediates traffic – potentially vesicular – between mother cell and the newly formed vacuole (Catlett and Weisman, 1998). This myosin-mediated exchange of membrane continues along actin tracks until late in the cell division cycle (Gomes de Mesquita *et al.*, 1991; Tang *et al.*, 2003). Accordingly, recent work by Han *et al.* suggests a key role for the G1 cyclin Cln3 in vacuole inheritance (Han *et al.*, 2003). Surprisingly, daughter cells of inheritance mutants are capable of generating vacuole(s) *de novo*. However, the mechanism for this phenomenon has not been elucidated (Gomes De Mesquita *et al.*, 1997).

While strains producing little or no PtdIns(3,5)P_2 (*fab1Δ, vac7Δ, and vac14Δ*) have marked inheritance defects, this is most likely a secondary consequence of the drastic vacuolar enlargement seen in these mutants (Weisman, 2003).

Thesis Overview

Studies to date have shown that the regulation of vacuole size, function, and inheritance is a highly complex process. Importantly, vacuolar

homeostasis depends on the proper coordination of several different routes of anterograde – and perhaps retrograde – membrane traffic and cannot be considered in isolation. Constitutive membrane traffic originating at the Golgi (endosomes), the PM (endocytic traffic), as well as the cytosol (Cvt and macroautophagy) is central in this regard. Many of the key players (e.g. phosphoinositides, SNAREs, Rab GTPases) that help establish and maintain organelle identity and direct traffic between these distinct compartments have been identified. However, important questions remain: for example, can we identify additional proteins required for endosome/vacuole maturation? How exactly does PtdIns(3,5)P_2 production lead to changes in vacuole size? Is there a bona fide retrograde membrane transport pathway originating at the vacuole, and can it be observed using endogenous cargo(es)? What is the membrane source for cytoplasm-to-vacuole (and macroautophagic) transport vesicles? In an effort to further our knowledge in these areas and others, this thesis details new insights into the regulation of membrane traffic at three consecutive waypoints: the Golgi, endosomes, and the vacuole.

Chapter 2 demonstrates roles for Mon2p, a member of a novel and highly conserved protein family, in Golgi and vacuole homeostasis. Mon2p is also shown to be required for cytoplasm-to-vacuole transport and maintenance of normal cell size and growth.

Research presented in Chapter 3 introduces the new technique of pathogen effector protein screening in yeast (PEPSY). Taking advantage of the high degree of conservation in membrane trafficking between yeast and higher eukaryotes, the former is used to screen genetically for bacterial proteins that prevent lysosome/vacuole maturation.

Finally, Chapter 4 aims to elucidate how the vacuolar lipid kinase Fab1 is able to affect gross changes in vacuole morphology by producing PtdIns(3,5)P_2 on the limiting membrane of this organelle. This work focuses on Atg18p: as an effector of PtdIns(3,5)P_2 , it is shown to be both necessary and sufficient for vacuole membrane remodeling. Moreover, the discovery of new protein interactors explains how Atg18p might interface with the PtdIns(3,5)P_2 production machinery and supports previous data suggesting that Atg18p is involved in retrograde transport from the vacuole.

ACKNOWLEDGEMENTS

This chapter includes, in part, material as it appears in *Current Opinion in Cell Biology* 17(4):402-8, 2005. Efe, J.A., Botelho, R.J., and S.D. Emr. The Fab1 phosphatidylinositol kinase pathway in the regulation of vacuole morphology. The dissertation author was the primary investigator and author of this paper.

CHAPTER 2

YEAST MON2P IS A HIGHLY CONSERVED PROTEIN THAT FUNCTIONS IN THE CYTOPLASM-TO-VACUOLE TRANSPORT PATHWAY AND IS REQUIRED FOR GOLGI HOMEOSTASIS

ABSTRACT

Although the small Arf-like GTPases Arl1-3 are highly conserved eukaryotic proteins, they remain relatively poorly characterized. The yeast and mammalian Arl1 proteins bind to the Golgi complex, where they recruit specific structural proteins such as Golgins. Yeast Arl1p directly interacts with Mon2p/Ysl2p, a protein that displays some sequence homology to the large Sec7 guanine exchange factors (GEFs) [1] of Arf1. Mon2p also binds the putative aminophospholipid translocase (APT) Neo1p, which performs essential function(s) in membrane trafficking. Our detailed analysis reveals that Mon2p contains six distinct amino acid regions (A to F) that are conserved in several other uncharacterized homologs in higher eukaryotes. Since the conserved A, E and F domains are unique to these homologues, they represent the signature of a new protein family. To investigate the role of these domains, we made a series of N-and C-terminal deletions of Mon2p. While fluorescence and biochemical studies showed that the B and C domains (also

present in the large Sec7 GEFs) predominantly mediate interaction with Golgi/endosomal membranes, growth complementation studies revealed that the C-terminal F domain is essential for the activity of Mon2p, indicating that Mon2p might also function independently of Arl1p. We provide evidence that Mon2p is required for efficient recycling from endosomes to the late-Golgi. Intriguingly, although transport of CPY to the vacuole was nearly normal in the *Dmon2* strain, we found the constitutive delivery of Aminopeptidase 1 from the cytosol to the vacuole to be almost completely blocked. Finally, we show that Mon2p exhibits genetic and physical interactions with Dop1p, a protein with a putative function in cell polarity. We propose that Mon2p is a scaffold protein with novel conserved domains, and is involved in multiple aspects of endomembrane trafficking.

INTRODUCTION

The late-Golgi and endosomal compartments are central protein sorting stations of the cell. They direct newly synthesized as well as endocytosed proteins to their final subcellular destinations. Transport of proteins and lipids between these specialized trafficking organelles is highly regulated. It requires sequential recruitment of cytosolic proteins that function in vesicle formation, motor recruitment, and vesicle tethering (Munro, 2002). This recruitment process is largely mediated by specific lipid modifications and the activation of small G proteins of the ADP-ribosylation factor (ARF) and Rab families. The Arf proteins are distinguished from the other small GTPases by the presence of a myristoylated N-terminal amphipathic helix that facilitates interaction with membranes (Nie et al., 2003). Like other small GTPases, Arf proteins cycle between inactive GDP-bound form, which is soluble and an active GTP-bound form, which is associated with membranes and selectively, interacts with effectors (reviewed in (Vetter and Wittinghofer, 2001). The stimulation of this cycle is mediated by the subsequent action of GTPase-activating proteins (GAPs) and guanine exchange factors (GEFs). The Arf GEFs represent a large and diverse protein family (Jackson and Casanova, 2000), sharing a conserved region of roughly 200 amino acids, termed the Sec7 domain. This Sec7 domain alone is sufficient for the GDP to GTP exchange activity (Chardin et al., 1996).

Mon2p/Ysl2p, a protein related to the Sec7 family, was identified in several independent genetic screens searching for mutants that are sensitive to the drugs monensin and brefeldin A (Muren et al., 2001), defective in endocytosis (Wiederkehr et al., 2001), defective in protein transport to the vacuole (Avaro *et al.*, 2002; Bonangelino *et al.*, 2002a), or synthetic lethal with *Δypt51*, a mutant that perturbs vesicular transport between the late-Golgi and endosomal compartments (Singer-Kruger and Ferro-Novick, 1997). Recently, Mon2p was proposed to be a GEF for the small GTPase Arl1p since the two proteins physically interact with each other and *Δmon2* and *Δarl1* mutants exhibit similar endocytic transport and vacuolar protein sorting defects (Jochum *et al.*, 2002b). Although Arl1p shares structural features with Arf proteins (Pasqualato et al., 2002), its precise function in membrane trafficking remains poorly established. Arllp is associated with the Golgi apparatus (Lu et al., 2001; Rosenwald et al., 2002) and the active Arl1-GTP form directly interacts with GRIP domains of several golgins, thus mediating their recruitment onto late-Golgi membranes (Lu and Hong, 2003; Panic et al., 2003a; Panic et al., 2003b; Setty et al., 2003). Golgins are long coiled coil proteins that maintain the structure of the Golgi complex and are necessary for vesicular tethering events (Barr and Short, 2003). Arl1p was also purified with the GARP complex, which is part of the tethering complex required for the fusion of endosome-derived vesicles at the late-Golgi (Panic et al., 2003b).

Mon2p also binds to Neo1p, a member of the putative aminophospholipid translocases (APTs) (Wicky et al., 2004). APTs couple ATP hydrolysis to the translocation of phosphatidylserine (PS) and phosphatidylethanolamine (PE) to the cytosolic leaflet of biological membranes (Balasubramanian and Schroit, 2003; Natarajan et al., 2004). A higher concentration of these lipids in this leaflet is believed to induce the recruitment of specific proteins or help to deform membranes during vesicle budding. The *NEO1* gene was originally isolated as a multicopy suppressor of neomycin sensitivity (Prezant et al., 1996) and performs essential function than cannot be replaced by the other APT members. Neo1p is involved in membrane transport within the endosomal and Golgi systems (Hua and Graham, 2003; Wicky et al., 2004), a function that could be linked to that of Mon2p and Arl1p.

In this study we show that Mon2p contains six domains that are conserved in several higher eukaryotic homologs, thus forming a new family of proteins. We found that Mon2p is active without its putative Sec7 and Arl1p binding domains, suggesting that Mon2p could function independently of Arl1p. Furthermore, our results demonstrate that Mon2p localizes to the late-Golgi/early endosomes, where it is involved in protein trafficking and maintenance of homeostasis. It is also required for the constitutive maturation of the hydrolase aminopeptidase I (Ape1), which relies on the cytoplasm-to-

vacuole transport (Cvt) pathway and requires the GARP complex. Finally, we show a genetic and biochemical interaction of Mon2p with Dop1p, a protein that functions in cell polarity.

MATERIALS AND METHODS

Yeast Strains, Plasmids and Reagents. Yeast strains used in this study are shown in Table 2.1, and their construction is described below. Strains were grown in complete medium (yeast extract-peptone-dextrose (YPD)) or synthetic dextrose (SD) growth medium (Sherman, 1991). Anti-Pep12p, monoclonal mouse 12CA5 anti-hemagglutinin (HA) and rabbit anti-GFP antibodies were purchased from Molecular Probes Inc. (Eugene, OR), Berkeley Antibody Co (Richmond, CA) and Clontech (Palo Alto, CA), respectively. The polyclonal antibodies against CPY and Ape1 were generous gifts of Dr. Randy Schekman, University of California, Berkeley and Dr. Daniel Klionsky, University of Michigan, Ann Arbor, respectively. The monoclonal anti-myc antibody (9E10) was purchased from the Developmental Studies Hybridoma Bank at the University of Iowa (Iowa City, IA). Chlorpromazine (C-8138) was obtained from Sigma Chemical Co. (St. Louis, MO).

The *mon2Δ::ADE2* (YFP93 and YFP94) and *MON2* (wild-type/YFP95) were constructed by inserting the *ADE2* gene into the internal *Nco*I/*Hpa*I restriction sites of the *MON2* gene in the wild-type diploid W303 strain and obtained after tetrad dissection, using standard yeast methods. The correct integration of the *mon2Δ::ADE2* disruption cassette was confirmed by Southern analysis. To construct diploid double mutants with the *mon2Δ::ADE2* allele, YFP93 was crossed with YFP71, CDK17-6B and YFP35 to give YFP72,

YFP155 and YFP38, respectively. YFP94 was crossed with RSY906 to give YFP103. The resulting diploid strains were sporulated and tetrads were dissected. Spore clones containing disrupted genes were selected by testing for the presence of the corresponding auxotrophic markers. Authentic *chc1-521*^{ts} strains were identified based on the absence of growth at the restrictive temperature. The ODY318/Y23304 strain was obtained from the EUROSCARF consortium.

Deletion of *MON2* in the SEY6210 strain background (AAY1120) and genomic integrations for C-terminal tagging (JEY001, JEY002, JEY003, and JEY069) were carried out by transformation of PCR-amplified constructs using the appropriate plasmids as templates (Longtine et al., 1998) and primers specific for *MON2*. Deletion and integrations were subsequently verified by PCR and western blot analysis (the latter only for fusion proteins). The diploid strain JEY026 was obtained by crossing JEY001 with JEY002. For the *DOP1*-3xHA-mRFP integration, a modified version of (Longtine) plasmid pFA6A-13Myc-HIS3-MX6 was used. Briefly, using *Pac*I/*Asc*I sites, the 13xMYC tag was replaced with a 3xHA-mRFP (kind gift of Dr. R. Tsien) PCR product, and *LEU2* (incl. 598 bp upstream and 46 bp downstream sequence) was substituted for the *HIS3* ORF using *Bgl*II and *Pme*I sites.

The relevant plasmids used in this study are listed in Table 2.2 and they were constructed as briefly described below. A 5.89 kb *Sal*I/*Spe*I fragment

containing the entire *MON2* open reading frame (ORF) was subcloned from a genomic library clone pDK7 into the *Sal*I/*Xba*I-restricted YEplac181 (2*μ*, *LEU2*), YEplac112 (2*μ*, *TRP1*) and YEplac195 (2*μ*, *URA3*) to form YEplac181-*MON2* (pDK30), YEplac112-*MON2* (pDK35) and YEplac195-*MON2* (pDK36), respectively. For the construction of GFP plasmids, the entire ORF of *MON2*[A-F (1-4911)], and all the 5'-DNA *MON2*[A-E (1-4500)], *MON2*[A-d (1-1800)], *MON2*[A-C (1-1230)], *MON2*[A-B (1-651)], *MON2*[A (1-180)] terminal fragments were fused upstream of a GFP-encoding fragment and cloned into the YEplac181 vector (2*μ*, *LEU2*) under the control of their own promoter. *MON2*[A-d (1-1800)] was also subcloned into the pRS315 vector (CEN, *LEU2*) (pOD130). All the 3'-DNA *MON2*[B-F (151-4911)], *MON2*[d-F (2383-4911)], *MON2*[E-F (3443-4911)] terminal fragments were fused downstream of a GFP, under the control of the ADH promoter into the pRS415-ADH-GFP vector (CEN, *LEU2*).

YEplac181-*DOP1* (pDK64) and pRS423-*DOP1* (pDK62) were obtained by subcloning a 8.3 kb *Sal*I/*Sac*I fragment containing the *DOP1* gene from pRS413-*DOP1* (pDK15) into the *Sal*I/*Sac*I-restricted YEplac181 and pRS423, respectively. YEplac181-*ARL1* (pRB95) and YEplac112-*ARL1* (pRB108) were constructed by subcloning a 1.25 kb *Sac*I/*Bam*HI fragment containing the *ARL1* gene from pN5 into the *Sac*I/*Bam*HI-restricted YEplac181 and YEplac112, respectively. Finally, YEplac181-*NEO1* (pRB111) and YEplac112-

NEO1 (pRB113) were obtained by subcloning a *Spe*I (Klenow blunt-ended)/*Xba*I fragment containing the *NEO1* gene from pA32 into the *Sma*I/*Xba*I-restricted YEplac181 and YEplac112, respectively. All cloned DNA fragments generated by PCR amplification were verified by sequencing.

Plasmids pCS198 and pCS212 have essentially been described previously (Stefan et al., 2002), except that GFP in the respective $FYVE_{(EEA1)}$ and $PH_{(FAPP1)}$ reporter constructs was replaced with DsRed using PCR amplification to introduce *Bgl*II and *Spe*I sites and subsequent (Klenow) blunt ligation.

Growth Complementation. YFP44 (*Δmon2/chc1-521*) cells harboring YEplac195-*MON2* and transformed with YEplac181-GFP, YEplac181*MON2*[1-4911]-GFP, YEplac181*mon2*[1-4500]-GFP, pRS415-ADH-GFP-*mon2*[151-4911], pRS415-ADH-GFP-*mon2*[2388-4911] or pRS415-ADH-GFP-*mon2*[3443-4911] were first streaked out on 5-FOA-containing plates to select for the loss of YEplac195-*MON2* at 22°C and then tested for growth on SD-LEU plates at the indicated temperatures. YFP93 (*Δmon2*) transformed with YEplac181-GFP, YEplac181*MON2*[1-4911]-GFP, YEplac181*mon2*[1-4500]-GFP, pRS415-ADH-GFP-*mon2*[151-4911], pRS415-ADH-GFP-*mon2*[2388-4911] or pRS415-ADH-GFP-*mon2*[3443-4911] were streaked on SD-LEU plates containing 50 mM potassium phosphate pH 7.0 and 20 μM CPZ as indicated.

Isolation of Multicopy Suppressors of the *Δmon2* Mutant. To obtain multicopy suppressors of the *Δmon2* null mutation, the CDK13-1A (*MAT*a *tif3Δ::TRP1 mon2Δ::ADE2* [pSEY18-*TIF3*]) strain was transformed with a YEp13-based yeast genomic library (Nasmyth library) or a YEplac181-based library (D. Kressler, unpublished). Transformants containing plasmids with suppressor activity were selected by replica plating onto 5-FOA-containing plates and re-tested by transformation into YFP44 (*Δmon2/chc1-521*), YFP101 (*Δmon2/Δvps1*) and YFP86 (*Δtif3/vps54*) double mutants. The specific suppressing genes of YFP44 and YFP101 strains were determined by subcloning.

Fluorescence Microscopy. For most GFP images, cells harboring GFP fusion constructs were grown in SD-LEU medium to mid-logarithmic phase at 30°C. Images were obtained using a Zeiss Axiovert S1002TV (Thornwood, NY) microscope equipped with an Axiocam color digital camera and the AxioVision™ software. Figures were prepared with the use of the Adobe Photoshop 8.0 (Adobe Systems Inc., San Jose, CA) software program.

For Mon2-GFP colocalization experiments and those using GFP-Ape1, cells were visualized using fluorescein isothiocyanate (FITC) and rhodamine filters, and images were captured with a Photometrix camera and processed with DeltaVision deconvolution software (Applied Precision, Seattle, WA). For the GFP-Ape1 experiments, cells were first labeled with the fluorescent

lipophilic dye N-[3-triethylammoniumpropyl]-4-[p-diethylaminophenylhexa-trienyl] pyridinium dibromide (FM4-64; Molecular Probes, Eugene, OR) as previously described to highlight vacuoles (Vida and Emr, 1995a). All observations are based on the examination of at least 100 cells, and representative fields are shown.

Electron Microscopy. Early log-phase cells (approximately 60 OD_{600} units) were grown in YPD, harvested, and fixed in 3% glutaraldehyde, 0.1 M Na cacodylate (pH 7.4), 5 mM $CaCl_2$, 5 mM $MgCl_2$, and 2.5% sucrose for 1 h. Cells were first washed in 100 mM Tris (pH 7.5), 25 mM DTT, 5 mM EDTA, and 1.2 M sorbitol for 10 min, then reuspended in 100 mM K_2HPO_4 (pH 5.9), 100 mM citrate, and 1 M sorbitol. Following addition of beta-glucuronidase (50 μl) and Zymolyase T100 (400 μg/ml), cells were incubated for 40 min at 30°C. They were then spun down, washed, and resuspended in cold buffer containing 500 mM Nacacodylate (pH 6.8) and 25 mM $CaCl_2$, followed by osmium-thiocarbohydrazide staining. Further processing details have been described previously (Rieder et al., 1996). Structural analyses were based on >50 cells examined for each strain.

Whole Cell Extracts, Subcellular Fractionation, and Co-immuprecipitation. The preparation of whole cell extracts for western blot analysis was made from cultures grown in SD medium to midlogarithmic

phase. Five OD_{600} units of cells were converted to spheroplasts and lysed by the addition of 200 μl of 1% SDS/8 M urea at 65°C for 10 min.

For subcellular fractionations, cells (approx. 20 OD_{600} units) were grown at 26°C to midlogarithmic phase and spheroplasted (Darsow et al., 1997). Spheroplasts were resuspended in 1 ml ice-cold lysis buffer (200 mM sorbitol, 50 mM potassium acetate, 20 mM HEPES, pH 7.2, 2 mM EDTA) containing protease inhibitors, and lysed by douncing (12x). Following a clearing spin at 500 x g for 5 minutes, lysates were spun at 13,000 x g for 10 min (4°C), whereafter the supernatant was treated as indicated for 15 min. with frequent agitation. Finally, the supernatant was further fractionated at 100,000 x g for 1 h (4°C), the S100 supernatant was removed, and the resulting P100 pellet was resuspended in lysis buffer. Proteins were precipitated from both fractions with trichloroacetic acid (TCA; 10% final concentration). SDS-PAGE and Western analyses were used to determine the relative amount of Dop1-HA-mRFP present in each fraction.

For co-immunprecipitations, cells (50 OD_{600} units) were lysed as above, and Tween-20 was added to the 13,000 x g supernatants to a final concentration of 0.5%. Following a 15-min. incubation, detergent-insoluble material was pelleted with a 10-min. 16,000 x g spin. After removing and TCA-precipitating 10% of the supernatant to determine total protein content, antibodies to the protein of interest were added to the remainder and

incubated at 4°C for four hours, with 20 μl Gammabind G-sepharose beads (Amersham Biosciences, Piscataway, NJ) being added two hours into the incubation. Protein complexes bound to the beads were recovered by washing three times with 1 ml ice-cold lysis buffer containing 0.5% Tween-20, and three times with detergent-free lysis buffer, followed by elution in boiling buffer (50 mM Tris, pH 6.8, 2% SDS, 5% b-mercaptoethanol, 10% glycerol, 0.005% bromophenol blue) at 100°C for 10 minutes. As above, SDS-PAGE and western analysis were used to detect proteins of interest.

Sucrose Density Gradients and Gel Filtration Chromatography.

For sucrose density gradient fractionation, cells transformed with the indicated plasmids were grown in 500 ml of SD medium to an OD_{600} of 1.2 at 30°C. Cells were subsequently lysed as described (Harsay and Bretscher, 1995). The yeast lysate was centrifuged for 20 min at 4°C at 13,000 x g in a SS34 rotor (Sorvall). The pellet was discarded and the supernatant was centrifuged for 60 min at 4°C at 100,000 x g in a SW41 rotor (Beckman Instruments) onto a 80 μl cushion of 60% sucrose. The membrane pellet was carefully resuspended in 2 ml of buffer containing 0.8 M sorbitol, 10 mM triethanolamine pH 7.2, 1 mM EDTA, 0.5 mM PMSF, 1 μg/ml pepstatin, 1 μg/ml leupeptin and 1 mM benzamidine. The resuspended pellet was then layered onto a 10.5 ml sucrose step gradient (1 ml 60%, 2 ml each at 42, 36, 24% and 1.5 ml of 18% sucrose) buffered with 0.8 M sorbitol, 10 mM triethanolamine pH 7.2 and 1 mM

EDTA. After a centrifugation of 18 h at 4°C at 100,000 x g in a SW41 rotor, fractions (0.4 ml) were manually collected from the top and equal volumes of each fraction were processed for immunoblotting.

In gel filtration chromatography experiments, approximately 100 OD_{600} units of cells were grown, spheroplasted, and lysed as described above (for subcellular fractionations), except that PBS (pH 7.2) was used as the lysis buffer. The S100 supernatants were run over a Sephacryl S-300 16/60 column (Pharmacia) in PBS. Fractions of 1.4 ml were eluted at a flow rate of 0.4 ml/min and, after TCA precipitation, a tenth of each fraction was analyzed by SDS-PAGE and western blot. Sizing standards for the column were blue dextran, ferritin, catalase, and thyroglobulin.

^{35}S Pulse-Chase Assays. Cell labeling and immunoprecipitations were performed as described previously (Gaynor et al., 1994). Briefly, mid-log (OD_{600}~0.6) phase cultures were concentrated to 3 OD_{600} units/ml and labeled with 3 μl Tran ^{35}S label per OD_{600} (PerkinElmer Life and Analytical Sciences, Boston, MA) for 10 min in SD-URA medium. Cells were chased with 10 mM methionine, 4 mM cysteine, and 0.4% yeast extract for the indicated times. Proteins were then precipitated in 10% TCA. Resulting protein pellets were washed twice with ice-cold acetone, dried and processed for immunoprecipitation as described previously (Gaynor et al., 1994). Labeling and immunoprecipitation of CPY was performed as described (Wilcox and

Fuller, 1991). Immunoprecipitated proteins were resolved on SDS-PAGE gels and analyzed by autoradiography.

Sequence Analyses. Iterative database searches using profiles were performed on the non-redundant database Swiss-Prot/TrEMBL for detection of Mon2p homologues. The default parameters of the pftools and the PSI-BLAST packages were used for the construction of profiles. The graphical representation of Mon2p was adapted from the PROSITE domain visualizer (http://www.expasy.org/tools/scanprosite/psview-doc.html). The alignment was shaded in conservation mode by using GeneDoc (version 2.6) according to the amino acid property. The secondary structure elements were predicted using the PHD program (Rost, 1996).

RESULTS

Mon2p contains six distinct domains present in several uncharacterized homologs. We originally isolated a *mon2* mutant in a synthetic lethal screen with a mutant of *TIF3*, which encodes a translation initiation factor (Coppolecchia et al., 1993). This genetic interaction helped us to establish a direct connection between protein synthesis and membrane trafficking (Deloche et al., 2004). Mon2p is a large protein of 186 kDa, with a weak homology to the large Sec7 GEFs. Initial sequence analysis revealed that this homology is not restricted to the catalytic Sec7 domain but to the other domains of unknown functions. To define the structural properties of these different domains, we performed iterative PSI-BLAST (Altschul et al., 1997) and generalized profile searches (Bucher et al., 1996) on the Swiss-Prot/TrEMBL non-redundant database (Bucher et al., 1996). We initiated our search with 6 conserved regions (A to F) that are clearly evident when aligning Mon2p with the various fungal homologues (Fig. 2.1A). Only sequences that matched a profile with a significant score (E-value< 0.01) were used for subsequent iteration cycles. After several cycles, our different profiles converged on two sets of sequences, shown in the different multiple sequence alignments (see supplemental figures). Profiles directed against domains B, C, and D revealed that these three domains of Mon2p are also present in the large Sec7 GEF proteins and closely correspond to the conserved upstream

and downstream regions of the Sec7 catalytic domain, as recently defined by B. Mouratou et al. (2005) (see Fig. 2.1B). Among these three domains, the B and C domains display important sequence conservation (41% and 40% similarity, respectively). A secondary structure prediction found ten α-helices in the C domain present in a region that was shown to interact with Arl1p (Jochum *et al.*, 2002b). As previously noted by Jochum et al. (Jochum *et al.*, 2002b), the number of these predicted a-helices suggests a possible structural similarity between the C domain and the Sec7 domains of GEFs (Cherfils et al., 1998). However, it is unclear whether the C domain is capable of nucleotide exchange since Mon2p does not bind to the the GDP-bound form Arl1p with higher affinity (Jochum *et al.*, 2002b). Moreover, Mon2p is not essential for stabilization of Arl1p on membranes (Panic et al., 2003b). Finally, a 100% conserved Y-D motif was detected in a predicted loop between the last two α-helices (Fig. 2.1A), a region that was previously described as being present in all members of the large Sec7 GEFs (Jackson and Casanova, 2000). Despite this homology, we found that Mon2p differs from the Sec7 GEF family in the following important aspects. First, Mon2p does not possess the typical Sec7 catalytic domain, and second, it contains three extra domains (A, E and F). These three domains are found associated with domain B, C, and D in a subgroup of well conserved proteins present in all eukaryotic kingdoms (Fig. 2.1A).

The identification of six conserved sequence regions suggests that Mon2p and its homologues function in a similar cellular process, and might interact with other highly conserved proteins. The alignments of the A and F domains show a sequence similarity of 42% and 40%, respectively, with a predominance of charged and hydrophobic residues (data not shown). The type of conserved amino acids, the small size, and the predicted secondary structure for these two domains suggest that they could be involved in protein binding activity. The E domain is remotely, if at all, conserved and is not present in all identified homologues.

The C-terminal region containing the F Domain is essential for Mon2p function. To assess the functions of the distinct domains of Mon2p, a series of N- and C-terminal deletions was generated by PCR and fused to a GFP reporter under the control of its own promoter in a 2μ plasmid or a constitutive ADH promoter in a centromeric plasmid (Fig. 2.2A). The different constructs were transformed into the *Δmon2* strain, and the level of protein expression was verified by western blot analysis. As shown in Figure 2.2B, each fusion protein migrates with the expected molecular mass, although the levels of expression are not completely uniform.

We next determined the minimal construct capable of suppressing the growth defect of the *Δmon2* mutant. For this purpose, we used the YFP44 (*mon2Δ/chc1-521*) strain, which does not grow at 30°C. As a positive control,

we first showed that the expression of the entire Mon2[A-F]p-GFP protein restores growth of the YFP44 mutant at 30°C (Fig. 2.2A). Subsequently, we examined the activity of the newly defined conserved A and F domains in the Mon2 protein family. The overproduction of a Mon2p construct lacking the A domain showed a normal growth complementation profile. In contrast, the deletion of only the F domain (*MON2*[A-E]) led to reduced restoration of cell growth (Fig. 2.2A), and larger deletions of the C-terminal part of Mon2p resulted in a complete loss of activity. In agreement with these results, we showed that overexpression of the C-terminal fragment containing only the E and F domains is sufficient to complement the growth defect of YFP44 cells at 25°C (data not shown), and partially at 30°C (Fig. 2.2A).

To confirm the presence of an active domain in the C-terminal region of Mon2p, we next used chlorpromazine (CPZ) as an agent to block the growth of the *mon2Δ* mutant. CPZ is a permeable cationic amphipathic molecule that changes the lateral organization of cellular membranes (Jutila et al., 2001) and interacts with negatively charged lipids (Chen et al., 2003). We previously observed that CPZ modifies internal membrane structures, making Golgi mutants such as *Δvps1* and *Δvps54* highly sensitive to CPZ (unpublished data). By analogy, we reasoned that a CPZ treatment would also be lethal to the *mon2Δ* mutant. As shown in Figure 2.2C, only, *mon2Δ* cells overexpressing Mon2[A-F]p-GFP and Mon2[B-F]p-GFP are resistant to CPZ

(20μM). Cells overexpressing Mon2[A-E]p-GFP remain sensitive, further supporting the conclusion that the F domain is essential for cell growth under membrane stress. Finally, in contrast to the growth complementation study in the YFP44 strain, the Mon2[E-F]p-GFP and Mon2[d-F]p-GFP are not sufficient to completely suppress the CPZ sensitivity and alleviate membrane transport defects, as judged by the presence of fragmented vacuoles (data not shown).

Mon2p localizes to late-Golgi/early endosomal membranes and the N-terminal B and C domains, conserved in the Sec7 GEFs, are sufficient to direct localization. Sequence analyses revealed that the N-terminal part of Mon2p has significant homology to the large Sec7 GEFs (yeast Sec7, BIG1 and BIG2) (Jochum *et al.*, 2002b). BIG1 and BIG2 were originally isolated as parts of large, cytosolic, macromolecular complexes (Morinaga et al., 1997; Togawa et al., 1999). However, these two proteins have been shown to interact with Golgi membranes via their N-termini containing the B and almost the entire C domains (Mansour et al., 1999; Yamaji et al., 2000). This prompted us to re-examine the localization of Mon2p since its previous localization was restricted to endocytic elements (Jochum *et al.*, 2002b). We first analyzed the subcellular localization of Mon2p by equilibrium sedimentation on a sucrose gradient. A whole cell extract from wild-type cells harboring a functional *MON2*-GFP allele was first subjected to differential centrifugation. Then, the enriched Mon2p-GFP high-

speed pellet (P100) was loaded on a sucrose gradient and centrifuged at 100,000 x g for 18 hours. Fractions were collected and analyzed by western blotting. Mon2p-GFP was detected in fractions containing Kex2p and Pep12p, markers of the late-Golgi/early endosome and the late endosomal compartment, respectively (Fig. 2.3A). Second, we examined the cellular localization of Mon2p by fluorescence microscopy in wild type cells. We detected Mon2p-GFP on multiple punctate structures, where it partially colocalized with two specific markers of the late-Golgi: a Sec7p-DsRed chimera and a $PH_{(FAPP1)}$-DsRed fusion that localizes to membranes enriched in phosphotidylinositol 4-phosphate [PI(4)P] (Fig. 2.3B). In contrast, no overlap was observed between Mon2p-GFP and DsRed-FYVE, a phosphotidylinositol 3-phosphate [PI(3)P] probe localizing to late endosomes. Altogether, our results indicate that Mon2p predominantly resides in the late-Golgi.

We next defined the minimal domains required for Mon2p to interact with late-Golgi/early endosomal membranes. Various N-terminal fragments still displayed a punctate pattern (Fig. 2.4A). In fact, our fluorescence experiments indicate that the A and B domains are sufficient to bind membranes, although an increase in the number of dots is observed, revealing perhaps a lower binding specificity (see below). In contrast, Mon2[d-F]p-GFP does not appear to associate with membranes, as judged by entirely cytosolic fluorescence, corroborating the finding that the N-terminus of Mon2p

possesses the specific amino acid sequences that interact with membranes. Interestingly, we observed that N-terminal fragments of Mon2p accumulate in a polarized manner in nascent buds (neck and cortical anchor) (Fig. 2.4A) and possibly colocalize with cytoskeletal elements, suggesting that Mon2p plays a function in polarized membrane transport (see below).

To confirm the identity of the domains that bind to membranes, we determined the Mon2p-GFP fragments that are enriched on membrane fractions separated by density sucrose gradient as performed in figure 2.3A. As expected, the overexpressed Mon2[A-F]p-GFP was detected as a single peak in fractions containing Kex2p and Pep12p (Fig. 2.4B). We subsequently analyzed the distributions of the different GFP fusion constructs on similar sucrose gradients (Fig. 2.4B). We confirmed that the Mon2[A-C]p-GFP fragment constitutes the core that associates with membranes since it is detected in the same fractions as Mon2[A-F]p-GFP. Surprisingly, in contrast to our fluorescence experiments, we failed to detect Mon2[A-B]p-GFP associated with membrane fractions (data not shown). These seemingly contradictory data are likely due to the fact that Mon2p is stabilized on membranes by multiple protein and lipid interactions. Perhaps the short Mon2[A-B]p fragment binds membrane fractions with a lower affinity and is released during the harsh cell lysis procedure. In this context, it is worth noting that the lysis of yeast cells often leads to the solubilization of certain

peripheral membrane proteins such as clathrins. We also showed that the distribution of the GFP-Mon2p protein lacking the A domain (Mon2[B-F]p-GFP) is not affected on gradients, supporting the notion that this domain is not essential for the localization of Mon2p. Taken together, we have demonstrated that Mon2p utilizes conserved domains present in other large Sec7 proteins to bind to late-Golgi/early endosomal membranes.

In addition, we tested whether Arl1p is needed to recruit Mon2p to membranes, since Jochum et al. (Jochum *et al.*, 2002b) previously demonstrated that the N-terminal part of Mon2p is capable of binding to Arl1p. The distribution of Mon2[A-F]p-GFP in a *Δarl1* strain was not affected, since it still cofractionated with endosomal and Golgi membranes (Fig. 2.4B). This result indicates that Arl1p is not needed for interaction of Mon2p with membranes.

The membrane transport of Ape1 to the vacuole is blocked in the *Δmon2* mutant. The localization of Mon2p on the late-Golgi coupled to the fact that Arl1p binds to the GARP complex (Panic et al., 2003b) suggested that Mon2p could function in protein recycling to the Golgi apparatus. Kex2p is a late Golgi endoprotease that functions in the proteolytic maturation of the a-factor mating pheromone (Fuller et al., 1988). The Golgi localization of Kex2p depends on the active retrieval pathways from a post-Golgi compartment (Wilsbach and Payne, 1993). Cells with missorted Kex2p secrete highly

glycosylated precursor a-factor (Payne and Schekman, 1989). Thus, to test whether Mon2p is required for the sorting of Kex2p, we analyzed the forms of the secreted a-factor in a *Δmon2* mutant where the open reading frame was replaced by the *ADE2* marker. No trace of incompletely matured forms of a-factor was detected in the *Δmon2* mutant in a pulse-chase labeling and immunoprecipitation experiment (data not shown). We also showed that the transport of the carboxypeptidase Y (CPY) to the vacuole, which is dependent on the recycling of its sorting receptor, Vps10p, is not affected (Fig. 2.5A).

We next examined the distribution of proteins (Snc1p, Tlg2p, and Chs3p), which are known to cycle through the late-Golgi and early endosome in normal growth conditions at 30°C. We found that all these proteins were properly sorted as judged in vivo by fluorescence microscopy (data not shown). However, at high temperature, where *Δmon2* cells display a severe growth defect, we found different internal distributions of Snc1p and Tlg2p, indicating a drastic membrane trafficking defect (data not shown). These observations support a role of Mon2p in membrane trafficking between the late-Golgi and early endosomes, despite the fact that none of the critical steps in vesicular transport, i.e. budding, docking or fusion, is completely blocked in the *Δmon2* mutant.

Recently, Reggiori et al. (Reggiori *et al.*, 2003) demonstrated that the late-Golgi GARP complex is required for the formation of Cvt vesicles. The

Cvt pathway mediates the constitutive and specific transport of the hydrolases Ape1 and a-mannosidase (Ams1) from the cytoplasm to the vacuole. Precursor forms of Ape1 and Ams1 are first enwrapped by a double membrane, leading to the formation of Cvt vesicles. Subsequently, these vesicles fuse with the vacuole, leading to digestion of the inner membranes and the cleavage of the two precursor proteins to their mature forms. To determine whether Mon2p is involved in this process, we analyzed the processing of prApe1 in the *Δmon2* mutant. Wild-type and *Δmon2* cells were subjected to pulse-chase labeling, and Ape1 was subsequently immunoprecipitated from cells and analyzed by SDS-PAGE and fluorography. We found that the processing of prApe1 is almost completely defective in the *Δmon2* mutant (Fig. 2.5B). This defect is not due to reduced proteolytic activity of the vacuole since the maturation of CPY was not affected under the same conditions. Nevertheless, to visually confirm a transport defect, we next determined the localization of a GFP-prApe1 fusion by fluorescence microscopy. In wild type cells expressing GFP-prApe1, fluorescence accumulates in the vacuole lumen (Fig. 2.5C). In contrast, GFP-prApe1 was observed on a few dots in close proximity to the highly fragmented vacuolar membranes of *Δmon2* cells (Fig. 2.5C). This localization is similar to that observed in mutants blocking either the formation or completion of Cvt vesicles, suggesting that Mon2p function is critical for one of these two events.

When the *Δmon2* strain was treated with rapamycin (to mimic starvation) prior to pulse-chase labeling, normal maturation of prApe1 was observed, indicating that the non-selective autophagy pathway is not affected in the mutant (data not shown).

We next tried to identify the domains that are required for the delivery of prApe1 into the vacuole. The *Δmon2* mutant was transformed with the various truncated forms of *MON2* and the maturation of prApe1 was subsequently analyzed. We found that the F domain must be present in truncations to restore Cvt pathway function to near-wild type levels in the deletion strain. This result suggests that the C-terminal region of Mon2p has a key function in endomembrane transport, which could also be linked to its requirement in cell growth.

The finding that constitutive transport of prApe1 is defective in the *Δmon2* mutant strengthens the idea that Mon2p functions in a similar capacity to the GARP complex and is needed to recycle materials to the late-Golgi. Therefore, we reasoned that mutants blocking membrane traffic through the late Golgi should display a synthetic growth defect when combined with the *Δmon2* null allele. The *Δmon2* mutant was crossed with mutants blocking vesicular trafficking to and from the late-Golgi such as *Δvps1, Δvps26* (retromer component)*, Δvps52, Δvps54* (members of the GARP complex), *Δrcy1*, *Δvps45,* and *Δarf1*. The resulting diploid strains were sporulated and

tetrads were dissected. Synthetic lethality was concluded on the basis of the inability of dissected spores containing both deletions to grow at 30°C. As expected, all the double mutants were synthetic lethal at 30°C or at 33°C for the *mon2Δ/arf1Δ* double mutant (data not shown).

Membrane transport defects at the late-Golgi often lead to a marked distortion of organelles of the late secretory pathway and appearance of aberrant membrane structures such as Berkeley bodies. To investigate endomembrane integrity in the *Δmon2* mutant, we grew cells at 26°C or at 38°C for 30 minutes to accentuate membrane alterations and performed an electron microscopy analysis. As previously observed (Jochum *et al.*, 2002b), *Δmon2* cells contain a large number of fragmented vacuoles (Fig. 2.6). In addition, accumulation of large membrane inclusions and what appear to be lipid droplets are seen throughout the cytoplasm at both temperatures (Fig.2.6B-D, F, H), very similar to what is observed in a *pik1^{ts}* strain (*pik1-83)* at the restrictive temperature (Fig. 2.6E, G). More surprisingly, multinucleated cells were also observed. These findings support a role for Mon2p in the regulation of membrane exchange at the Golgi (and perhaps on endosomes) and may play a role in nuclear segregation during cell division.

Mon2p forms oligomers and associates with very large protein complexes. Our structural protein analysis along with previous studies (Jochum *et al.*, 2002b; Wicky *et al.*, 2004) indicates that Mon2p interacts with

multiple protein partners. This lead us to investigate the nature of protein complexes associated with Mon2p. Cells expressing Mon2p-HA were lysed under native conditions and protein complexes resolved by gel filtration chromatography. Mon2p-HA was detected in two distinct high molecular weight complexes of approximately 550 and 900 kDa (Fig. 2.7A). The large size of these complexes suggests that Mon2p may oligomerize *in vivo*, potentially acting as a scaffold for recruitment of its protein partners. To address this possibility, we first constructed a diploid strain harboring both a Mon2p-myc and a Mon2p-HA chimera. Detergent-solubilized whole cell native extracts from a Mon2p-HA control strain and the doubly tagged diploid were then subjected to centrifugation at 13,000 x g. Proteins were immunoprecipitated from the soluble fractions (S13) using a-HA antibodies. In subsequent western blotting, Mon2p-myc was found to be specifically immunoprecipitated only in the presence of Mon2p-HA (Fig. 2.7B).

Mon2p genetically and physically interacts with Dop1p. To further elucidate the cellular function of Mon2p, we next searched for new partners of Mon2p. To do this, we performed a multicopy suppressor analysis of a *Δmon2* mutant by using a yeast genomic library cloned in a multicopy vector (2m, *LEU2*). The candidate genes capable of suppressing the *Δmon2* growth defect were isolated and subsequently identified by comparing their DNA sequences to that of the yeast genome database. Three distinct genes, *ARL1*, *NEO1* and

DOP1 were able to restore the growth of *mon2Δ/chc1-521* at 30°C (Fig. 2.8). The isolation of Arl1p and Neo1p is consistent with the finding that these two proteins are genetically and biochemically linked to Mon2p (Jochum *et al.*, 2002b; Wicky *et al.*, 2004). The *DOP1* gene is essential for cell growth and is implicated in cell polarity since the overexpression of the N-terminal region of Dop1p in wild-type cells leads to an abnormal budding pattern (Pascon and Miller, 2000).

Based on computer sequence analyses, Dop1p is a large protein of 195 kDa that does not contain any putative transmembrane domain(s). However, Dop1p was detected mostly in the high speed pellet fraction (P100) by differential centrifugation (data not shown), indicating that Dop1p is peripherally associated with light membranes. To substantiate this finding, we tested the conditions required to release Dop1p-HA-mRFP from the P100 membrane pellet into the supernatant. Lysates were subjected to various treatments prior to centrifugation at 100,000 x g for separation into pellet and supernatant fractions. Most of Dop1p-HA-mRFP was solubilized by 1 M NaCl, 0.1 M Na_2CO_3 pH 11, and 2 M urea (Fig. 2.9A). We next determined whether Dop1p resides in close proximity to Mon2p membranes in a double immunofluorescence experiment. The Mon2p-GFP fusion was co-expressed with a Dop1p-HA-mRFP chimera. As shown in Figure 2.9B, Dop1p-HA-mRFP displays a very similar punctate fluorescence to that of Mon2p-GFP. The

merge reveals a partial colocalization of the two proteins, with approximately 50% overlapping signal (n=50). Next, we tested for *in vitro* interaction of Dop1p with Mon2p by coimmunoprecipitation. Detergent-solubilized whole cell native extracts from wild type cells expressing Mon2p-GFP either alone or together with Dop1p-HA-mRFP were processed as previously described in figure 8B. Mon2p-GFP was found to be specifically immunoprecipitated only in the presence of Dop1p-HA-mRFP (Fig. 2.9C). Collectively, these results indicate that Dop1p is a peripheral membrane protein, which binds to Mon2p on Golgi and/or endosomal elements, and that its function(s) might be at least partly linked to Mon2p.

DISCUSSION

In the present study, we show that Mon2p belongs to a new protein family, with nine homologues identified. The presence of six distinct domains suggests that this group of proteins shares similar functions via conserved protein interactions. The B, C and D domains, whose functions have not yet been determined, are present in the large Sec7 GEFs. As already noted by Jochum et al. (2002), the C domain has structural similarity to the catalytic Sec7 domain with a high content of a helices. The remaining A, E and F domains were only detected in this new group of conserved proteins and thus, we propose that they represent the signature of this family.

The N-terminal region of Mon2p is necessary and sufficient to associate with the late-Golgi/endosomal fractions. This membrane association does not require the first 50 amino acid residues representing the A domain, but is dependent on the B and C domains. Our results suggest that the B domain is the key region that interacts with membrane fractions, while the C domain might increase Mon2p's affinity for membranes. Interestingly, the Arl1p binding domains have been shown to reside in the B and C domains (Jochum *et al.*, 2002b), which are conserved in the large Sec7 GEFs. This raises the possibility that Arl1p also binds to the large Sec7 GEFs. Further, we have shown that the activity of Mon2p is dependent on the F domain. The presence of highly conserved hydrophobic and charged residues indicates that the F

domain could interact with a specific protein, which is likely present and conserved in most eukaryotic species. Altogether, we could imagine a model in which Neo1p and Arl1p are required to maintain Mon2p in a specific lipid and protein environment, allowing Mon2p to interact with other cellular components.

Mon2p acts on the late-Golgi and is required for the cytoplasm-to-vacuole transport pathway. Previously, Mon2p was reported to bind Arl1p and Neo1p and to play a role in endocytosis and in vacuolar biogenesis (Jochum *et al.*, 2002b). Here, we extend the role of Mon2p to the late-Golgi compartment. Our data show that Mon2p predominantly colocalizes with late-Golgi markers, which is consistent with the partial localization of Arl1p and Neo1p on late-Golgi structures (Lu et al., 2001; Wicky et al., 2004) and the existence of a genetic link between Mon2p and several late-Golgi proteins. Furthermore, the presence of fragmented vacuoles, as already observed by others, and an accumulation of aberrant membrane structures resembling Berkeley bodies are typical of membrane transport defects due to compromised late-Golgi function.

Recently, Arl1p was proposed to be involved in a retrograde pathway from endosomal compartments to the late-Golgi by interacting with Golgins and the GARP complex (Panic et al., 2003b). Our data show that the transport of prApe1 into the vacuole, which requires the GARP complex, also

depends on the functional C-terminal domains of Mon2p. This finding further supports the conclusion that the F domain is essential for the activity of Mon2p, and that the requirement for the N-terminal late-Golgi binding domains can be bypassed under overexpression conditions (Reggiori et al., 2003). Surprisingly, we were unable to detect a direct interaction between Mon2p and components of the GARP complex (Vps53p and Vps54p; data not shown). This result suggests that Mon2p is not part of the docking/tethering complex implicated in retrograde transport to the late-Golgi. Consistent with this, we only observed a protein trafficking defect between late-Golgi and endosomal compartments in the absence of Mon2p at 37°C, while other type of protein transport from the late-Golgi such the ALP delivery to the vacuole, bypassing the endosomes, is already delayed in the *Δmon2* mutant at 30°C (Bonangelino *et al.*, 2002a). Altogether, our results suggest that Mon2p interacts with multiple partners in regulating late-Golgi homeostasis, and that the protein recycling defect in the *Δmon2* mutant is most likely an indirect consequence of the alteration of Golgi and/or endosomal structures.

Mon2p is linked to cell growth and polarity. Golgins regulate the structure and dynamics of Golgi apparatus by associating membranes with cytoskeletal elements (Barr and Short, 2003). The yeast actin cytoskeleton is organized into morphologically distinct structures, which provide the structural basis for the polarized transport of membranes during cell division (Pruyne

and Bretscher, 2000). Interestingly, actin organization is adversely affected in a *Δmon2* mutant (Singer-Kruger and Ferro-Novick, 1997). In this respect, we found that N-terminal fragments of Mon2p accumulate at the polarized sites of nascent bud and a synthetic lethality between *Δmon2* and the *Δarc18* mutant (data not shown). Arc18p is a subunit of Arp2/3 complex, which initiates the nucleation of actin filaments in cortical patches (Winter et al., 1999). In agreement with a putative function of Mon2p in polarized growth, we found that the highest conserved Mon2p homolog is a protein encoded by *A. gossypii* YNL297C (40% identity). *A. gossypii* is a filamentous fungus that grows by hyphal extension, which represents an extreme example of polarized growth. Even more interestingly, we found that Mon2p genetically and physically interacts with Dop1p. Dop1p is an essential protein that shares conserved functions in cell polarity with DopA, its *A. nidulans* homolog (Pascon and Miller, 2000). DopA also plays a role in directed nuclear movement in *A. nidulans* cells (Pascon and Miller, 2000). Similarly, we often observed appearance of multinucleated cells in the *Δmon2* mutant, which could imply a function for Mon2p in nuclear dynamics during cell division.

In summary, we have identified a new group of conserved proteins, which likely share similar functions in the coordination of membrane trafficking between the late-Golgi and early endosomes, as well as in polarized growth.

Table 2.1 *S. cerevisiae* strains used in this study

Strain	Genotype	Reference or Source
SEY6210	*MATα leu-3,112 ura3-52 his3-D200 trp1-D901 lys2-801 suc2-D9*	Lab strain
AAY1120	SEY6210; *mon2Δ::HIS3MX6*	This study
AAY104	SEY6210; *pik1D::HIS3* carrying pRS314 *pik1-83* (*TRP1 CEN6 pik1-83)*	Audhya *et al.* 2000
JEY001	SEY6210; *MON2-3xHA::HIS3MX6*	This study
JEY002	SEY6210; *MON2-13xMYC::HIS3MX6*	This study
JEY003	SEY6210; *MON2-GFP::HIS3MX6*	This study
JEY026	*MAT***a**/α *MON2-3xHA::HIS3MX6/MON2-13xMYC::HIS3MX6 leu-3,112/leu-3,112 ura3-52/ura3-52 his3-D200/his3-D200 trp1-D901/trp1-D901 lys2-801/lys2-801 suc2-D9/suc2-D9*	This study
JEY069	JEY003; *DOP1-3xHA-mRFP::LEU2*	This study
W303	*MAT***a**/α *ade2-1/ade2-1 ura3-1/ura3-1 his3-11,15/his3-11,15*	Lab strain
YFP93	W303 ; *MATα mon2Δ::ADE2*	This study
YFP94	W303 ; *MAT***a** *mon2Δ::ADE2*	This study
CDK17-6B	W303 ; *MAT***a** *vps54Δ::LEU2*	Lab strain
YFP71	*MAT***a** *vps1Δ::LEU2 ade2 ura3 his3 leu2 trp1*	Lab strain
YFP35	*MAT***a** *chc1-521^{ts} TPI::SUC2::HIS3 pep4::TRP1*	Lab strain
RSY906	*MATα arf1Δ ::HIS3 ura3-52 his3Δ200 leu2-3,112*	Sheckman lab
ODY318	*MAT***a** *arl1::kanMX4 his3Δ leu2Δ ura3Δ*	EUROSCARF
YFP72	*MAT***a**/α *mon2Δ::ADE2/MON2 vps1Δ::LEU2/VPS1*	(YFP93xYFP71)
YFP155	*MAT***a**/α *mon2Δ::ADE2/MON2 vps54Δ::LEU2/VPS54*	(YFP93xCDK17-6B)
YFP38	*MAT***a**/α *mon2Δ::ADE2/MON2 chc1-521^{ts}/CHC1*	(YFP93xYFP35)
YFP103	*MAT***a**/α *mon2Δ::ADE2/MON2 arf1 ::HIS3/ARF1*	(YFP94xRSY906)
YFP101	*MAT***a** *mon2Δ::ADE2 vps1Δ::LEU2 ade2 ura3 his3 leu2 trp1* [YEplac195-*MON2*]	YFP72-E4
YFP156	*MAT***a** *mon2Δ::ADE2 vps54Δ::LEU2* [YEplac195-*MON2*]	YFP155-C4
YFP44	*MAT***a** *mon2Δ::ADE2 chc1-521^{ts} pep4::TRP1 ade2-1 ura3 his3 leu2 trp1* [YEplac195-*MON2*]	YFP38-K2
CDK13-1A	W303 ; *MATα tif3Δ::TRP1 mon2Δ::ADE2* [pSEY18-*TIF3*]	Lab strain
YFP86	W303 ; *MAT***a** *tif3Δ::TRP1 vps54* [pSEY18-*TIF3*]	Lab strain

For simplicity the genotypes of crossing strains are not indicated.

Table 2.2 Plasmids used in this study

Plasmid	Description	Source
pDK7	pRS413-*MON2*; isolated from genomic library; *(CEN, HIS3)*	Lab plasmid
pDK36	YEplac195-*MON2*; 5.89 kb *Sal*I/*Spe*I fragment from pDK7; (2*μ*, *URA3)*	This study
PFP22	pHAC181-*MON2*-HA (2*μ*, *LEU2*)	This study
pFP45	YEplac181-*MON2*[1-4911]-GFP; (2*μ*, *LEU2*)	This study
pOD123	YEplac181-*MON2*[1-4500]-GFP; (2*μ*, *LEU2*)	This study
pFP46	YEplac181-*MON2*[1-1800]-GFP; (2*μ*, *LEU2*)	This study
pOD124	YEplac181-*MON2*[1-1230]-GFP; (2*μ*, *LEU2*)	This study
pOD125	YEplac181-*MON2*[1-651]-GFP; (2*μ*, *LEU2*)	This study
pFP46	YEplac181-*MON2*[1-180]-GFP; (2*μ*, *LEU2*)	This study
pOD126	pRS415-ADH-GFP-*MON2*[151-4911]; (*CEN, LEU2*)	This study
pOD122	pRS415-ADH-GFP-*MON2*[2388-4911]; (*CEN, LEU2*)	This study
pOD127	pRS415-ADH-GFP-*MON2*[3443-4911]; (*CEN, LEU2*)	This study
pFP36	pRS316-*KEX2*-HA; (*CEN*, *URA3*)	Deloche *et al*., 2001
pDK15	pRS413-*DOP1*; isolated from genomic library (*CEN*, *HIS3*)	This study
pDK64	YEplac181-*DOP1*; 8.3 kb *Sal*I/*Sac*I fragment of *DOP*; (2*μ*, *LEU2*)	This study
pDK62	pRS423-*DOP1*; 8.3 kb *Sal*I/*Sac*I fragment of *DOP*; (2*μ*, *HIS3*)	This study
pN5	YEp13-*ARL1*; isolated from genomic library (2*μ*, *LEU2*)	This study
pRB95	YEplac181-*ARL1*; 1.25 kb *Sac*I/*Bam*HI fragment from pN5; (2*μ*, *LEU2*)	R. Boeck
pRB108	YEplac112-*ARL1*; 1.25 kb *Sac*I/*Bam*HI fragment from pN5; (2*μ*, *TRP1*)	R. Boeck
pA32	YEp13-*NEO1*; isolated from genomic library; (2*μ*, LEU2)	This study
pRB111	YEplac181-*NEO1*; *Spe*I(Klenow blunt)/*Xba*I fragment from pA32; (2*μ*, *LEU2*)	R. Boeck
pRB113	YEplac112-*NEO1*; *Spe*I(Klenow blunt)/*Xba*I fragment from pA32; (2*μ*, *TRP1)*	R. Boeck
pGFP-Ape1	pRS414-GFP-*APE1* (*CEN, TRP1*)	Shintani *et al.,* 2002
pCS198	pRS426-$PH_{(FAPP1)}$-DsRed *(CEN, URA3)*	C. Stefan, unpublished
pCS212	pRS425-DsRed-$FYVE_{(EEA1)}$ (*CEN, LEU2)*	Stefan *et al.,* 2002
pRC2240	pRS316-*SEC7*-T4DsRed (*CEN, URA3)*	Calero *et al.,* 2003

Figure 2.1 Identification of a Mon2p protein family. (A) Representation of 6 conserved domains (A to F) present in Mon2p and in nine other uncharacterized proteins. Blue boxes are domains with significant levels of sequence similarity, which were only detected in Mon2p and the identified proteins. Green boxes represent domains that are also present in all members of the large Sec7 protein family. The dark-green bar is a Y-D motif detected in the conserved region described by (Jackson and Casanova, 2000). The percent (%) similarity of each domain is indicated. (B) Representation of Sec7p (*S. cerevisiae*) and BIG1 (*H. sapiens*), two members of the large Sec7 protein family, with their Sec7 catalytic domain represented by orange boxes. Recently, B. Mouratou et al. (Mouratou *et al.*, 2005) have redefined the domain architecture of the Sec7/BIG1 protein family, and this alternative configuration is depicted below the dashed line for comparison. The first two conserved DCB (dimerization/Cyclophilin Binding) and HUS (Homology Upstream of Sec7) domains correspond to our B and C domains respectively, while the three HDS1, HDS2 and HDS3 (Homology Downstream of Sec7) regions overlap with our D domain. All protein sequences were taken from the Swiss-Prot/EMBL databases. *S.c., Saccharomyces cerevisiae; H.s., Homo sapiens; M.m., Mus musculus; N.c., Neurospora crassa; As.g., Ashbya gossypii; S.p., Schizosaccharomyces pombe; C.e., Caenorhabditis elegans; An.g., Anopheles gambiae; D.m., Drosophila melanogaster; O.s., Oryza sativa*.

A

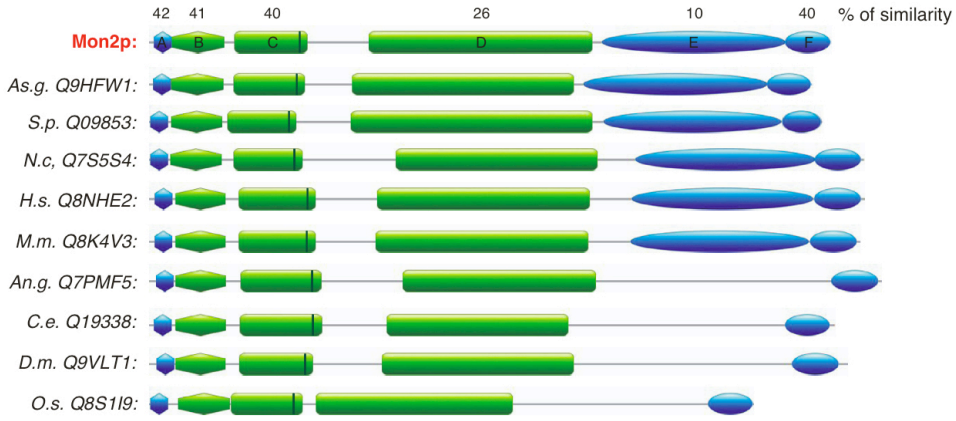
42
41
40
26
10
40
% of similarity
Mon2p:
A
B
C
D
E
F
As.g. Q9HFW1:
S.p. Q09853:
N.c, Q7S5S4:
H.s. Q8NHE2:
M.m. Q8K4V3:
An.g. Q7PMF5:
C.e. Q19338:
D.m. Q9VLT1:
O.s. Q8S1I9:

B

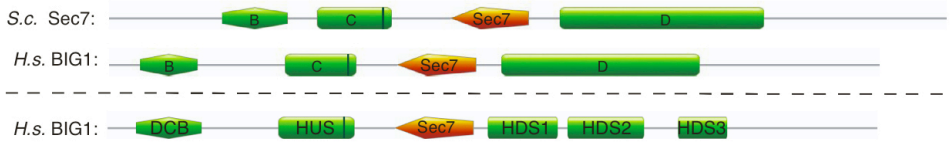
S.c. Sec7:
B
C
Sec7
D
H.s. BIG1:
B
C
Sec7
D
H.s. BIG1:
DCB
HUS
Sec7
HDS1
HDS2
HDS3

Figure 2.2 The C-terminal region of Mon2p is essential for cell growth under membrane stress. (A) Schematic representation of the Mon2p-GFP fusion with its six conserved domains (A to F) and various truncated Mon2p-GFP derivatives: Mon2[A-F]p /(pFP45), Mon2[A-E]p /(pOD123), Mon2[A-d]p /(pFP46), Mon2[A-C]p /(pOD124), Mon2[A-B]p /(pOD125), Mon2[A]p /(pFP46), Mon2[B-F]p /(pOD126), Mon2[d-F]p /(pOD122) and Mon2[E-F]p /(pOD127). The D domain is denoted with a lowercase ("d") when it is not entirely expressed. Growth complementation of the different Mon2p-GFP derivatives were tested in YFP44 (*Δmon2/chc1-521*) cells at 30°C and indicated as followed: +++, growth identical to wild type cells; ++ and +, growth is slightly and strongly reduced, respectively; - no growth. (B) Western blotting. Whole cell extracts of YFP93 (*Δmon2*) cells transformed with constructs encoding GFP-tagged truncations were resolved by SDS-PAGE. The expressed protein fragments were detected by GFP antibody; (1) represents a released GFP fragment; (2) presence of a doublet. (C) YFP93 (*Δmon2*) cells expressing the Mon2p-GFP derivatives containing the indicated domains were grown on SD-LEU plates containing 0 or 20 μM CPZ for 36 hours at 25°C.

A

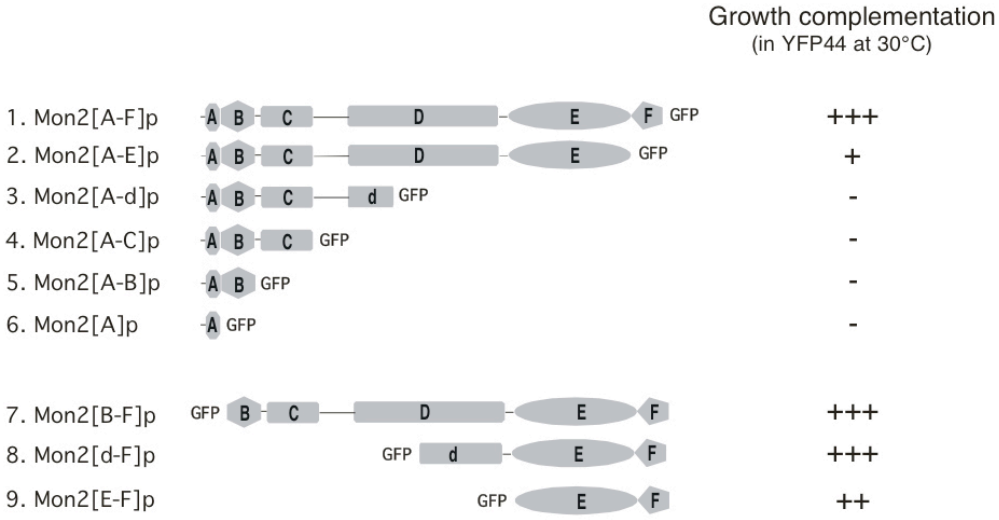
Growth complementation
(in YFP44 at 30°C)
1. Mon2[A-F]p
2. Mon2[A-E]p
3. Mon2[A-d]p
4. Mon2[A-C]p
5. Mon2[A-B]p
6. Mon2[A]p
7. Mon2[B-F]p
8. Mon2[d-F]p
9. Mon2[E-F]p
GFP
+++
+
-
-
-
-
+++
+++
++

B

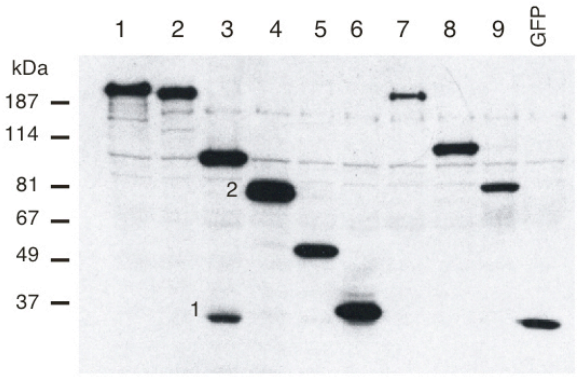
1 2 3 4 5 6 7 8 9 GFP
kDa
187
114
81
67
49
37
1
2

C

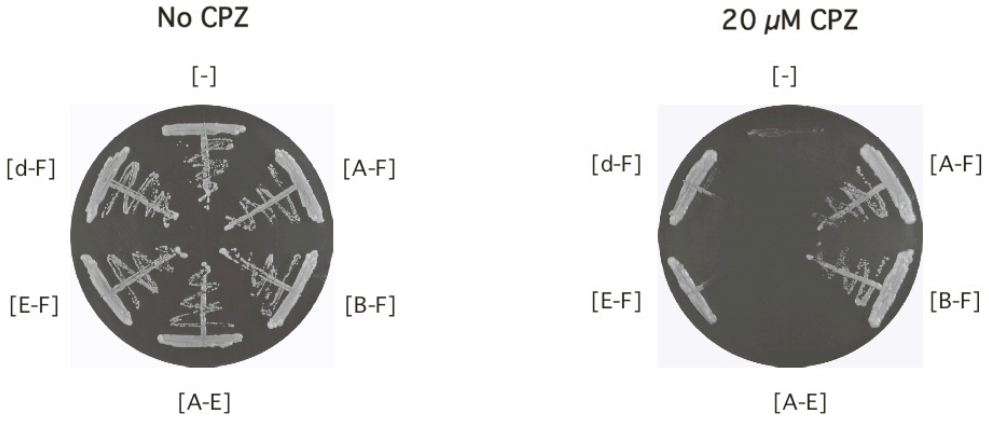
No CPZ
20 μM CPZ
[-]
[d-F]
[A-F]
[E-F]
[B-F]
[A-E]

Figure 2.3. Mon2p is associated with the late-Golgi and early endosomes. (A) Mon2p-GFP colocalizes with Kex2p-HA and Pep12p on a sucrose density gradient. JEY003 (*MON2*-GFP) cells harboring pRS316-*KEX2*-HA were grown to mid-logarithmic phase at 30°C and subsequently lysed. The P100 fraction was prepared and subjected to equilibrium sedimentation through a sucrose gradient. Fractions were collected from the top, subjected to SDS-PAGE and analyzed by Western blotting using anti-GFP, anti-HA, anti-Mnn1p and anti-Pep12p antibodies. (B) Mon2p-GFP partially colocalizes with late-Golgi markers (Sec7p-DsRed and PH_{FAPP1}-DsRed), but shows no overlap with a late endosomal marker (DsRed-$FYVE_{EEA1}$). Strains chromosomally expressing Mon2p-GFP and harboring the indicated fusion construct on a plasmid were grown to mid-logarithmic phase and observed by fluorescence microscopy as described in materials and methods. Images are representative of >100 cells observed.

A

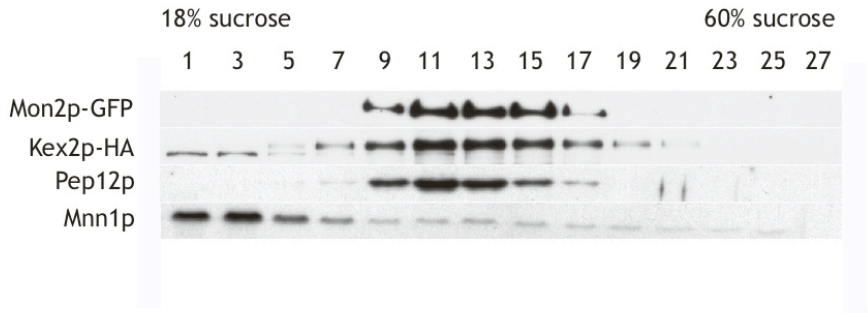
18% sucrose
60% sucrose
1 3 5 7 9 11 13 15 17 19 21 23 25 27
Mon2p-GFP
Kex2p-HA
Pep12p
Mnn1p

B

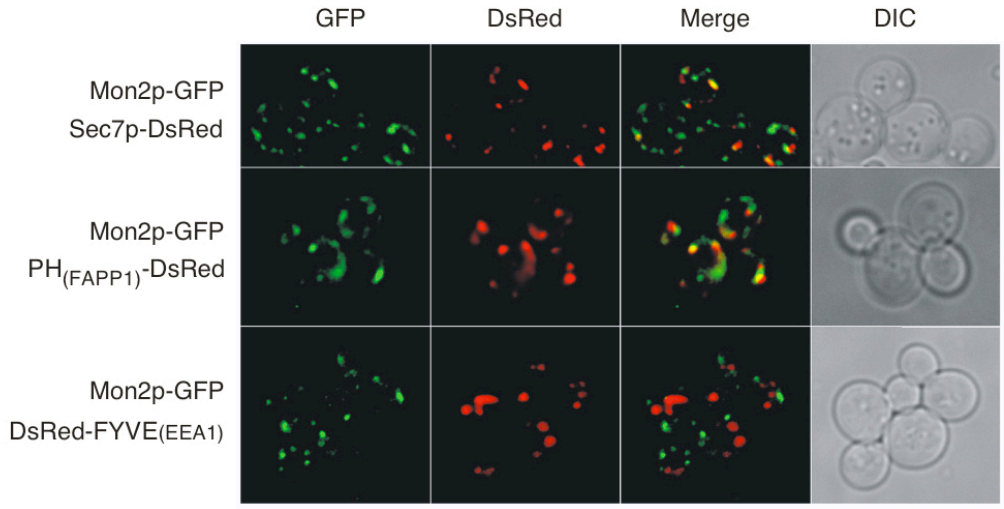
GFP
DsRed
Merge
DIC
Mon2p-GFP
Sec7p-DsRed
Mon2p-GFP
PH(FAPP1)-DsRed
Mon2p-GFP
DsRed-FYVE(EEA1)

Figure 2.4 The N-terminal region binds to the late-Golgi/endosomal membranes. (A) YFP93 *(Δmon2*) cells expressing Mon2[A-F]p-GFP /(pFP45), Mon2[A-E]p-GFP /(pOD123), Mon2[A-B]p-GFP /(pOD125), Mon2[A]p-GFP /(pFP46), Mon2[d-F]p-GFP /(pOD122), Mon2[A-C]p /(pOD124), and Mon2[A-d]p /(pFP46) were grown to mid-logarithmic phase at 30°C and processed for fluorescence microscopy. *MON2*[A-d] was subcloned into a centromeric (CEN) plasmid (pOD130) to reduce protein expression level and the fluorescence was detected with a confocal microscope (Nipkow). The observed localization pattern is indicated below each image. (B) For sucrose density gradients, YFP93 cells transformed with pRS316*KEX2*-HA and pFP45; YFP93 cells transformed with pOD123, pOD124, pOD126 or pOD127; and ODY318 (*arl1::kanMX4*) cells containing pFP45 were grown to mid-logarithmic phase at 30°C and subjected to equilibrium sedimentation through a sucrose gradient. Fractions were collected from the top and analyzed by western blotting using anti-HA, anti-Pep12p and anti-GFP antibodies. The first 3 proteins, indicated by a vertical bar, were detected from the same sucrose gradient.

A

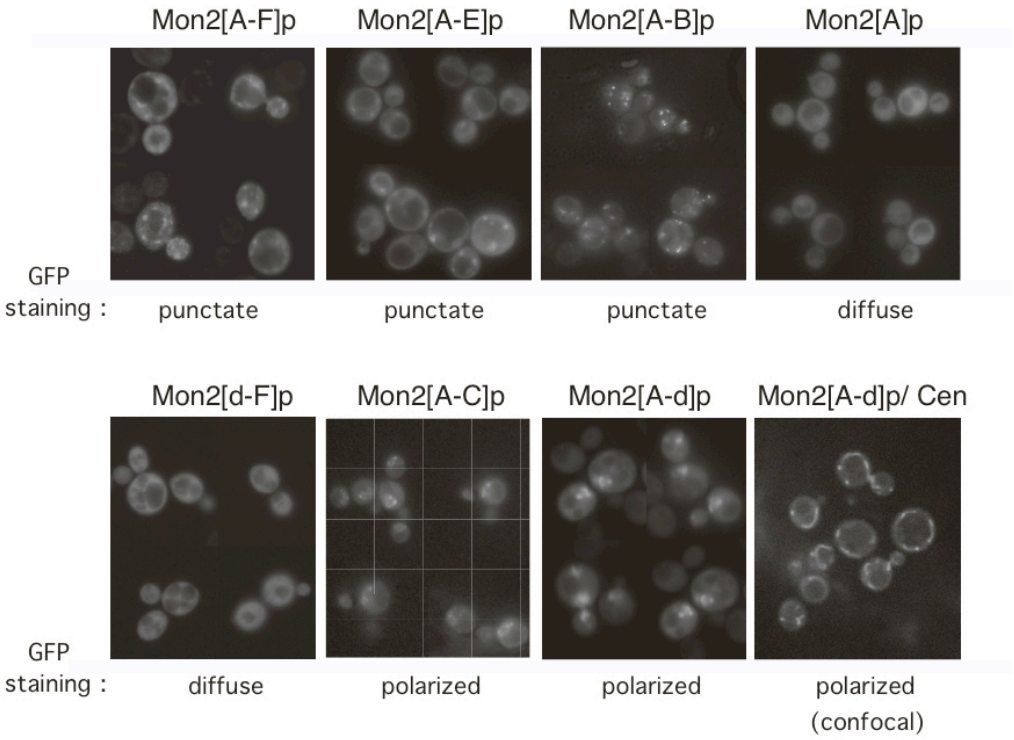
Mon2[A-F]p
Mon2[A-E]p
Mon2[A-B]p
Mon2[A]p
GFP staining :
punctate
punctate
punctate
diffuse
Mon2[d-F]p
Mon2[A-C]p
Mon2[A-d]p
Mon2[A-d]p/ Cen
GFP staining :
diffuse
polarized
polarized
polarized (confocal)

B

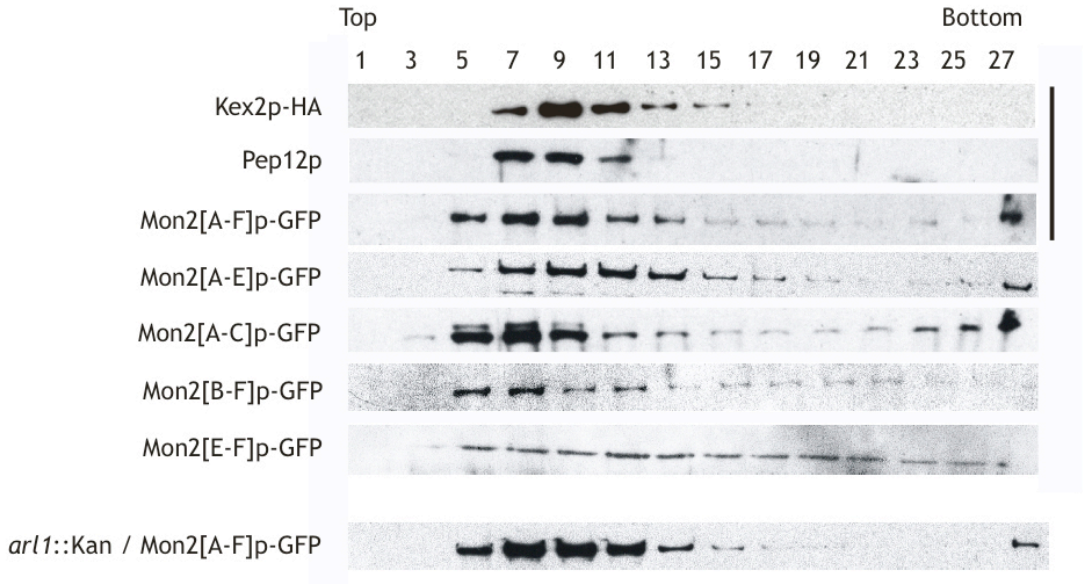
Top
Bottom
1 3 5 7 9 11 13 15 17 19 21 23 25 27
Kex2p-HA
Pep12p
Mon2[A-F]p-GFP
Mon2[A-E]p-GFP
Mon2[A-C]p-GFP
Mon2[B-F]p-GFP
Mon2[E-F]p-GFP
arl1::Kan / Mon2[A-F]p-GFP

Figure 2.5 The transport of prApe1 to the vacuole is blocked in the *Δmon2* mutant. (A) YFP95 (wild-type) and YFP93 (*mon2Δ*) were metabolically (^{35}S) labeled at 30°C for 10 min and chased for the indicated times. The ER, Golgi and mature forms of CPY are labeled p1, p2 and m, respectively. (B) SEY6210 (wild-type) and AAY1120 (*Dmon2*) cells were metabolically (^{35}S) labeled at 26°C for 20 min and chased for the indicated times. CPY and Ape1 were immunoprecipitated from extracts, and analyzed by SDS-PAGE and autoradiography. (C) Subcellular localization of GFP-prApe1. SEY6210 and AAY1120 cells expressing GFP-prApe1were grown at 26°C to mid-logarithmic phase and labelled with FM4-64 to visualize vacuoles. Analysis was done by fluorescence microscopy, and images shown are representative of >100 cells observed.

A

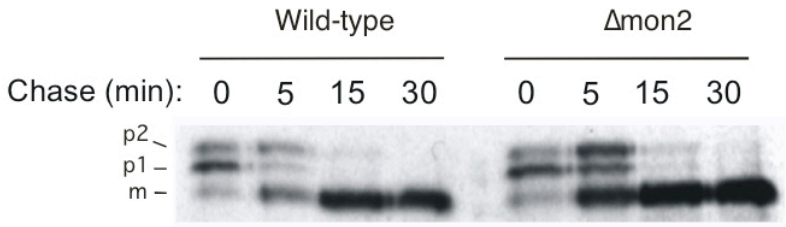
Wild-type
Δmon2
Chase (min): 0 5 15 30 0 5 15 30
p2
p1
m

B

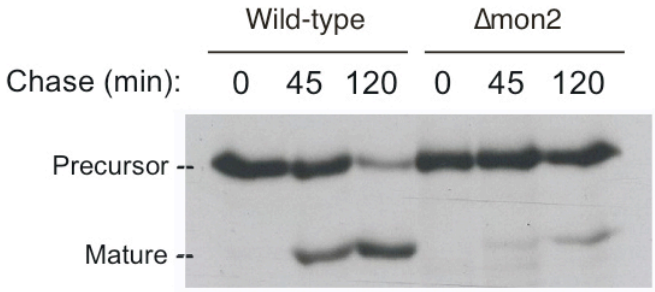
Wild-type
Δmon2
Chase (min): 0 45 120 0 45 120
Precursor
Mature

C

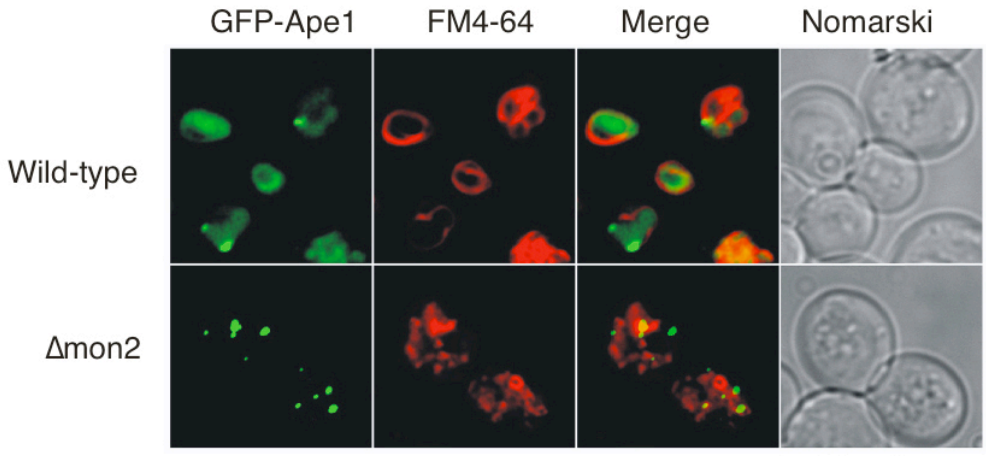
GFP-Ape1
FM4-64
Merge
Nomarski
Wild-type
Δmon2

Figure 2.6 EM analysis of subcellular structure. SEY6210 (wild-type) (A), AAY1120 (*Dmon2*) cells grown at 26°C (B, C, D) and shifted 38°C for two hours (F, H), and AAY104 (pik1^{ts}) cells pre-shifted to the restrictive temperature for one hour (E, G) were processed for and visualized by EM as described in materials and methods. Black arrows point to enlarged aberrant membrane structures shown in the panels on the right. Vacuoles (v), nuclei (n), and mitochondria (m) are also indicated. Cells shown are representative of >90% of the population (except for multinucleation, which was observed in approx. 15% of *Dmon2* cells). Bars, 0.5 mm.

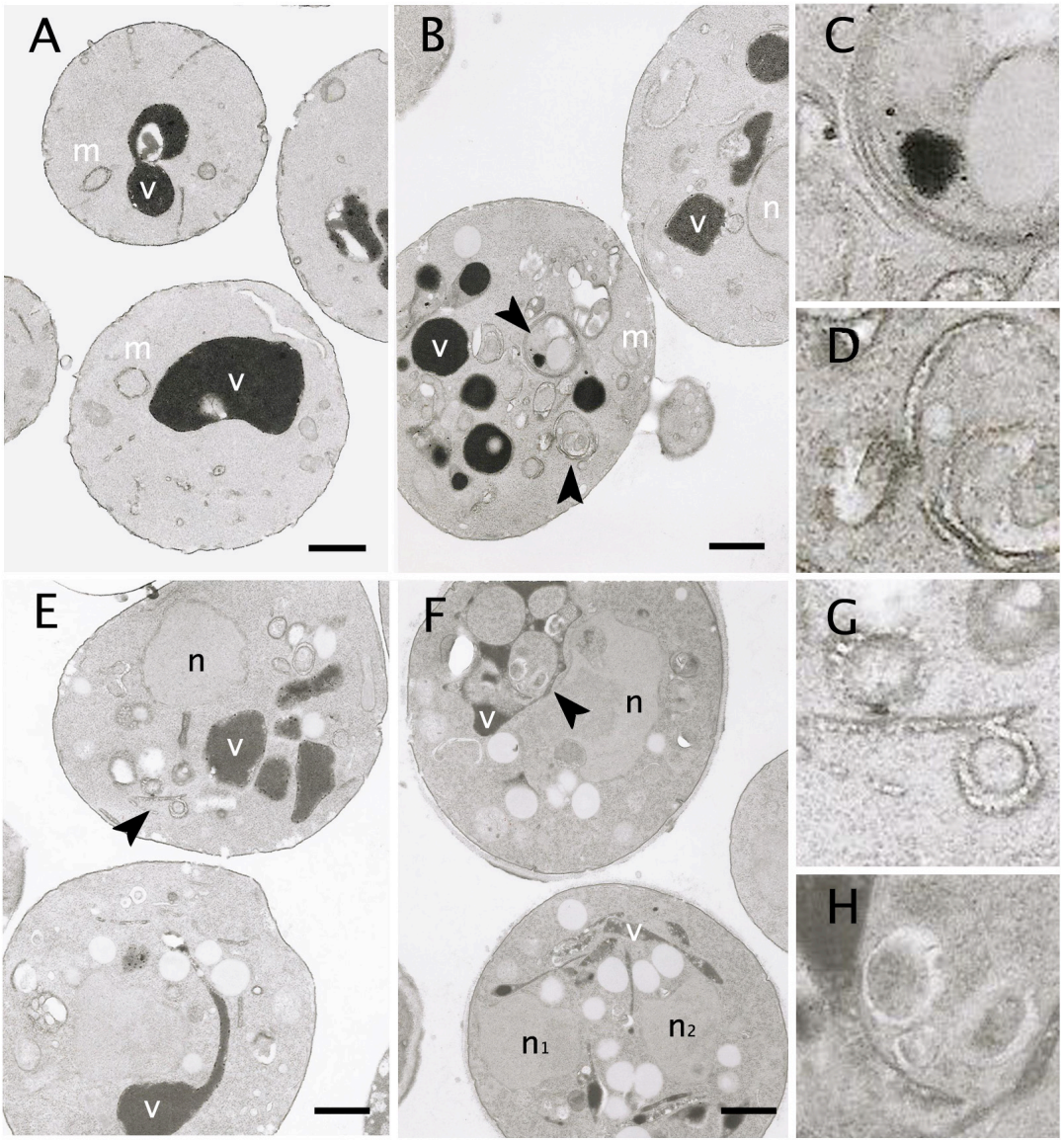
A
m
v
m
v
B
v
n
v
m
C
D
E
n
v
v
F
v
n
v
n1
n2
G
H

Figure 2.7 Mon2p associates with large protein complexes and forms oligomers. (A) Native lysate from JEY001 cells (Mon2p-HA; approx. 100 OD_{600} units) was cleared by ultracentrifugation at 100,000 x g for one hour and subjected to gel filtration chromatography. Fractions were analyzed by SDS-PAGE and western blotting using a monoclonal a-HA antibody. All fractions containing Mon2p-HA are shown and approximate complex size (based on a prior run of sizing standards) is indicated. (B) Mon2p-Myc co-immunoprecipitates with Mon2p-HA. Detergent-solubilized native lysates from cells (50 OD_{600} units) expressing Mon2p-myc alone (JEY003) or with Mon2p-HA (JEY026) were cleared at 16,000 x g and subjected to immunoprecipitation using a-HA antibody. Purified proteins were subjected to SDS-PAGE and western blotting analysis with a-myc and a-HA antibodies

.

A

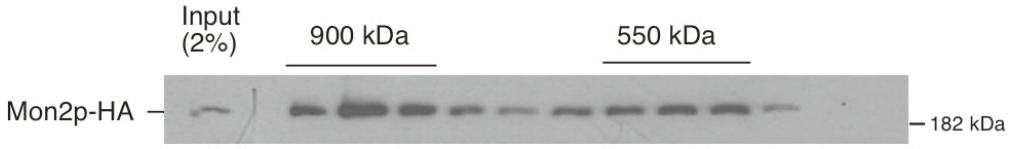
Input
(2%)
900 kDa
550 kDa
Mon2p-HA
182 kDa

B

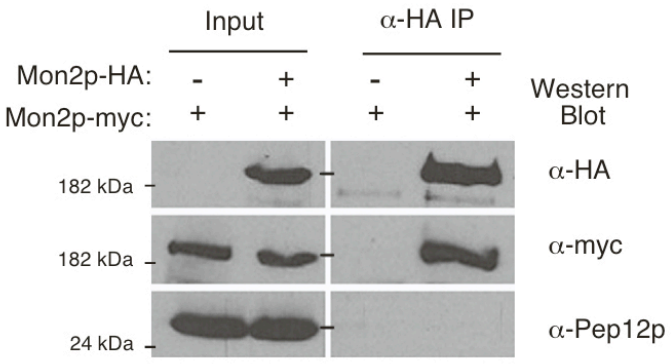
Input
α-HA IP
Mon2p-HA: - + - +
Mon2p-myc: + + + +
Western
Blot
182 kDa
α-HA
182 kDa
α-myc
24 kDa
α-Pep12p

Figure 2.8 Isolation of *ARL1, NEO1 and DOP1* as multicopy suppressors of the *Δmon2* mutant. The *ARL1, NEO1 and DOP1* were isolated in CDK13-1A (*Δmon2/Δtif3*) double mutant as described in materials and methods. The complementation of the *Δmon2* mutant was subsequently tested in YFP44 (*Δmon2/chc1-521*^{ts}) double mutant. YFP44 cells were transformed with plasmids (2*μ*, and the appropriate auxotrophic markers) alone or plasmids containing *MON2* (pFP45), *DOP1* (pDK64), *NEO1* (pRB111) or *ARL1* (pRB95). The resulting transformants were then tested for growth at 30°C on 5-FOA-containing plates as indicated. As controls no growth complementation was observed in YFP86 (*Δtif3/vps54*) double mutant (data not shown).

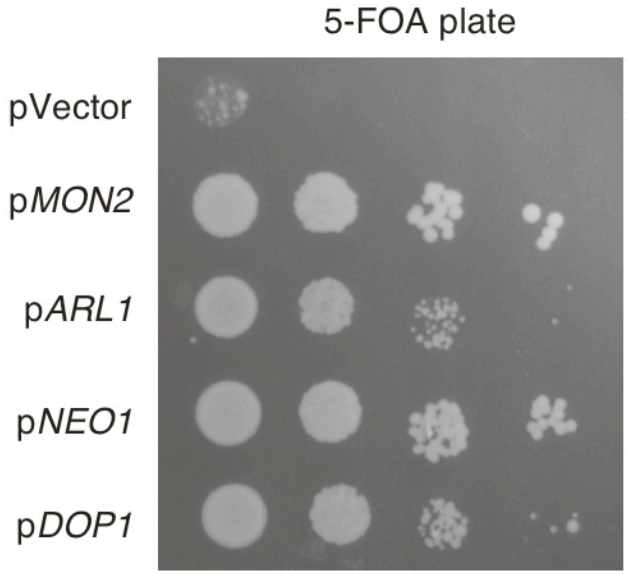
5-FOA plate
pVector
p*MON2*
p*ARL1*
p*NEO1*
p*DOP1*

Figure 2.9 Mon2p associates with the peripheral membrane protein Dop1p. (A) Dop1p-HA-mRFP is peripherally associated with membranes. JEY069 (*MON2-GFP DOP1-HA-mRFP*) cells (20 OD_{600} units) were osmotically lysed and centrifuged at 13,000 x g. The supernatant (S13) fraction was differentially treated as indicated, and further separated by ultracentrifugation at 100,000 x g. The resulting high-speed pellet (P) and supernatant (S) fractions were analyzed for relative Dop1p-HA-mRFP content by western blotting. (B) Mon2p colocalizes with Dop1p. JEY069 cells were grown to mid-logarithmic phase at 26°C, shifted to 4°C for 10 minutes to minimize rapid movement of Golgi and endosomal elements, and observed by fluorescence microscopy. (C) Mon2p-GFP co-immunoprecipitates with Dop1p-HA-mRFP. Detergent-solubilized native lysates (50 OD_{600} units) from JEY003 (*MON2-GFP*) and JEY069 were cleared at 16,000 x g and subjected to immunoprecipitation using a-HA antibody. Purified proteins were subjected to SDS-PAGE and western blotting analysis with a-GFP and a-HA antibodies. (*) indicates a possible breakdown product of Dop1p-HA-mRFP.

A

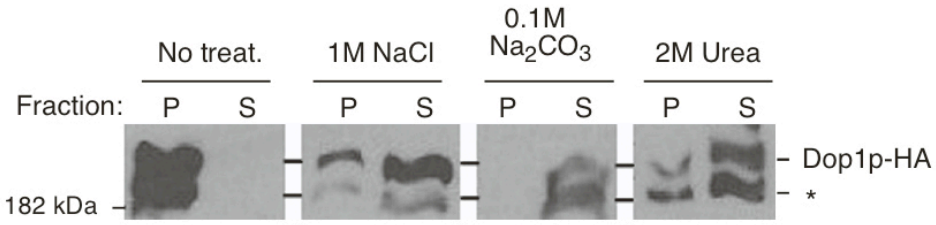
No treat.
1M NaCl
0.1M Na_2CO_3
2M Urea
Fraction:
P S P S P S P S
182 kDa
Dop1p-HA
*

B

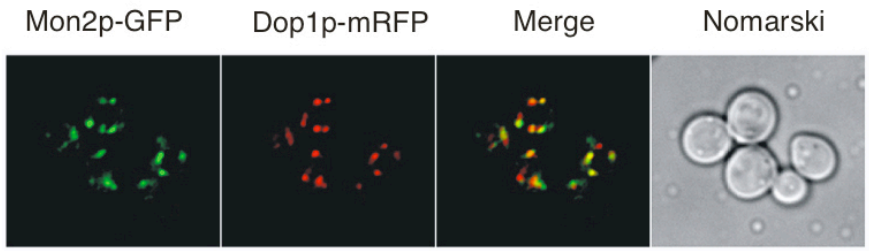
Mon2p-GFP
Dop1p-mRFP
Merge
Nomarski

C

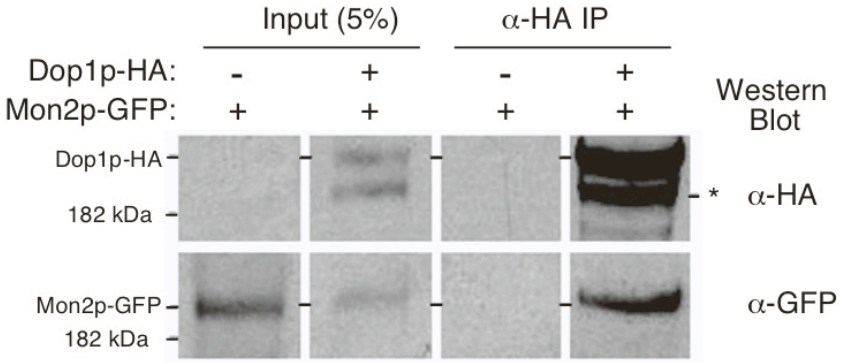
Input (5%)
α-HA IP
Dop1p-HA: - + - +
Mon2p-GFP: + + + +
Western Blot
Dop1p-HA
182 kDa
*
α-HA
Mon2p-GFP
182 kDa
α-GFP

ACKNOWLEDGEMENTS

We are extremely grateful for continuous support from Costa Georgopoulos and Patrick Linder. We thank R. Boeck, I. Iost, M.-C. Daugeron, H. Pelham and K. Nasmyth for providing plasmids and libraries. We also thank Drs. Anjon Audhya, William Parrish, Christopher Stefan, and Simon Rudge for key reagents and helpful discussions, Ingrid Niesman for EM processing (Immunoelectron Microscopy Core B of Program Project grant CA58689 headed by M. Farquhar), and Alexander Rusnak for technical assistance. This work was supported by grants from the Swiss National Science Foundation and the Canton of Geneva to C. Georgopoulos (FN-31-65403) and P. Linder (FN-31-43321) and NIH training grant #5T32CA67754-08 (to J.A.E). S.D.E is an investigator of the Howard Hughes Medical Institute.

This chapter, in full, is a reprint of the material as it appears in *Journal of Cell Science* 118(20):4751-64, 2005. Efe, J.A., Plattner, F., Hulo, N., Kressler, D., Emr, S.D., and O. Deloche. Yeast Mon2p is a highly conserved protein that functions in the cytoplasm-to-vacuole transport pathway and is required for Golgi homeostasis. The dissertation author was the primary investigator and author of this paper.

CHAPTER 3

PATHOGEN EFFECTOR PROTEIN SCREENING IN YEAST IDENTIFIES LEGIONELLA FACTORS THAT INTERFERE WITH MEMBRANE TRAFFICKING

ABSTRACT

L. pneumophila invades and replicates intracellularly in human and protozoan hosts. The bacteria use the Icm/Dot Type IVB secretion system to translocate effectors that inhibit phagosome maturation and modulate host vesicle trafficking pathways. To understand how *L. pneumophila* modulates organelle trafficking in host cells, we carried out a novel Pathogen Effector Protein Screening in Yeast (PEPSY), identifying *L. pneumophila* genes that produced membrane trafficking (vps) defects in yeast. We identified four *L. pneumophila* DNA fragments that perturb sorting of vacuolar proteins. Three encode ORFs of unknown function that are translocated via the Icm/Dot transporter from Legionella into macrophages. VipA (VPS Inhibitor Protein) is a novel coiled-coil protein, VipD is a patatin domain-containing protein and VipF contains an acetyltransferase domain. Processing studies in yeast indicate that VipA, VipD and VipF inhibit lysosomal protein trafficking by

different mechanisms; overexpressing VipA only has an effect on carboxypeptidase Y (CPY) trafficking, while VipD interferes with multivesicular body (MVB) formation at the late endosome and ER-to-Golgi transport. Such differences highlight the multiple strategies *L. pneumophila* effectors employ to subvert host trafficking processes. Using yeast as an effector gene discovery tool allows for a powerful, genetic approach to both identify novel virulence factors and study their function.

INTRODUCTION

Legionella pneumophila is a gram-negative facultative intracellular pathogen of protozoa and human alveolar macrophages. Human infection results in a severe pneumonia known as Legionnaires' disease. *L. pneumophila* alters host cell trafficking pathways in both types of host cells. The bacteria reside in a vacuole that does not fuse with lysosomes or acidify but recruits ER-derived vesicles (Horwitz and Silverstein, 1983; Horwitz and Maxfield, 1984; Cianciotto, 2001; Kagan and Roy, 2002). These properties require a Type IVB Secretion System (TFBSS) known as the Icm/Dot system (Segal *et al.*, 1998; Vogel *et al.*, 1998). The essential nature of the TFBSS predicts that Icm/Dot translocated effectors modulate host organelle trafficking by interacting with host components to inhibit phagolysosome formation and promote establishment of a permissive, replicative vacuole. Several Icm/Dot substrates have been identified: LidA, RalF, LepA, LepB, SdeB, SdeC, SdhB, SidA-H (Nagai *et al.*, 2002; Conover *et al.*, 2003; Chen *et al.*, 2004; Luo and Isberg, 2004). Among these, only RalF has been shown to directly perturb vesicle trafficking by inhibiting acquisition of the ARF1 GTPase to the *Legionella* vacuole. The LepA and LepB proteins are involved in release of Legionella from protozoa by an unknown mechanism. Mutants in all the above effectors have no discernable defects in inhibition of phagolysosome maturation or intracellular growth. This suggests the presence of additional

effectors that interact with host trafficking factor(s) and contribute to modulation of host organelle traffic.

To identify novel effectors that alter eukaryotic trafficking pathways we took advantage of a well-characterized system in budding yeast used to study organelle trafficking pathways. In *Saccharomyces cerevisiae*, vacuole protein sorting pathway components (VPS proteins) control several distinct vesicle trafficking pathways (Bankaitis *et al.*, 1986b; Robinson *et al.*, 1988a; Bryant and Stevens, 1998b). Moreover, numerous mammalian VPS orthologs play similar roles in endosomal trafficking pathways. Examples include hVPS34, a human phosphatidylinositol 3-kinase involved in endosomal transport events including phagosome maturation (Siddhanta *et al.*, 1998; Fratti *et al.*, 2001); Tsg101, a human homolog of Vps23p (Babst *et al.*, 2000); SKD1 and mVps18p, mouse homologs of Vps4p and Vps18p, respectively (Yoshimori *et al.*, 2000; Poupon *et al.*, 2003).

We screened a *L. pneumophila* genomic library for genes that induce a Vps^- phenotype in yeast as candidate effectors capable of altering endosomal traffic. Using this novel Pathogen Effector Protein Screening in Yeast (PEPSY), we have identified three genes (*vipA, vipD, vipF*; *V*PS *i*nhibitor *p*rotein) that encode proteins, which specifically interfere with trafficking in yeast, and are translocated from *L. pneumophila* into host macrophages via the Icm/Dot TFBSS.

MATERIALS AND METHODS

Bacterial and Yeast Strains. Bacterial strains, media and antibiotic concentrations were used as previously described (Chen *et al.*, 2004). The diploid NSY01 was generated from the haploid BHY10 (Horazdovsky *et al.*, 1994) by HO endonuclease induction (Herskowitz and Jensen, 1991). BHY10 was transformed with YCp50::HOc12 (a gift by Aaron Mitchell) and the diploid was isolated (Herskowitz and Jensen, 1991).

Plasmid Construction. Genomic DNA was isolated from stationary phase *Legionella pneumophila* Philadelphia-1 isolate grown overnight in AYE using the DNeasy Kit (Qiagen). 30μg gDNA was partially digested with Sau3AI for 15 minutes at 37°C. Digested DNA was run on an agarose gel and the region corresponding approximately to 0.8-5kb was excised and DNA was purified. pWS93 (a gift by Marian Carlson) was linearized by BamHI/BglII digestion to remove a 3xHA tag located between those two sites. Sau3AI digested *L. pneumophila* DNA was ligated to linearized pWS93 and transformed into DH5α. Approximately 35,000 Carbenicillin resistant colonies were scraped and plasmid DNA prepared. Plasmid DNA was transformed into NSY01 and transformants were plated on SC-Ura plates with 2% fructose as the only carbon source. pNS00 was generated by self-ligating pWS93 linearized by BamHI/BglII digestion. *VPS4*^{E233Q} was amplified from pMB66 (Babst *et al.*, 1998) and cloned into the SalI site of pNS00. To make cyclase

fusions *vipA*, *vipD*, *vipE* and *vipF* were amplified from *L. pneumophila* genomic DNA and cloned in the KpnI/XbaI site of pJC141 (Chen *et al.*, 2004). Plasmids encoding *vip-cyaA* fusions were electroporated into JR32 or *dotA* and plated on CYE-Cm. Construction of the GFP-CPS plasmid is described elsewhere (36).

Invertase Assay Assays were based on previous methodologies (Darsow *et al.*, 2000). For the qualitative plate assay, NSY01 transformant colonies on SC-Ura/fructose plates were overlaid with agar containing 125mM sucrose, 100mM sodium acetate (pH 5.5), 0.5mM NEM, 10μg/mL horseradish peroxidase, 8 units/mL glucose oxidase and 2mM *O*-dianisidine. The trafficking defect was assessed by intensity of brownness compared to vector-only strain (white, Vps^{+}) and $Vps4^{E233Q}$ strain (brown, Vps^{-}). The quantitative assay was performed on stationary phase liquid cultures as previously described (Bankaitis *et al.*, 1986b; Klionsky *et al.*, 1988; Darsow *et al.*, 2000). Stationary phase liquid cultures of *vip* expressing strains were grown in SC-Ura/fructose and divided into two samples: Total Invertase Activity and Exogenous Invertase Activity. For Total Activity, yeast were first lysed by 4x freeze/thaw cycles. Samples were then tested for invertase activity by addition of sucrose and glucostat reagent. Reactions were stopped using 6N HCl and the absorbance at 540nm measured. One unit of invertase activity is defined as the amount of enzyme that hydrolyzes sucrose to produce 1μmol of

glucose per minute at 30°C. Values for Exogenous and Total Invertase activity were obtained and used to calculate the Percent Secreted. To test for a plasmid-dependent Vps$^-$ effect, plasmid DNA was isolated from Vps$^-$ clones, amplified in *E. coli* and used to transform NSY01. Vps$^-$ clones were cured of their plasmids by streaking once on YP/fructose plates, followed by growth on SCC/fructose plates supplemented with 5-fluoroorotic acid (5-FOA). 5-FOA resistant colonies were restreaked on SCC/fructose plates. The qualitative invertase plate assay was performed on these cured strains.

Immunoprecipitations. Cell labeling and immunoprecipitations were performed as described previously (37). Briefly, mid-log (OD_{600}~0.6) phase cultures were concentrated to 3 OD_{600} units/ml and labeled with 3 μl Tran ^{35}S label per OD_{600} (PerkinElmer Life and Analytical Sciences, Boston, MA) for 10 min in SC-Ura medium. Cells were chased with 5mM methionine, 2mM cysteine, and 0.2% yeast extract for the indicated times. Proteins were then precipitated in 10% trichloroacetic acid. Protein pellets were washed twice with ice-cold acetone, dried in vacuo, and processed for immunoprecipitation as described previously (37). Immunoprecipitated proteins were resuspended in sample buffer for resolution by SDS-PAGE, and gels were developed by autoradiography.

Fluorescence Microscopy. Cells expressing GFP-CPS were grown to an OD_{600} of 0.6 and labeled with the fluorescent lipophilic dye N-[3-

triethylammoniumpropyl]-4-[p-diethylaminophenylhexatrienyl] pyridinium dibromide (FM4-64; Molecular Probes, Eugene, OR) as previously described (38). Cells were visualized using a Zeiss Axiovert S1002TV (Thornwood, NY) inverted fluorescent microscope equipped with fluorescein isothiocyanate (FITC) and rhodamine filters. Images were captured with a Photometrix camera and processed with DeltaVision deconvolution software (Applied Precision, Seattle, WA) and Adobe Photoshop 8.0 (Adobe Systems Inc., San Jose, CA). All observations are based on the examination of at least 100 cells, and representative fields are shown.

cAMP Measurement. cAMP measurement was performed as previously described (Chen *et al.*, 2004). Briefly, $4x10^6$ J774 cells in RPMI (Cellgro) + 10% Normal Human Serum were infected with *L. pneumophila* strains using an MOI of 50 and incubated at 37°C for 30 minutes. After removal of supernatant, lysates were extracted by addition of cold 2.5% perchloric acid for 10 minutes, followed by neutralization with KOH. cAMP levels were measured using the cAMP Biotrak Enzymeimmunoassay System (Amersham Biosciences).

RESULTS

PEPSY screening identifies *L. pneumophila* genes that inhibit vacuolar traffic. The methodology used to identify a Vps phenotype (Bankaitis *et al.*, 1986b; Robinson *et al.*, 1988a; Horazdovsky *et al.*, 1994; Darsow *et al.*, 2000) takes advantage of the properties of a hybrid protein resulting from a fusion between invertase and carboxypeptidase Y. The *SUC2* gene encodes an invertase (β-D-fructofuranoside fructohydrolase) that is normally localized at the cell surface. The *PRC1* gene encodes carboxypeptidase Y (CPY), a vacuolar hydrolase that undergoes post-translational modifications in the Golgi, followed by trafficking to the late endosome and sorting to the lysosome-like yeast vacuole. Because the sorting signals for CPY lie in the amino terminal region, when the first 50 amino acids of CPY are fused to the 433 C-terminal amino acids of invertase, the CPY-Inv hybrid protein traffics from the ER to the Golgi and then to the vacuole via the late endosome. Because the CPY-Inv hybrid is sequestered in the vacuole and cannot reach the cell surface, the cell is unable to hydrolyze exogenous sucrose. However, if normal trafficking of CPY-Inv is perturbed, cargo vesicles are blocked from reaching the vacuole, resulting in missorting of the hybrid protein and subsequent spillover into vesicles destined for the cell surface. This aberrant secretion of the CPY-Inv hybrid allows the cell to hydrolyze exogenous sucrose. This phenotype can be scored at the colony level by a

simple agar overlay containing sucrose and chromogenic reagents that indicate glucose production by a brown precipitate. A wild-type Vps^+ phenotype is scored as a white colony whereas a Vps^- phenotype is scored as a brown colony (Darsow *et al.*, 2000).

To look for *L. pneumophila* proteins that would perturb vacuole protein sorting, we screened for bacterial genes capable of inducing a Vps^- phenotype in yeast. A random library of *L. pneumophila* genomic DNA was generated by a Sau3AI partial digest. Fragments were cloned into the $URA3^+$ 2μ yeast expression vector pNS00. Gene expression from inserted DNA in this plasmid is under the control of the strong constitutive ADH1 promoter. Plasmid pools were transformed into the diploid Ura^- indicator yeast strain NSY01 that expresses the CPY-Inv hybrid protein. Transformants were plated on SC–Ura plates with fructose as the sole carbon source. We screened approximately 80,000 colonies by overlaying with agar containing glucose detection reagents and those that turned brown were restreaked and re-tested (Figure 3.1A). CPY-Inv secretion was also quantified in liquid cultures (Figure 3.1B). Plasmid DNA was isolated from brown Vps^- colonies and re-transformed into NSY01. In parallel, the Vps^- yeast strains were cured of the plasmids and their Vps phenotype was re-tested. Candidates in which the Vps phenotype was linked to the plasmid by both retransformation and curing were kept for further analysis. Of the Vps^- colonies, 17% were plasmid dependent. The DNA

sequences of the inserts in these plasmids were determined and analyzed using the *L. pneumophila* genome database (Chien *et al.*, 2004). Our positive control in our assays was expression of a dominant negative allele of the AAA ATPase Vps4p. Mutation of a conserved glutamate at position 233 of Vps4p abolishes its vacuolar protein sorting function in a dominant negative manner (Babst *et al.*, 1998). We identified four independent clones that induce a Vps^- phenotype in yeast. The genes carried by the clones were designated *vipA, D, E, F* (***VPS*** ***i****nhibitor* ***p****rotein*). Clones containing *vipA* and *vipF* were isolated more than once.

Protein similarities and properties. The fragment expressing *vipA* contained two other ORFs downstream of *vipA*, but mutational analysis determined that only removal of the *vipA* coding region abolished CPY-Inv secretion (data not shown). We cloned the full-length *vipA* gene into pNS00 and the corresponding NSY01 strain exhibited similar CPY-Inv secretion as the original Sau3AI *vipA* fragment (data not shown). The sequence of VipA is predicted to have a coiled-coil region but exhibits no extensive homologies to known proteins. The fragment designated *vipD* contained an 848bp sequence encoding a C-terminal region of the VipD protein where the initiating methionine is at residue 341. This results in a polypeptide encompassing residues 341-613 of the full length VipD. The full-length gene encodes a patatin domain and shows strong homology to the *Pseudomonas aeruginosa*

Type III translocated effector ExoU. The patatin domain also showed considerable homology to eukaryotic phospholipase A genes. However, the *vipD* fragment that results in a Vps^- phenotype does not include the catalytic patatin domain. Interestingly, when cloned into pNS00, the full-length *vipD* gene also caused a Vps^- phenotype but mis-secreted only 24% ± 3% of total CPY-Inv (data not shown), significantly less than the 72% ± 8% mis-secreted by the fragment encoding the C-terminal region (Figure 3.1B). Expression of full length VipD in yeast did not result in any detectable toxicity (data not shown). The *vipE* clone contained a single ORF that exhibited no extensive homology to other genes. The *vipF* clone contained a single gene that exhibited homologies to genes that encode acetyltransferases (e scores between e^{-4} to e^{-24}, data not shown).

Characterization of trafficking pathways affected in yeast by Vip expression. To characterize the defects in trafficking produced by *vip* gene expression, we examined the proteolytic maturation of proteins that are sorted to the vacuole via the three major pathways in yeast (Figure 3.2A): (a) the CPY sorting pathway (13), (b) the MVB (multivesicular body) pathway, (Katzmann *et al.*, 2002) and (c) the ALP (alkaline phosphatase) pathway (Odorizzi *et al.*, 1998c). CPY is a soluble hydrolase that traffics to the vacuole via endosomes in a receptor-mediated fashion and does not require all components of the MVB pathway. CPS, however, is a transmembrane protein

that is sorted into MVB vesicles at the late endosome prior to final delivery and maturation at the vacuole. Finally, ALP, a transmembrane protein residing in the vacuolar membrane, bypasses endosomes entirely and reaches the vacuole by the AP3 adaptor-mediated sorting pathway (Piper *et al.*, 1997; Stepp *et al.*, 1997).

Processing of these proteins in the Golgi and the vacuole results in precursor and mature forms of different molecular weights. In order to examine maturation in yeast strains expressing different Vip proteins, we ^{35}S-labeled nascent proteins by pulse-chase, and determined the extent of CPS, CPY, and ALP processing by immunoprecipitation and SDS-PAGE (Figure 3.2, data not shown for ALP). VipA expression resulted in partial accumulation in p2CPY (Golgi form), indicating a block in trafficking between the Golgi and the late endosome and/or between the late endosome to the vacuole. VipA expression also caused a partial accumulation of precursor CPS but no detectable effect on ALP. Strains expressing the VipD C-terminal fragment caused a more severe defect in processing; there was a partial kinetic delay in the conversion of the p1 (ER) form to the p2 (Golgi) form, and most of the intracellular CPY accumulated in the p2 form, indicating a defect in Golgi-to-vacuole trafficking. Furthermore, given the strong CPY-Inv secretion exhibited by this strain, it is likely that the majority of the p2-CPY is secreted into the growth medium and therefore was not detected on the gel. Similarly, expression of the VipD C-

terminal region inhibited nearly all CPS and ALP processing (ALP data not shown). In contrast, VipF expression did not cause a detectable alteration in the processing of any of the three proteins.

We also analyzed the localization of GFP-tagged CPS in the Vip-expressing strains by fluorescence microscopy (Figure 3.3). Although the GFP-CPS protein is normally localized in the vacuole lumen, VipA expression resulted in partial mislocalization to the membrane. Expression of the VipD C-terminal region resulted in a more striking phenotype, where some cells showed localization of the GFP-CPS protein exclusively in the vacuole membrane, while others showed partial membrane localization. Interestingly, all cells exhibited an accumulation of GFP-CPS on punctate structures on or near the vacuole membrane. These structures are reminiscent of an aberrant endosomal membrane compartment observed in class E *vps* mutants (Raymond *et al.*, 1992), where MVB sorting is impaired (Odorizzi *et al.*, 1998b). As in the case of the processing assays, VipF had no discernable effect on GFP-CPS localization.

Legionella translocates the VipA, D, and F proteins into macrophages via the Icm/Dot TFBSS. If the Vip proteins are *bona fide* effectors, they should be substrates of the Icm/Dot TFBSS. To determine if they are translocated into host cells by *L. pneumophila*, we used a reporter that has been used to study the translocation of many bacterial effectors into

eukaryotic cells. This reporter, the *cyaA* sequence of *Bordetella pertussis,* encodes an adenylate cyclase that is activated by eukaryotic calmodulin. Thus, increased intracellular cAMP levels following infection by strains expressing effector-cyclase hybrids is indicative of CyaA translocation from bacteria into the host cytosol (Ladant and Ullmann, 1999). The *vipA*, *vipD, vipE* and *vipF* genes were cloned into pJC141, a reporter plasmid derived from pMMB207C that is used for creating upstream translational fusions to *cyaA* (Chen *et al.*, 2004). Plasmids containing the Vip-CyaA hybrids were transformed into the wild-type JR32 strain and a *dotA* mutant in which the TFBSS is inactive. Because the VipE-CyaA hybrid was unstable and had low intrinsic adenylate cyclase activity, it was not analyzed further. J774 macrophages were infected with *L. pneumophila* expressing the Vip-CyaA hybrid proteins or unfused CyaA (Figure 3.4). The levels of cAMP produced by the strains containing the Vip-CyaA hybrids resembled the levels produced by the positive control LepA-CyaA, a previously characterized translocated effector hybrid (Chen *et al.*, 2004). The differences in cAMP levels produced by infection by wild-type and *dotA* strains were between 10-100 fold, similar to values obtained with other effectors (Chen *et al.*, 2004), indicating that a functional Icm/Dot TFBSS is required for translocation. Constructs expressing only CyaA resulted in very low levels of cAMP, indicating that increased cAMP levels required the presence of the Vip sequences. We conclude that the

VipA, D, and F proteins that produce trafficking defects in yeast are also substrates of the Icm/Dot TFBSS.

DISCUSSION

L. pneumophila modulates host vesicle traffic to create a protective, replicative vacuole. This is likely accomplished by injecting effector proteins into the host via the Icm/Dot TFBSS. Effectors modulate phagosome trafficking by unknown mechanisms. Despite the identification of numerous Icm/Dot substrates, all appear to be dispensable for proper phagosome trafficking and intracellular growth. It has been proposed that *L. pneumophila* possesses a high degree of functional redundancy and species specificity in effector function (Chen *et al.*, 2004; Chien *et al.*, 2004; Luo and Isberg, 2004). We sought to directly identify effectors that can interact with endosomal trafficking pathways. We took advantage of the CPY-Inv assay, previously used to identify the *vps* genes (Bankaitis *et al.*, 1986b; Robinson *et al.*, 1988a) that encode components of these pathways in both lower and higher eukaryotes. Using PEPSY screening, we identified four Sau3AI fragments and characterized three genes: *vipA*, *vipD* and *vipF*, whose expression in yeast results in mistrafficking of vacuolar proteins. Using calmodulin-activated adenylate cyclase as a reporter, we determined that *L. pneumophila* indeed translocates the VipA, VipD and VipF proteins via the Icm/Dot TFBSS into host macrophages.

At present, it is difficult to identify the precise nature of the defects caused by the Vip proteins or their direct targets. However, some information

can be gleaned from the Vip protein sequences. VipA contains a relatively large coiled-coil region as do previously documented *L. pneumophila* effectors such as LepA, LepB, LidA, SidC, SidE, SdeA, SdeB and SdhB. Coiled-coils are highly versatile structures involved in protein interactions and several trafficking components possess coiled-coils such as SNAREs, EEA1, and Uso1p (Burkhard *et al.*, 2001; Gillingham and Munro, 2003). We speculate that *L. pneumophila* effectors may interact with similar host proteins via their coiled-coil regions. The N-terminal domain of VipD contains a patatin domain that is found in the *Pseudomonas aeruginosa* effector ExoU. ExoU has lipolytic activity that is lethal to eukaryotic cells; however this activity depends on activation by unknown eukaryotic cell-derived factors (Phillips *et al.*, 2003; Rabin and Hauser, 2003; Sato *et al.*, 2003). The VipD patatin domain also bears strong homology to eukaryotic phospholipase A2 proteins that generate the signaling lipid arachidionic acid, which is also the precursor for other important lipid molecules such as leukotrienes and prostaglandins. Recent work from various labs has also implicated a role for phospholipase A2 in Golgi membrane dynamics, ER-to-Golgi traffic and even phagosome biogenesis (de Figueiredo *et al.*, 2001; Kuroiwa *et al.*, 2001; Girotti *et al.*, 2004). However, the fragment isolated from the Vps screen encodes only the C-terminal domain and lacks the patatin domain. This C-terminal region does not bear any sequence or structural homology to known proteins or motifs, yet

causes the strongest defect in vacuolar traffic, even when compared to the dominant negative Vps4p^{E233Q} allele. Expression of the VipD C-terminal region significantly delayed the trafficking of CPY from the ER to the Golgi and from Golgi to vacuole. Additionally trafficking of CPS and ALP to the vacuole was also delayed. When we expressed the full length VipD protein it resulted in a less severe defect in CPY-Inv trafficking. This could be due to differential stability or expression levels between the two forms of VipD, or the N-terminal domain may be negatively regulating the C-terminal domain. It is also possible that the C-terminal region targets or titrates a limiting host trafficking component more efficiently than the full-length protein. In support of the latter model it has been hypothesized that the C terminus of ExoU (that also excludes the patatin domain) interacts with a eukaryotic factor necessary for ExoU function and cytotoxicity (Sato and Frank, 2004; Rabin and Hauser, 2005). Unlike ExoU, expression of full length VipD was not lethal in yeast but was sufficient to cause a Vps$^-$ phenotype. VipF is a protein that has an acetyltransferase domain. Despite its ability to cause mistrafficking of CPY-Inv, pulse-chase experiments and fluorescence microscopy did not reveal a detectable phenotype. However, it is important to note that several of the original *vps* mutants also exhibited stronger defects in CPY-Invertase sorting than for the wild-type protein; a likely explanation for this observation is that

the fusion protein is sorted less efficiently than CPY because it is recognized less well by the CPY receptor Vps10p (12).

Yeast has been used as a tool to understand bacterial virulence by many groups and was the subject of a recent review (Valdivia, 2004). However these studies used yeast to characterize known virulence factors. We wanted to use yeast in a new way as a gene discovery tool to identify previously unrecognized effectors that inhibit vesicle traffic. We were encouraged by earlier work showing that many bacterial effectors normally involved in mammalian infection retain their biological function in yeast (Lesser and Miller, 2001; Valdivia, 2004). Furthermore, *L. pneumophila* infects and modulates host traffic in species from different kingdoms. This may be due to interactions between effectors and host targets that are highly conserved. There may be other host specific effectors, such as LepA and LepB which appear to function in protozoa but not in mammalian hosts (Chen *et al.*, 2004). The fact that we recovered Icm/Dot translocated effectors that interfere with organelle trafficking in yeast supports the idea that some effector: host interactions are conserved. The three Vip proteins do not share common structures nor do they appear to inhibit organelle trafficking by the same mechanisms. This may reflect multiple strategies that *L. pneumophila* effectors use to intersect with the host trafficking pathways. We found four other patatin domain-containing VipD paralogs in the *L. pneumophila* genome database lpg1227, lpg2410,

lpg1426 and lpg0670. Interestingly, they share strong homology between their N-terminal patatin-like domains but not in their C-terminal regions. There may be additional *vip* genes that we did not find due to lack of a proximal Sau3AI site or because of lethality in yeast. For example, *lepB* expression is lethal in yeast and tolerated only under low-copy, repressing conditions (data not shown). Furthermore it has been shown that expression of *lepA* in yeast results in a Vps^- phenotype (Pericone, CD, Shohdy, N and Shuman, HA, unpublished data).

It should be possible to use other yeast tools such as suppressor analysis to identify host factors that either dampen or enhance the Vip-dependent Vps^- phenotype. The PEPSY approach can also be applied to other pathogens that modulate host cell trafficking such as *Salmonella typhimurium* and *Mycobacterium tuberculosis* and less characterized pathogens such as *Coxiella burnetti* and *Brucella abortus*. This strategy provides additional approaches to both identify novel virulence factors and study their mode of action, thus contributing to the understanding of host-pathogen interactions during intracellular survival and multiplication.

Figure 3.1 Invertase assays on selected *vip* clones. (A) Qualitative Invertase Assay on NSY01 strains transformed with plasmids carrying empty vector, *VPS4*^{E233Q}, *vipA*, *vipD, vipE and vipF* clones. SC-Ura/fructose plate was overlaid with top agar containing chromogenic reagents that result in a brown precipitate upon secretion of the CPY-Inv hybrid protein. (B) Quantitative Invertase Assay on *vip* clones. Stationary phase liquid cultures of *vip* expressing strains were grown in SC-Ura/fructose and divided into two samples: Total Invertase Activity and Exogenous Invertase Activity. For Total Activity, yeast were first lysed by 4x freeze/thaw cycles. Samples were then tested for invertase activity by addition of chromogenic reagents. Reactions were stopped using 6N HCl and the absorbance at 540nm measured. One unit of invertase activity is defined as the amount of enzyme that hydrolyzes sucrose to produce 1μmol of glucose per minute at 30°C. Values for Exogenous and Total Invertase activity were obtained and used to calculate the Percent Secreted. Assays were done in triplicate at least twice.

A.

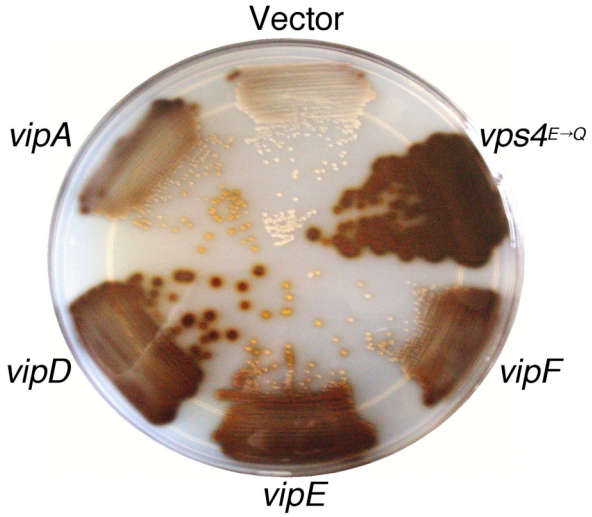
Vector
vipA
vps4E→Q
vipD
vipF
vipE

B.

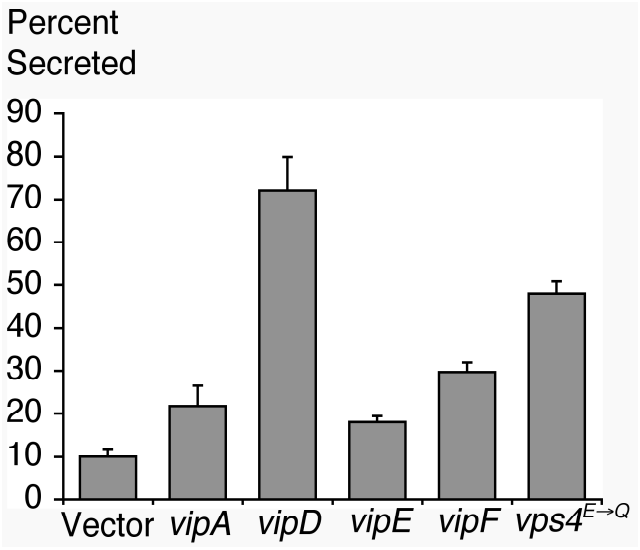
Percent
Secreted
90
80
70
60
50
40
30
20
10
0
Vector
vipA
vipD
vipE
vipF
vps4E→Q

Figure 3.2 Biosynthetic trafficking of CPY and CPS is differentially affected by overexpression of *vip* clones. (A) Golgi-to-vacuole sorting pathways in *S. cerevisiae*. The CPY and MVB (CPS) pathways diverge at the late endosome, where the latter involves internal vesicle formation. Following fusion with the vacuole, MVBs are degraded in the lumen by various enzymes. ALP is sorted via an AP3-dependent pathway that bypasses endosomes. B-C. Immunoprecipitation of vacuolar proteins in *vip*-expressing strains. Cells were [^{35}S]methionine-labeled at 26°C with with a 10-minute pulse, followed by a chase to the indicated time points as described in Materials and Methods. Intracellular CPY (B) and CPS (C) were immunoprecipitated using the appropriate antibodies, samples were resolved by SDS-PAGE, and visualized by autoradiography. Precursor (p) and mature (m) forms are indicated to the left. For CPY, the endoplasmic reticulum-modified (p1), Golgi-modified (p2), and mature (m) forms are shown. For CPS, the Golgi-modified (p) and mature (m) forms are shown.

A.

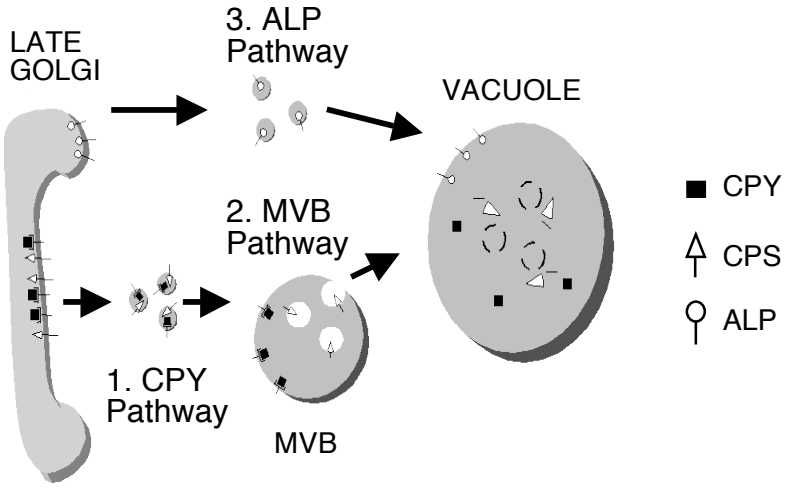
LATE
GOLGI
3. ALP
Pathway
VACUOLE
2. MVB
Pathway
1. CPY
Pathway
MVB
CPY
CPS
ALP

B.

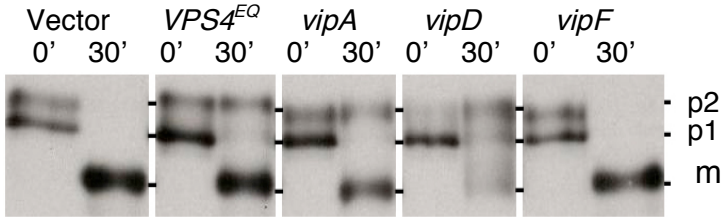
Vector
VPS4EQ
vipA
vipD
vipF
0’ 30’ 0’ 30’ 0’ 30’ 0’ 30’ 0’ 30’
p2
p1
m

C.

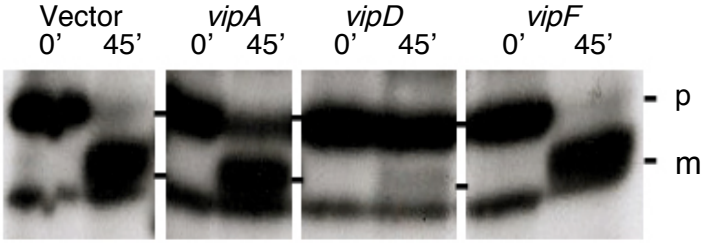
Vector
vipA
vipD
vipF
0’ 45’ 0’ 45’ 0’ 45’ 0’ 45’
p
m

Figure 3.3 Steady-state localization of a GFP-CPS fusion in *vip*-expressing strains. Cells were harvested in mid-log phase and labeled with FM4-64 to visualize the vacuole membrane (as described in Materials and Methods). Fluorescence was observed and imaged using a DeltaVision system (Applied Precision, Seattle, WA) (DIC: Nomarski optics).

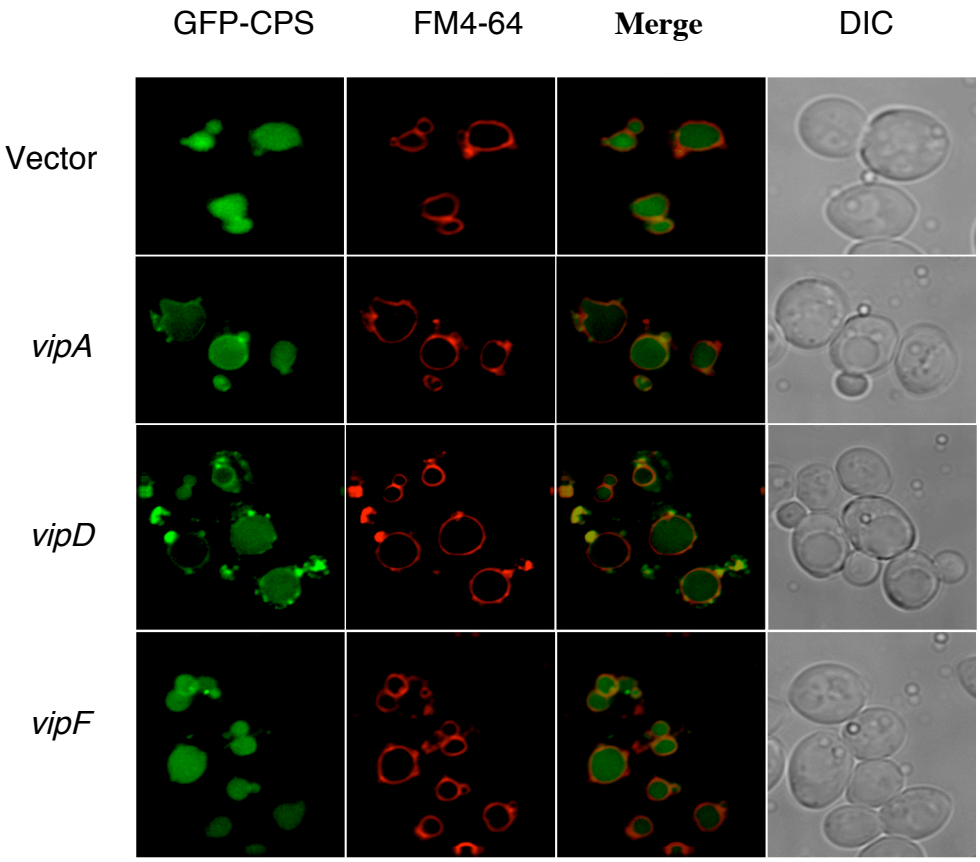
GFP-CPS
FM4-64
Merge
DIC
Vector
vipA
vipD
vipF

Figure 4.4 Cyclase translocation assays. J774 macrophages were seeded into 96-well tissue culture plates and infected with *L. pneumophila* strains for 30 minutes. After removal of supernatant, cells were lysed with cold 2.5% perchloric acid and neutralized with KOH. cAMP levels measured as in previous studies (Chen *et al.*, 2004) using cAMP Biotrak Enzymeimmunoassay System (Amersham Biosciences).

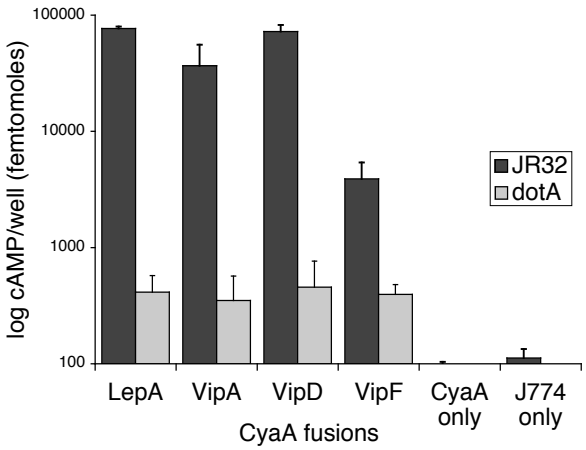
100000
10000
1000
100
log cAMP/well (femtomoles)
JR32
dotA
LepA
VipA
VipD
VipF
CyaA only
J774 only
CyaA fusions

ACKNOWLEDGEMENTS

This work was supported by grant AI23549 (HAS) and CA58689 (SDE). SDE is an Investigator of the Howard Hughes Medical Institute. We thank Marian Carlson and Aaron Mitchell for advice and materials, Chris Pericone and Jonathan Dworkin for helpful comments on the manuscript.

This chapter, in full, is a reprint of the material as it appears in Shohdy, N., Efe, J.A., Emr, S.D., and H.A. Shuman. *Proceedings of the National Academy of Sciences* 102(13):4866-71. Pathogen effector protein screening in yeast identifies Legionella factors that interfere with membrane trafficking. The dissertation author was a co-investigator and co-author of this paper.

CHAPTER 4

ATG18 REGULATES ORGANELLE MORPHOLOGY AND FAB1 KINASE ACTIVITY INDEPENDENT OF ITS MEMBRANE RECRUITMENT BY PHOSPHATIDYLINOSITOL 3,5-BISPHOSPHATE

ABSTRACT

The lipid kinase Fab1 plays a central role in the regulation of vacuole morphology by generating PtdIns(3,5)P_2. Cells lacking Atg18p, an effector of this phospholipid, have enlarged vacuoles and high levels of PtdIns(3,5)P_2. We show that Atg18 puncta on the vacuole often colocalize with Fab1p. However, it is unlikely that Atg18 acts directly on the kinase, as deletion of *VAC7* or *VAC14* is epistatic to that of *ATG18*: *atg18Δvac7Δ* cells have no detectable PtdIns(3,5)P_2. A fusion consisting of two tandem copies of Atg18 localizes to the vacuole membrane in the absence PtdIns(3,5)P_2, but requires Vac7p for recruitment. Like EEA1, Atg18 membrane binding may have both a phospholipid and a protein component. When the lipid requirement is bypassed by fusing Atg18 to ALP, a vacuolar transmembrane protein, *vac14Δ* vacuoles can be fragmented. Rescue is independent of PtdIns(3,5)P_2 when Atg18 is tethered to the vacuole, as mutation of the phospholipid binding site does not abrogate fragmentation or Fab1 kinase inhibition. Finally, Vac17p

interacts with Atg18p, perhaps mediating cytoskeletal attachment during retrograde membrane transport. Atg18p is likely a PtdIns(3,5)P_2 “sensor”, acting as an effector of this phospholipid to remodel membranes as well as regulating its synthesis via feedback that might involve Vac7p.

INTRODUCTION

Eukaryotic cells have evolved highly sophisticated macromolecular machinery to orchestrate the complex and dynamic process of membrane trafficking. These protein complexes vary widely in structure and function, but are all tightly coordinated in order to catalyze a sequence of specific events with the goal of transferring membrane cargo from one compartment to another. Despite the constant flux of membrane and proteins, organelles maintain distinct identities. To achieve the formation and maintenance of organelle size, shape and function, trafficking complexes must be properly targeted and subsequently recycled (Munro, 2004; Behnia and Munro, 2005; Jordens *et al.*, 2005). Lipids have been shown to play an increasingly important role in these processes, especially phosphoinositides (PtdIns*P*s).

PtdIns*P*s are phosphorylated derivatives of phosphatidylinositol, of which there are seven species that can be rapidly interconverted by phosphorylation or dephosphorylation reactions. The occurrence of a specific PtdIns*P* transiently recruits cognate effector proteins that bind the PtdIns*P* via short modular motifs such as the FYVE and PH domains (Lemmon, 2003; Balla, 2005; Behnia and Munro, 2005; Di Paolo and De Camilli, 2006; Takenawa and Itoh, 2006). Hence, PtdIns*P*s are particularly suited to serve as membrane surface tags. Importantly, PtdIns*P*-binding modules differ greatly in their affinity and specificity for the various PtdIns*P*s, which when

coupled with protein partners, generates a specificity code for each organelle (Lawe *et al.*, 2000; Balla, 2005).

PtdIns(3)*P* and PtdIns(3,5)P_2 respectively label early and late endosomal structures (Burd and Emr, 1998a; Cooke *et al.*, 1998; Gary *et al.*, 1998; Gillooly *et al.*, 2000; Jeffries *et al.*, 2004; Kim *et al.*, 2005). While PtdIns(3)*P* predominantly controls protein sorting and membrane dynamics at the early endosome, PtdIns(3,5)P_2 appears to govern events associated with later endosomal compartments such as the yeast vacuole (Schu *et al.*, 1993a; Cooke *et al.*, 1998; Gary *et al.*, 1998; Clague *et al.*, 1999). Cells depleted for PtdIns(3,5)P_2 exhibit numerous vacuolar defects including non-acidic vacuoles, impaired vacuole-to-endosome retrograde transport, abnormal vacuolar inheritance and most conspicuously, these cells possess a drastically enlarged, single-lobed vacuole (Yamamoto *et al.*, 1995; Cooke *et al.*, 1998; Gary *et al.*, 1998; Jeffries *et al.*, 2004). In contrast, increasing the levels of PtdIns(3,5)P_2 during hypertonic shock or through genetic manipulation causes vacuolar fragmentation (Dove *et al.*, 1997; Gary *et al.*, 2002). Together, this suggests that PtdIns(3,5)P_2 principally modulates membrane traffic and dynamics of the vacuole.

PtdIns(3,5)P_2 is generated from PtdIns(3)*P* phosphorylation by the yeast PtdIns(3)*P* 5-kinase Fab1p (PIKfyve in mammals), (Cooke *et al.*, 1998; Gary *et al.*, 1998; Sbrissa *et al.*, 1999). Synthesis of PtdIns(3,5)P_2 is

modulated by at least two vacuolar proteins, Vac7p and Vac14p. Vac7p is a transmembrane protein with no known homologs in higher eukaryotes, whereas Vac14p is likely an adaptor protein. PtdIns(3,5)P_2 is reduced 10-fold or more in *vac14*Δ and *vac7*Δ and consequently, these cells exhibit a phenotype similar to *fab1*Δ cells (Bonangelino *et al.*, 1997; Dove *et al.*, 2002; Gary *et al.*, 2002). Interestingly, Vac14p binds to Fig4p, a PtdIns(3,5)P_2-specific 5'-phosphatase thought to antagonize Fab1p (Rudge *et al.*, 2004). Indeed, a loss of function mutant of FIG4 was originally isolated as a suppressor of *vac7*Δ, partially rescuing the levels of PtdIns(3,5)P_2 and vacuolar morphology (Gary *et al.*, 2002). However, Fig4p appears to be necessary for maximal synthesis of PtdIns(3,5)P_2 during hypertonic shock, pointing to a more complex role for Fig4 than to simply turnover PtdIns(3,5)P_2 (Duex *et al.*, 2006a).

Several putative protein effectors of PtdIns(3,5)P_2 have been identified. The mammalian ESCRT-III component, mVps24 (Whitley P, 2003), and the ENTH-containing proteins Ent3p/Ent5p were shown to bind PtdIns(3,5)P_2 and are suggested effectors for PtdIns(3,5)P_2-dependent sorting into MVBs (Friant *et al.*, 2003; Eugster *et al.*, 2004). In addition, Dove *et al.* identified *SVP1* in a screen for cells with swollen vacuoles and demonstrated that Svp1p bound to PtdIns(3,5)P_2 (Jeffries *et al.*, 2004). Interestingly, Svp1p was shown to be the same as Atg18p (used herein), a previously identified component of the

autophagic and the cytosol-to-vacuole transport (CVT) pathways (Barth *et al.*, 2001). It is noteworthy that PtdIns(3,5)P_2 does not appear to play a direct role in autophagy or the CVT pathways, suggesting that Atg18p has at least two distinct functions in the cell (Jeffries *et al.*, 2004).

ATG18 encodes a multi-WD-containing protein that is postulated to fold into a b-barrel. It is related to the yeast Atg21p and Hsv2p and to the WIPI proteins in mammals (Jeffries *et al.*, 2004). Atg18p does not possess a distinct PtdIns-binding module. Instead, an intact b-barrel comprising almost the entire length of Atg18p is required to associate with PtdIns(3,5)P_2. However, the FRRG^{287} motif on the b-barrel is a strong candidate for the direct site of interaction with PtdIns(3,5)P_2. Mutation of the double arginines disrupts binding to PtdIns(3,5)P_2 and shifts Atg18p from the vacuole to the cytosol (Jeffries *et al.*, 2004).

The precise role and molecular mechanism of Atg18p as a PtdIns(3,5)P_2 effector remains uncertain. Dove *et al.* suggest that Atg18p is required for PtdIns(3,5)P_2-dependent retrograde membrane traffic from the vacuole to the Golgi apparatus via the endosomes. This conclusion was deduced from the lack of the mature isoform of RS-ALP in the Golgi membrane fraction in *atg18*Δ cells (Bryant and Stevens, 1998a; Jeffries *et al.*, 2004). RS-ALP is an ALP isoform modified with a FXFXD motif that enables recycling from the vacuole, where it undergoes proteolytic maturation, to the

Golgi (Bryant and Stevens, 1998a; Jeffries *et al.*, 2004). On the other hand, deletion of ATG18 causes an abnormal elevation in the levels of PtdIns(3,5)P_2, which suggests that Atg18p is also a negative regulator of the Fab1 kinase pathway (Bryant and Stevens, 1998a; Jeffries *et al.*, 2004). Clearly, Atg18p is a key component of the PtdIns(3,5)P_2 signaling network, being an apparent effector and modulator of this lipid.

Here, we employed several engineered isoforms of Atg18p that deliver it to the vacuole independently of PtdIns(3,5)P_2 to explore the requirement for PtdIns(3,5)P_2-binding in governing vacuolar morphology and lipid levels. We also found that Vac7 plays a role in membrane recruitment of Atg18. Finally, we identify Vac17 as a protein partner of Atg18p. Putative interaction with Vac7p may provide a model for Atg18p-dependent inhibition of the Fab1 kinase while binding to Vac17p suggests a possible role of Atg18p in vacuole inheritance.

MATERIALS AND METHODS

Strains and Media. A list of all *S. cerevisiae* strains used in this study and their genotypes can be found in Table 4.1. Strains were grown in rich (YPD) or minimal (SD) media supplemented with the appropriate amino acids. Standard growth conditions and manipulations have been described previously by Rose *et al*. (Rose, 1990).

Genetic and DNA manipulations. Restriction enzymes were purchased from New England Biolabs (Ipswich, MA), and PCR reactions were carried out with KOD polymerase (EMD Biosciences, San Diego, CA) or ExTaq (Takara Mirus Bio, Madison, WI) for cloning and diagnostic reactions, respectively. Standard molecular biology techniques as described by Maniatis *et al.* (Maniatis, 1992) were used for all DNA manipulations. Yeast transformations were done by the method of Ito *et al.*(Ito *et al.*, 1983), and yeast genomic preparations were carried out as described by Hoffman and Winston (Hoffman and Winston, 1987).

Deletions and chromosomal epitope-tagging were all done in the SEY6210 wild-type background (Table 4.1) using PCR-amplified genomic integrations as described by Longtine *et al.* (Longtine *et al.*, 1998). All deletions and integrations were verified by PCR analysis, and expression (chromosomal and plasmid-based) of fusion proteins was confirmed by western blot analysis. For all PCR-based cloning procedures, unique

restriction enzyme sites were generated at the 5' and 3' ends of ORFs by incorporating them into their respective primers.

Plasmids pJE181 (encoding GFP-Atg18) and pJE191 (GFP-Vac17) are based on the vector pBP73G, a kind gift from Dr. Willliam R. Parrish. Briefly, pBP73G was created by cloning the *GPD1* promoter (beginning 500 basepairs upstream of start) between the SacI and XbaI sites of pRS416 (Sikorski and Hieter, 1989) by PCR amplification, followed by the subcloning of GFP between the XbaI and BamHI sites. pJE181 and pJE191 contain the full length *ATG18* and *VAC17* ORFs amplified by PCR and ligated in-frame between the EcoRI/XhoI and BamHI/SalI site pairs, respectively. pJE182 was generated from pJE181 by mutating $_{285}$RR$_{286}$ to $_{285}$GG$_{286}$ in Atg18 using site-directed mutagenesis (Stratagene Corp., La Jolla, CA). Plasmids pJE183 (encoding GFP-Atg18-ALP), pJE184 (GFP-Atg18-ALP with a $_{285}$GG$_{286}$ mutation in Atg18), pJE185 (GFP-2xAtg18), and pJE186 (myc-2xAtg18) are all based on the vector pRB415A, a modified version of pBP74A (also a gift from Dr. William R. Parrish). Briefly, pBP74A was generated from pRS415 (Sikorski and Hieter, 1989) by cloning the *ADH1* promoter (beginning 500 basepairs upstream of start) by PCR as a SacI-XbaI fragment, followed by ligation of GFP between the XbaI and BamHI sites. pRB415A modifies pBP74A by integrating the restriction sites BglII-AvrII-AatI-SpeI-NruI-NheI-BspEI-SacII between the HindIII and SalI sites of pBP74A. pJE183 contains full-length

ATG18 and *PHO8* ligated in-frame between the EcoRI/HindIII and AvrII/NruI site pairs, respectively. pJE184 was generated from pJE183 using site-directed mutagenesis as described above. pJE185 is identical to pJE183, except that a second copy of *ATG18* was cloned in-frame between the XmaI and XhoI sites instead of *PHO8* as above. pJE186 was generated form pJE185 by excision of GFP using XbaI and EcoRI, followed by ligation of a 12xmyc tag (amplified from pFA6a-13myc-TRP1, (Longtine *et al.*, 1998)) into the gapped plasmid using the same sites.

Primer sequences for all of the above genetic manipulations are available upon request.

Fluorescence Microscopy. In vivo labeling of the vacuole limiting membrane with the lipophilic dye N-[3-triethylammoniumpropyl]-4-[p-diethylaminophenylhexa-trienyl] pyridinium dibromide (FM4-64; Molecular Probes, Eugene, OR) was done as outlined previously by Vida and Emr (Vida and Emr, 1995b).

Fluorescence and differential interference contrast (DIC) images of cells labeled with FM-64 and those expressing GFP fusion proteins were generated with a Delta Vision RT microscopy system (Applied Precision, LLC, Issaquah, WA). Specifically, data were acquired using an Olympus IX71 inverted microscope (Tokyo, Japan) equipped with fluorescein isothiocyanate (FITC) and rhodamine filters and coupled to a Photometrics CoolSNAP HQ camera

(Tucson, AZ). Images were processed using Delta Vision deconvolution software (Applied Precision) and Adobe Photoshop 8.0 (Adobe Systems Inc., San Jose, CA).

Quantification of Fluorescence Intensity and Coincidence.

Fluorescence intensity of the FM4-64 (rhodamine) and GFP (FITC) channels of unprocessed TIFF images was quantified by using ImageJ 1.36b (NIH, Bethesda, USA). Typically, plot profiles were acquired by drawing a 5-pixel wide line from the cytosol to the vacuole lumen; lines started around the mid-point of the cytosol and were typically 20-40 pixels long. Line positioning across the vacuole was random, but puncta were avoided. Fluorescence intensity values were exported to Excel 2004 (Microsoft Corp., Redmond, WA) where the background was subtracted. For graphical representation in Figures 4.1 and 4.5, intensity values were normalized against the highest intensity value to achieve a peak of 1. For the values depicted in Tables 4.2 and 4.3, intensity values were normalized against the value of the first cytosolic pixel. The vacuole membrane was defined as the pixel with the highest FM4-64 intensity and the corresponding GFP intensity was used to measure the relative enrichment of the GFP-fusion protein between the vacuole membrane and the cytosol. The relative GFP fluorescence intensity of vacuole/cytosol for Atg18-GFP and GFP-2xAtg18 was statistically analyzed against that of soluble GFP using the one-tail, unpaired Student's t-test. Note

that the contrast and the brightness of the images shown in Figures 4.1 and 4.5 have been adjusted after acquiring line plot profiles.

Immunoprecipitation and Western Blot Analysis. ^{35}S metabolic labeling and immunoprecipitations were performed as described previously (Gaynor *et al.*, 1994). Briefly, mid-log (OD_{600}~0.6) phase cultures were concentrated to 3 OD_{600} units/ml and labeled with 3 μl Tran ^{35}S label per OD_{600} (PerkinElmer Life and Analytical Sciences, Boston, MA) for 20 min in SD medium. Cells were chased with 20 mM methionine, 8 mM cysteine, and 0.8% yeast extract for 120 minutes. Proteins were precipitated in 10% TCA and resulting pellets were washed twice with ice-cold acetone, dried and processed for immunoprecipitation as described previously (Gaynor *et al.*, 1994). Anti-APeI antibody was a kind gift from Dr. Daniel Klionsky. Immunoprecipitated proteins were resolved on SDS-PAGE gels and analyzed by autoradiography.

Cross-linking immunoprecipitations using ^{35}S-labeled extracts were carried out essentially as described by Rieder and Emr (Rieder and Emr, 1997). Briefly, osmotic whole cell lysates were treated with the cross-linker DSP [dithiobis(succinimidyl-propionate); Pierce, Rockford, IL] and TCA-precipitated proteins were subjected to two successive overnight immunoprecipitations using anti-HA antibody (Roche Diagnostics, Indianapolis, IN). Following cleavage of the cross-linker and resolution by

SDS-PAGE, autoradiography was used to reveal any proteins cross-linked to Atg18-HA.

For co-immunoprecipitation of Atg18 and Vac17, cells (20 OD_{600} units) were grown at 26°C to midlogarithmic phase and spheroplasted (Darsow *et al.*, 1997). Spheroplasts were resuspended in 1 ml ice-cold lysis buffer (200 mM sorbitol, 50 mM potassium acetate, 20 mM HEPES, pH 7.2, 2 mM EDTA) containing protease inhibitors, and lysed by douncing (10x). Tween-20 (Sigma, St. Louis, MO) was added to the 500 x g supernatants to a final concentration of 0.5%. Following a 10-min. incubation, detergent-insoluble material was pelleted with a 10-min. 13,000 x g spin. After removing and TCA-precipitating 5% of the supernatant to determine total protein content, anti-FLAG antibody (Sigma) and 20 μl Gammabind G-sepharose beads (Amersham Biosciences, Piscataway, NJ) were added to the remainder and incubated at 4°C for 90 minutes. Protein complexes bound to the beads were recovered by washing twice with 1 ml ice-cold lysis buffer containing 0.5% Tween-20, and twice with detergent-free lysis buffer, followed by elution in boiling buffer (50 mM Tris, pH 6.8, 2% SDS, 5% b-mercaptoethanol, 10% glycerol, 0.005% bromophenol blue) at 100°C for 10 minutes. SDS-PAGE and western blot analysis were used to detect Atg18-FLAG and GFP-Vac17.

In Vivo Analysis of Phosphoinositides. Phosphoinositide levels were analyzed as previously described by Rudge *et al*. (Rudge *et al.*, 2004). Briefly, 5 OD_{600} units of cells (per strain) were labeled with 60 mCi of myo-[2-^{3}H]inositol (Amersham Biosciences) in SD media lacking inositol for one hour. Following precipitation in 4.5% perchloric acid (final concentration) for 5 minutes, phospholipids were deacylated by incubation in methylamine reagent (10.7% methylamine, 45.7% methanol, 11.4% 1-butanol) for 50 minutes at 53°C. Excess methylamine was removed by drying in a vacuum chamber, followed by two washes (resuspension by sonication and subsequent drying) of the pellet in 300 ml sterile water. After a third resuspension in water, an equal volume of extraction reagent (1-butanol/ethyl-ether/formic acid ethyl ester at a ratio of 20:4:1) was added and [^{3}H]gylcero-phosphoinositides were extracted into the aqueous phase by vortexing for 5 minutes and centrifugation at 14,000 rpm for 2 minutes. The extraction was repeated twice more and the final aqueous phase was collected and dried as above.

For quantitative analyses, dried pellets were resuspended in sterile water and $1x10^{7}$ cpm quantities of sample were separated on a Partisphere SAX column (Whatman, Inc., Florham Park, NJ) attached to a Shimadzu high-performance liquid chromatography (HPLC) system (Shimadzu Manufacturing, Kyoto, Japan) and a 610TR on-line radiomatic detector (PerkinElmer, Inc., Whaltham, Massachusetts) using Ultima Flo scintillation fluid (PerkinElmer).

The HPLC and on-line detector were controlled with EZStart 7.2.1 and ProFSA 3.3 software, respectively, with final data analysis taking place in the latter.

RESULTS

Atg18p colocalizes with the PtdIns(3,5)P_2 core synthesis machinery on vacuolar foci. Using a *fab1Δ* strain, Dove *et al.* have previously shown that the localization of Atg18-GFP to the vacuole limiting membrane depends on the presence of the Fab1 kinase (Dove *et al.*, 2004). However, this result does not establish whether the observed failure to localize is solely due to a lack of PtdIns(3,5)P_2. The Fab1 protein could be playing at least as important a role in recruiting Atg18p to the vacuole membrane as its phospholipid product, especially since these proteins interact in two-hybrid experiments (Georgakopoulos *et al.*, 2001). To differentiate between the two possibilities, we examined Atg18-GFP localization in strains deleted for *VAC7* or *VAC14*, which encode the two upstream activators of the Fab1 kinase. In both *vac7Δ* and *vac14Δ* strains, Fab1p properly localizes to the vacuole membrane (Bonangelino *et al.*, 2002b; Dove *et al.*, 2002). We found that Atg18-GFP is entirely cytosolic in both cases, indicating that PtdIns(3,5)P_2 is necessary for recruitment even in the presence of a fully functional (but inactive) Fab1 kinase on the vacuole membrane (Figure 4.1A and Table 4.2).

In wild-type cells, Atg18-GFP does not appear uniformly distributed along the vacuolar membrane; prominent punctate structures are frequently seen as well (Guan *et al.*, 2001). It has been speculated that these puncta represent autophagic membrane compartments and an association with

PI(3)P may be necessary for recruitment to them (Guan *et al.*, 2001; Stromhaug *et al.*, 2004); however, it is important to note that punctate enrichment on the vacuole membrane is also characteristic of most components of the PtdIns(3,5)P_2 synthesis machinery (i.e. Fab1p, Vac14p and Fig4p). Importantly, there is a significant degree of overlap between them (our unpublished observations), and we have found that Atg18-mRFP puncta frequently coincide with foci of Fab1-GFP or Vac14-GFP (Figure 4.1B).

While Atg18-GFP puncta are moderately motile, their movement is almost always confined to the vacuole membrane. In the rare instances that we do observe cytosolic foci of Atg18, it is in the context of what appears to be retrograde vesicular membrane transport from the vacuole. Time-lapse microscopy clearly shows an FM4-64-positive vesicle budding from a site of Atg18-GFP enrichment, followed by movement of this vesicle into the daughter cell and subsequent fusion with endocytic and/or vacuolar compartment(s) (Figure 4.1C).

Hyperactivation of the Fab1 kinase in *atg18Δ* requires both activators of the kinase as well as the Fig4 phosphatase. Unlike the deletion of genes encoding the core machinery for PtdIns(3,5)P_2 synthesis and turnover, the *atg18Δ* strain has dramatically elevated levels of this phosphoinositide (Dove *et al.*, 2004). This observation, coupled with the finding that Atg18p is recruited to its site of function by PtdIns(3,5)P_2, suggests

that this protein is part of a negative feedback pathway regulating synthesis of this phospholipid. More specifically, we hypothesized that Atg18p most likely inhibits Fab1 kinase function rather than upregulating Fig4 phosphatase activity, because phosphoinositide levels and vacuole morphology are unaltered in a *fig4Δ* strain (Gary *et al.*, 2002; Efe *et al.*, 2005). Although a two-hybrid interaction between *FAB1* and *ATG18* suggests Atg18p might directly inhibit Fab1 kinase function (Georgakopoulos *et al.*, 2001), indirect regulation via one or both of the kinase's upstream regulators, Vac7p and Vac14p, is also possible. To address this issue, we examined PtdIns(3,5)P_2 levels in *atg18Δvac7Δ* and *atg18Δvac14Δ* strains. In both cases, deletion of the upstream activator was epistatic to *atg18Δ* (Figure 4.2A). The precipitous drop in PtdIns(3,5)P_2 levels associated with the individual deletion of *VAC7* or *VAC14* is not even partially suppressed by additionally deleting *ATG18* (which, on its own, elevates lipid levels approximately 8-fold) (Dove *et al.*, 2004). The *atg18Δvac14Δ* strain also displays a very severe synthetic phenotype: compared to either single deletion, the double mutant grows approximately three times more slowly and is temperature-sensitive (practically no growth is observed at 30°C; data not shown). Based on these results, Atg18p most likely inhibits Fab1p function indirectly via one or both of its upstream regulators. However, a direct interaction with Fab1p cannot be ruled out at this time.

Paradoxically, *atg18Δ* cells also lacking the Fig4 phosphatase exhibit a very similar phenotype: in an *atg18Δfig4Δ* strain PtdIns(3,5)P_2 levels drop to 10% of wild-type, or just over 1% of *atg18Δ* (Figure 4.2B). However, this result is in agreement with a recent study showing that activation of the Fab1 kinase by Vac14p is largely dependent on the presence of Fig4p, either as a co-activator of the kinase itself or a scaffold for a putative kinase complex (Duex *et al.*, 2006a).

Tethering Atg18p to the vacuole membrane restores normal vacuole morphology in the *vac14Δ* mutant. While wild-type *S. cerevisiae* vacuoles are small and multi-lobed, the vacuoles of cells lacking Atg18p are significantly enlarged and almost exclusively single-lobed (Dove *et al.*, 2004). Thus, in addition to the Fab1 kinase hyperactivation previously described, *atg18Δ* cells show a defect in vacuole size control similar to that of a *fab1Δ* strain. Numerous studies have established a firm and clear link between high levels of PtdIns(3,5)P_2 and vacuole fragmentation, especially in the context of hyperosmotic shock (Gary *et al.*, 1998; Bonangelino *et al.*, 2002b; Gary *et al.*, 2002). To date, *atg18Δ* is the only mutant strain in which very high levels of PI(3,5)P_2 and enlarged vacuoles can coexist. In light of this observation, we have proposed that Atg18p might be the PtdIns(3,5)P_2 effector involved in vacuole fragmentation (Efe *et al.*, 2005). To test this hypothesis, we asked whether tethering Atg18p to the vacuole limiting membrane is sufficient to

fragment enlarged mutant vacuoles lacking PtdIns(3,5)P_2 on their surface. Membrane anchoring was achieved by fusing GFP-Atg18p C-terminally to alkaline phosphatase (ALP), a transmembrane protein of the vacuole (Klionsky and Emr, 1989). The requirement for the phospholipid in the proper localization of Atg18p is thus bypassed, and the stable vacuolar association of Atg18 is sufficient to shrink and fragment not only *atg18Δ* vacuoles, but also the grossly enlarged vacuoles of a *vac14Δ* strain. Conversely, overexpression of GFP-Atg18 without a membrane anchor fails to restore wild-type vacuole morphology in the same strain (Figure 4.3A). Interestingly, the Atg18-ALP fusion does not rescue the vacuoles of *vac7Δ* or *fab1Δ* cells (data not shown). It is important to note that, unlike these strains, *vac14Δ* cells do synthesize a small amount of PtdIns(3,5)P_2 – approximately 10% of wild-type – and this residual phospholipid is most likely what allows for effective function of Atg18p on the membrane, either via allosteric regulation or recruitment of an additional PtdIns(3,5)P_2 effector required for vacuole size regulation.

The Atg18-ALP fusion construct also allows one to assess whether restricting Atg18p activity to the vacuole limiting membrane has any adverse effects on autophagy. To gauge the efficiency of both the cytoplasm-to-vacuole (cvt) and macroautophagy pathways, we examined the proteolytic maturation of aminopeptidase I (APeI) that takes place upon its delivery to the vacuole in cvt vesicles or autophagosomes (Nair and Klionsky, 2005). In the

atg18Δ strain, metabolic labeling followed by a 120-minute chase shows no maturation of APeI, both under vegetative (cvt) and starvation (macroautophagy) conditions, where the latter is induced by treatment with rapamycin (Figure 4.3B). Interestingly, while adding back GFP-Atg18 rescues both defects, the GFP-Atg18-ALP fusion is incapable of cvt transport and exhibits a very substantial (50%) kinetic delay in macroautophagy. Thus, Atg18p must be able to detach from the vacuole membrane in order to effectively mediate its autophagic function(s), a requirement we do not observe in the context of PI(3,5)P_2 homeostasis and vacuole size regulation.

The putative phosphoinositide binding site in Atg18p is not critical for its regulation of the Fab1 kinase and vacuole morphology. Since PtdIns(3,5)P_2 might be required for Atg18 activity at the vacuole membrane, we sought to determine if the putative phospoinositide-binding region identified by Dove *et al*. (2004) as critical for recruitment of Atg18 also plays a role the activation of Atg18p. We first made a $_{284}$F**RR**G$_{287}$ to $_{284}$F**GG**G$_{287}$ mutation in GFP-Atg18 and showed that this construct, even when overexpressed, is not recruited to the vacuole membrane in an *atg18Δ* strain and cannot properly regulate vacuole size (Figure 4.4A). However, when we made the same mutation in the context of our GFP-Atg18-ALP chimera – thereby bypassing the recruitment step and highlighting any adverse effect(s) on activity – we observed a complete rescue of vacuole morphology. Moreover, the ability to

attenuate Fab1 kinase activity also remained intact in the chimeric point mutant (Figure 4.4B). These results indicate that the $_{284}$FRRG$_{287}$ basic patch of Atg18, while absolutely necessary for proper localization, is not required for its vacuole size regulation function or for suppression of Fab1 kinase activity.

Membrane recruitment of a GFP-2xAtg18 fusion requires Vac7p. As alluded to above, it is unclear whether Atg18p directly interacts with the Fab1 kinase or its upstream regulators; a strict requirement for PtdIns(3,5)P_2 in proper localization of Atg18p makes it impossible to determine the role of protein-protein interactions, if any, in the process. To test for the potential contribution of protein-protein interactions, we expressed a chimera consisting of GFP fused N-terminally to two tandem copies of Atg18 (GFP-2xAtg18) in the *fab1Δ*, *vac7Δ*, and *vac14Δ* strains. We hypothesized that the increased avidity an Atg18 dimer would have for putative protein interactor(s) might allow recruitment to the vacuole limiting membrane even in the absence of PtdIns(3,5)P_2. Indeed, we observed that GFP-2xAtg18 localizes predominantly to the vacuole membrane in the *fab1Δ* and *vac14Δ* strains, indicating that (a) PtdIns(3,5)P_2 is not required for localization of the chimera and (b) any potential interaction with Fab1p or Vac14p is also not required for recruitment (Figure 4.5A and Table 4.3). In agreement with our previous results indicating a requirement for PtdIns(3,5)P_2 in activation of Atg18p, GFP-2xAtg18 was only able to rescue the vacuole size defect in *vac14Δ* cells.

Strikingly, the chimera was entirely cytosolic in the *vac7Δ* strain, indicating that Vac7p likely constitutes the protein component of Atg18p's interaction with the vacuole membrane.

Atg18p interacts with Vac17p. In order to visualize various proteins interacting with Atg18, we metabolically labeled cells with ^{35}S and carried out *in vivo* cross-linking experiments. We found only one protein clearly co-immunoprecipitating with Atg18-HA under these conditions, and it migrated to approximately 50 kDa on a PAGE gel (Figure 4.6A). Of the previously identified interactors of Atg18p (putative or biochemically demostrated), three proteins fit this electrophoretic profile: Bio3p, Rtg3p, and Vac17p. In a two-hybrid screen, Georgakopoulos *et al.* (2001) found that *VAC17* was one of the most frequently recovered genes and the highest-ranking gene encoding a protein localizing to the vacuole membrane (Ishikawa *et al.*, 2003).

We were able to replicate this result using a synthetic two-hybrid library engineered by PCR-amplification of all *S. cerevisiae* ORFs. More than 100,000 colonies were screened using high stringency, ultimately resulting in the isolation of ten clones, all of which turned out to harbor *VAC17* plasmids (data not shown). More importantly, we also found that Vac17p and Atg18p interact in vivo by co-immunoprecipitation analysis (Figure 4.6B).

DISCUSSION

Atg18p was first identified as an essential component of the autophagy, Cvt, and pexophagy pathways in *S. cerevisiae* (Guan *et al.*, 2001). Its vacuolar rim localization is unique among proteins in these pathways, and it was subsequently found to bind PtdIns3*P* and PtdIns(3,5)P_2, which plays a key role in its membrane association (Dove *et al.*, 2004; Stromhaug *et al.*, 2004). Moreover, deletion of *ATG18* results in a nine-fold increase in PtdIns(3,5)P_2 levels. Here we show that Atg18p colocalizes with components of the PtdIns(3,5)P_2 synthesis machinery on the vacuole, and that vacuole recruitment of a tandem 2xAtg18 fusion requires Vac7p, suggesting a possible mechanism of Fab1 kinase inhibition. Further, Atg18p is necessary and sufficient for proper vacuole morphology in wild-type and *vac14Δ* strains. By tethering wild-type Atg18 or a mutant defective in PtdIns(3,5)P_2 binding to the vacuole membrane, we show that PtdIns(3,5)P_2 binding is not required for vacuole fragmentation or restoration of wild-type levels of this phosphoinositide in these strains. Finally, we show that Atg18p co-immunoprecipitates with the vacuole inheritance protein Vac17p and might be involved in a vesicular transport pathway originating at the vacuole membrane.

Regulation of PtdIns(3,5)P_2 levels by Atg18p. Atg18-mRFP partially co-localizes with Fab1-GFP and Vac14-GFP on areas of punctate enrichment along the vacuole membrane. As has been previously suggested (Rudge *et*

al., 2004), these puncta may represent a large number of protein complexes capable of rapidly phosphorylating PtdIns3*P* to PtdIns(3,5)P_2. The cell could efficiently regulate this process by recruiting Atg18p to a subset of these sites as a direct or indirect inhibitor of the Fab1 kinase.

Although it has been reported that Atg18p and Fab1p interact by yeast two-hybrid analysis (Georgakopoulos *et al.*, 2001), it is noteworthy that this interaction was weak compared to others listed. Instead, our data suggest that Atg18p regulates Fab1 activity indirectly. Epistasis tests show that the dramatic rise in PtdIns(3,5)P_2 levels observed upon deletion of *ATG18* requires *VAC7, VAC14* and FIG4. The latter result confirms a previously reported role for the Fig4 phosphatase in Fab1 kinase activation (Duex *et al.*, 2006a), especially under circumstances that require dramatic and/or sustained increases in phosphoinositide levels. Furthermore, the very low level of PtdIns(3,5)P_2 in the *atg18Δvac14Δ* strain is especially striking, as *vac14Δ* cells have detectable but low (10% of wild-type) steady-state PtdIns(3,5)P_2 and can still partially respond to hyperosmotic shock by elevating levels of this phosphoinositide (Bonangelino *et al.*, 2002b; Duex *et al.*, 2006b).

Importantly, Vac7p is the only known protein in the PtdIns(3,5)P_2 synthesis pathway that is required for recruitment of GFP-2xAtg18 to the vacuole membrane. GFP-2xAtg18 is associated with the vacuole even in the complete absence of PtdIns(3,5)P_2 (i.e. in a *fab1Δ* strain), and we can rule out

recruitment by PtdIns3*P* alone since the *vac7Δ* strain actually produces slightly higher than normal levels of this phosphoinositide. Therefore, the data support a model in which PtdIns(3,5)P_2 and the transmembrane protein Vac7 function together on the vacuole to recruit Atg18 specifically to this organelle. A similar synergistic requirement is observed for the recruitment of EEA1 to endosomes; proper localization requires both PI(3)*P* and the small GTPase Rab5 (Simonsen *et al.*, 1998). Conceivably, Atg18p might indirectly inhibit PtdIns(3,5)P_2 synthesis by sequestering Vac7 away from Fab1p or by recruiting an unknown inhibitor of Vac7. Thus far, in vivo co-immunoprecipitation experiments (both native and cross-linking) have only shown a very weak interaction between a myc-2xAtg18 construct and HA-tagged Vac7 (data not shown). However, Vac7 is highly unstable under these conditions, and it is quite possible that rapid degradation is masking a stronger physical association between the two proteins.

Mechanistically, a plausible hypothesis is that the putative phosphoinositide binding pocket of Atg18p, $_{284}$F**RR**G$_{287}$, is involved in calibrating lipid levels by an allosteric mechanism. However, making the $_{284}$F**GG**G$_{287}$ mutation in the Atg18-ALP fusion construct did not ablate its ability to suppress hyperactivation of the Fab1 kinase in the *atg18Δ* background. Our data support a model in which the binding pocket $_{284}$F**RR**G$_{287}$ is implicated in Atg18p-recruitment to the vacuole. However, this does not rule out allosteric

regulation by PtdIns(3,5)P_2 at the vacuole membrane; there might be still other site(s) of phospholipid interaction, albeit these sites are not sufficient for vacuolar localization in $_{284}$F**GG**G$_{287}$ Atg18 mutant.

Atg18p control of vacuolar morphology. We and others have consistently observed an inverse relationship between vacuole size and steady-state PtdIns(3,5)P_2 levels in yeast: low or non-existent PtdIns(3,5)P_2 gives rise to enlarged and single-lobed vacuoles, while excessive production of this phospholipid results in smaller-than-normal and highly fragmented vacuoles. The *atg18Δ* strain is the only exception to this rule, and we have found that vacuoles in this strain remain enlarged even when expressing *fab1-5*, a hyperactive allele of the Fab1 kinase (lipid levels are at least 20x higher than wild-type in this case; our unpublished results). This finding corroborates the report by Dove *et al.* that hypertonic shock of *atg18Δ* cells does not alter vacuole morphology either, even though PtdIns(3,5)P_2 levels rise to an unprecendented 60x of wild-type (Dove *et al.*, 2004). These results indicate that *atg18Δ* cells are not able to properly respond to the synthesis of the phospholipid, and implicate Atg18p as a fragmentation-specific PtdIns(3,5)P_2 effector – in addition to its role in a negative feedback loop constraining Fab1 kinase activity.

In agreement with the above model, we found that Atg18p is not only required for the process of vacuole fragmentation, but is also sufficient: a

membrane-anchored Atg18-ALP fusion bypasses the requirement for PtdIns(3,5)P_2 in recruitment to the vacuole and ameliorates the large vacuole phenotype of *atg18Δ* and *vac14Δ* strains. Interestingly, this construct fails to rescue the large vacuole defect in a *vac7Δ* or *fab1Δ* strain. Possible explanations for this observation include: (a) Atg18p-mediated fragmentation might require a small amount of PtdIns(3,5)P_2 for allosteric activation and the residual amount in *vac14D* is sufficient [*vac7Δ* and *fab1Δ* have no detectable PtdIns(3,5)P_2]; (b) another protein functioning at the same level or downstream of Atg18p is not properly localized in *vac7Δ* and *fab1Δ* strains; or (c) deleting *VAC7* or *FAB1* has a more pleiotropic effect on vacuole homeostasis, rendering fragmentation physiologically impossible. Indeed, Vac7p and Fab1p have very poorly acidified and larger vacuoles that appear more rigid. These proteins may eventually be found to have roles above and beyond PtdIns(3,5)P_2 synthesis and regulation.

The ability to localize Atg18p to the vacuole membrane in the absence of PtdIns(3,5)P_2 by fusing it to ALP also enabled us to ascertain that the putative phosphoinositide binding pocket $_{284}$F**RR**G$_{287}$ is not relevant for Atg18-mediated regulation of vacuole morphology. Making the $_{284}$F**GG**G$_{287}$ mutation in the Atg18-ALP fusion construct did not ablate its ability to restore wild-type morphology to *atg18Δ* and *vac14Δ* vacuoles. These results clearly show that

the putative phosphoinositide binding pocket is not required for lipid or vacuole morphology regulation by Atg18p following its recruitment to the membrane.

Autophagy and vacuole size regulation functions of Atg18p are distinct. Atg18 has been shown to bind both PtdIns3*P* and PtdIns(3,5)P_2 (Dove *et al.*, 2004; Stromhaug *et al.*, 2004). However, since only one phosphoinositide binding site has been found in Atg18 to date – and mutation of this site ablates binding to both lipids – it was unclear whether the ability to bind different phospholipids is simply promiscuity resulting from structural similarity or whether it actually signifies a dual role on two different membrane compartments. Our results confirm the latter hypothesis, insofar as Atg18p is fully competent for vacuole size control when tethered to the vacuole membrane, but either partially (macroautophagy) or completely (Cvt) loses its autophagic functionality under these circumstances. An $_{284}$F**TT**G$_{287}$ point mutation that renders Atg18p completely cytosolic results in essentially the same deficiencies in these pathways (Krick *et al.*, 2006). Thus, it would appear that Atg18p must be be able to cycle on and off one or more target membrane compartment(s) to be fully functional, at least in the context of macroautophagy. We have shown that no such requirement exists for vacuole size control and PtdIns(3,5)P_2 by Atg18p, providing definitive evidence for two distinct areas of function.

However, there is also a significant parallel between the otherwise distinct roles of Atg18p. Our model suggests Atg18p may mediate vesicular budding and transport from the vacuole membrane, and previous studies have found that Atg18p has a similar role in autophagy: it is required for the recycling of the transmembrane protein Atg9p from the pre-autophagosomal structure (PAS) (Reggiori *et al.*, 2004a; Reggiori *et al.*, 2005). It is tempting to postulate that Atg18p, once recruited to the PAS and the vacuole by PtdIns3*P* and PtdIns(3,5)P_2, respectively, is essentially carrying out the same function on different membranes: recycling of protein(s) and membrane.

Atg18p may mediate retrograde and/or vacuole inheritance-related vesicular traffic. Atg18p-containing foci are not entirely confined to the vacuole membrane. Very rarely, a membrane patch enriched in Atg18-GFP can be observed budding from the vacuole membrane and traveling into a nascent bud. The relatively slow speed of these vesicles that allows them to be clearly visualized, as well as the non-Brownian nature of the movement suggest they might be moving along cytoskeletal track(s). Our results showing that Atg18p associates with Vac17p *in vivo* provide a mechanistic model for this type of vesicular membrane traffic. Vac17p is the vacuole inheritance-specific adapter for the type-V myosin Myo2p, which enables the transport of vacuoles into buds on actin cables in a cell-cycle coordinated fashion (Weisman, 2003). However, experiments to gauge the integrity of this type of

membrane traffic in a *vac17Δ* strain were inconclusive, and it remains at present unclear whether Vac17p is required for this process.

We have found that Vac17p plays no role in PtdIns(3,5)P_2 synthesis or regulation (our unpublished results). However, it has been long known that proper vacuole inheritance requires PtdIns(3,5)P_2, and others have postulated that Atg18p might be required for membrane fission during the formation and/or termination of the segregation structure (Weisman, 2003). Alternatively, Vac17p may, as a separate but related function, facilitate the budding and transport of vesicles enriched in Atg18p from the vacuole membrane for recycling purposes; further testing of this hypothesis awaits the discovery of a reliable endogenous cargo protein as a marker to probe the integrity of a vacuolar retrograde transport pathway.

We propose (Fig. 4.7) that that Atg18p regulates vacuole morphology by modulating the activity of the Fab1 lipid kinase, possibly via sequestration of Vac7p to alter PtdIns(3,5)P_2 levels on the vacuole membrane, and by acting as an effector of the phospholipid to induce vacuole fission and/or fragmentation by an as of yet uncharacterized mechanism. Finally, Atg18p is involved in a form of vesicular transport originating at the vacuole membrane, and this function most likely requires cytoskeletal associations mediated by Vac17p and Myo2p (Figure 4.7). In coordinately performing these various functions, Atg18 is essentially acting as a “sensor” of PtdIns(3,5)P_2,

remodeling membranes and concurrently regulating phosphoinositide synthesis as it dynamically cycles on and off the vacuole membrane.

Table 4.1 ***S. cerevisiae*** **strains used in this study**

Strain	Genotype	Reference or Source
fab1Δ2	SEY6210; fab1Δ::HIS3	Gary et al., 1998
JGY134	SEY6210; vac7Δ::HIS3	Gary et al., 2002
JGY138	SEY6210; fig4Δ::LEU2	Gary et al., 2002
JGY145	SEY6210; vac14Δ::TRP1	Gary et al., 2002
SRY13	SEY6210; atg18Δ::HIS3	This study
SRY14	SEY6210; Atg18-GFP:HIS3	This study
SRY15	SEY6210; Atg18-GFP:HIS3 fab1Δ::HIS3	This study
JEY35	SEY6210; Atg18-HA:TRP1	This study
JEY38	SEY6210; Atg18-GFP:HIS3 vac14Δ::TRP1	This study
JEY40	SEY6210; Atg18-GFP:HIS3 vac7Δ::HIS3	This study
JEY41	SEY6210; atg18Δ::HIS3 vac14Δ::TRP1	This study
JEY48	SEY6210; atg18Δ::HIS3 vac7Δ::HIS3	This study
JEY53	SEY6210; atg18Δ::HIS3 fig4Δ::LEU2	This study
JEY66	SEY6210; Atg18-FLAG:TRP1	This study
JEY85	SEY6210; Atg18-HA-mRFP:LEU2 Fab1-GFP:HIS3	This study
JEY89	SEY6210; Atg18-HA-mRFP:LEU2 Vac14-GFP:HIS3	This study

Table 4.2 Ratio of the Atg18-GFP intensity on the vacuolar membrane versus the cytosolic signal.

STRAIN	GFP VACUOLAR/ CYTOSOLIC SIGNAL	t-TEST, p VALUE[ſ]	SAMPLE NUMBER (n)
Wt-GFP	1.04±0.05	N/A	13
*atg18*Δ	1.70±0.27	p<0.05	13
*vac14*Δ	1.12±0.1	p<0.05	17
*fab1*Δ	1.07 ±0.08	p>0.05	11
*vac7*Δ	1.05 ±0.03	p>0.05	16

[*] GFP signal intensity on the vacuolar membrane was defined by colocalization with the highest intensity of FM4-64 signal in line scan profiles. [ſ]Student's t-test, one tail was employed to test the null hypothesis that the vacuole/cytosol ratio of Atg18-GFP was not significantly greater than the ratio obtained with soluble GFP expressed in wild-type cells. Values are normalized against first cytosolic pixel value.

Table 4.3 Ratiometric measurement of GFP-2xAtg18 signal present on the vacuolar membrane versus that of the cytosol.

STRAIN	GFP VACUOLAR*/ CYTOSOLIC SIGNAL	t-TEST, p VALUE∫	SAMPLE NUMBER (n)
Wt-GFP	1.04±0.05	N/A	13
*atg18*Δ	1.84±0.22	p<0.05	10
*vac14*Δ	1.88±0.30	p<0.05	13
*fab1*Δ	2.55 ±0.54	p<0.05	11
*vac7*Δ	1.08 ±0.13	p>0.05	12

* GFP signal intensity on the vacuolar membrane was defined by colocalization with the highest intensity of FM4-64 signal in line scan profiles. ∫Student's t-test, one tail was employed to test the null hypothesis that the vacuole/cytosol ratio of GFP-2xAtg18 was not significantly greater than the ratio obtained with soluble GFP expressed in wild-type cells. Values are normalized against first cytosolic pixel value.

Figure 4.1 Atg18 is entirely cytosolic in *fab1Δ*, *vac7Δ*, and *vac14Δ* mutants. (A) Fluorescence microscopy was used to determine the localization of an Atg18-GFP fusion in relation to the vacuoles of wild-type and mutant cells, as labeled with FM4-64. Overlap with the vacuolar membrane was quantified with ImageJ software by plotting normalized fluorescence intensity along a path traversing the vacuole membrane (indicated by the white bars). For orientation purposes, the cytosol (left) is separated from the lumen of the vacuole (right) by a dotted line. (B) Atg18-RFP localizes to puncta on the vacuolar rim that partially overlap with Vac14-GFP and Fab1-GFP. RFP/GFP pairs were co-expressed and their localization was compared by fluorescence microscopy. Arrows in the merge panels indicate areas of extensive overlap. (C) Atg18-GFP puncta are highly mobile. Representative still images from a 64-second time-lapse movie depict a patch of membrane enriched in Atg18-GFP (arrows) budding from the mother cell vacuole and traveling into the daughter cell. Simultaneously acquired FM4-64 fluorescence images highlight the vacuolar membranes. Bars, 4 mm.

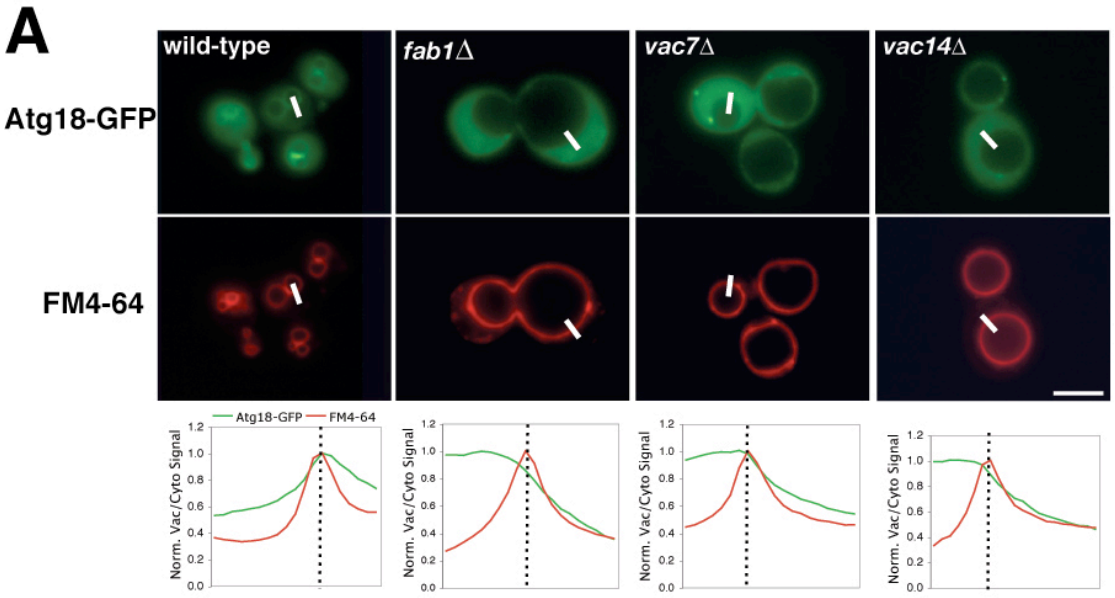
A
wild-type
fab1Δ
vac7Δ
vac14Δ
Atg18-GFP
FM4-64
Atg18-GFP
FM4-64
Norm. Vac/Cyto Signal
1.2
1.0
0.8
0.6
0.4
0.2
0.0

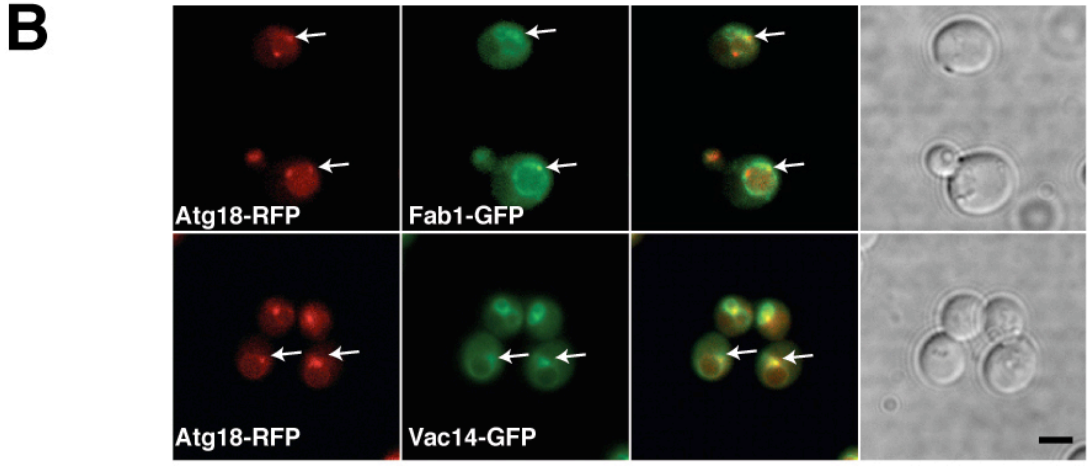
B
Atg18-RFP
Fab1-GFP
Atg18-RFP
Vac14-GFP

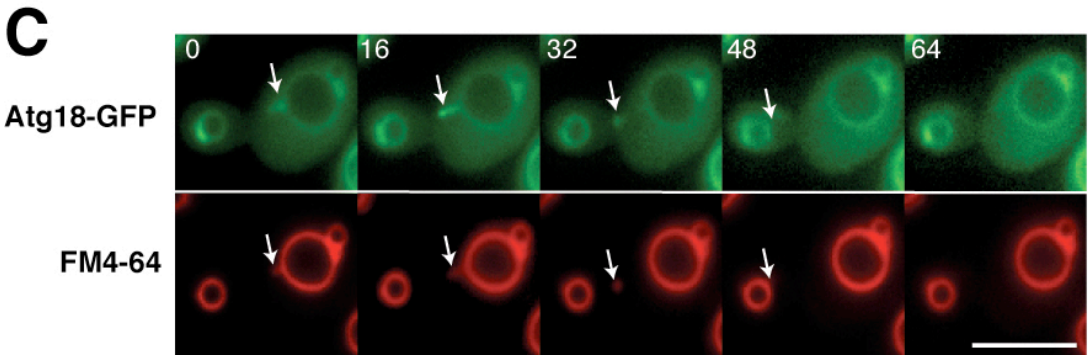
C
Atg18-GFP
FM4-64
0
16
32
48
64

Figure 4.2 Deletion of *FIG4, VAC7,* or *VAC14* is epistatic to that of *ATG18*. PtdIns(3)*P* and PtdIns(3,5)P_2 levels in (A) *vac7Δ*/*atg18Δ* and *vac14Δ*/*atg18Δ* or (B) *atg18Δ*/*fig4Δ* strains were analyzed and compared to those of the single mutant parents and a wild-type strain. ^{3}H-labeled phosphoinositides were isolated and measured by HPLC as described in MATERIALS AND METHODS.

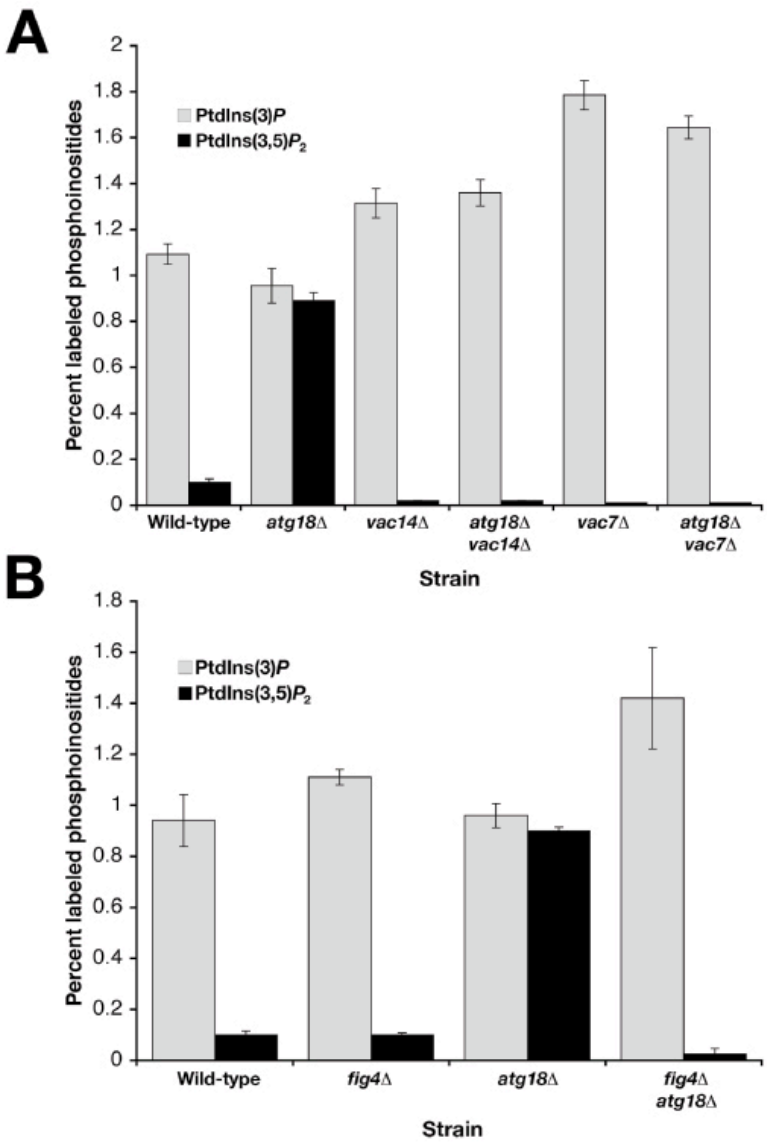
A
Percent labeled phosphoinositides
PtdIns(3)P
PtdIns(3,5)P2
Wild-type
atg18Δ
vac14Δ
atg18Δ vac14Δ
vac7Δ
atg18Δ vac7Δ
Strain
B
Percent labeled phosphoinositides
PtdIns(3)P
PtdIns(3,5)P2
Wild-type
fig4Δ
atg18Δ
fig4Δ atg18Δ
Strain

Figure 4.3 A GFP-Atg18-ALP fusion restores wild-type vacuole morphology in a *vac14Δ* strain. (A) Fluorescence microscopy comparison of GFP-Atg18 and GFP-Atg18-ALP fusion protein localization and the resulting vacuole morphology in a *vac14Δ*/*atg18Δ* strain. Bars, 4 mm. (B) GFP-Atg18-ALP is defective in the cytoplasm-to-vacuole and macroautophagy pathways. APe1 was immunoprecipitated from whole-cell lysates of cells metabolically labeled with ^{35}S-methionine (chase time is two hours for all samples) in the presence or absence of rapamycin. Proteolytic maturation of APe1 was analyzed by SDS-PAGE.

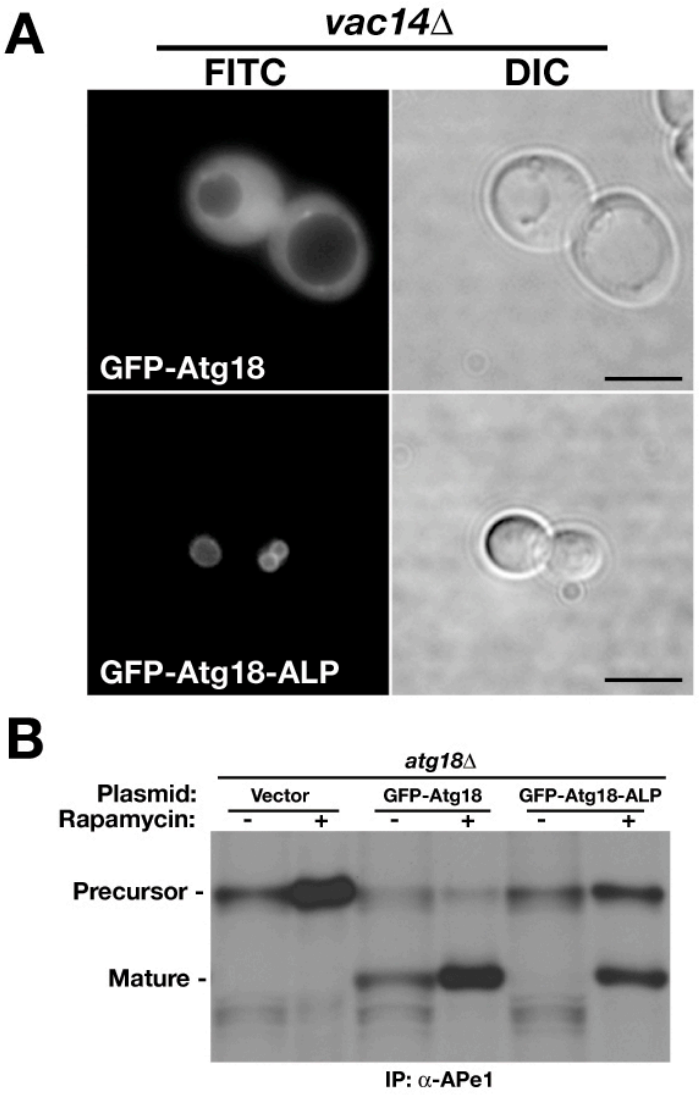
A
vac14Δ
FITC
DIC
GFP-Atg18
GFP-Atg18-ALP
B
atg18Δ
Plasmid:
Vector
GFP-Atg18
GFP-Atg18-ALP
Rapamycin:
- + - + - +
Precursor -
Mature -
IP: α-APe1

Figure 4.4 GFP-Atg18-ALP can alleviate *atg18Δ* phenotypes even if the putative PtdIns(3,5)P_2 binding site is mutated. (A) GFP-Atg18 and GFP-Atg18-ALP fusions harboring either wild-type or an $_{285}RR_{286}$-to-$_{285}GG_{286}$ point mutant of Atg18 were transformed into *atg18Δ* cells and visualized by fluorescence microscopy. Bars, 4 mm. (B) PtdIns(3,5)P_2 levels in the same set of transformants were measured as described in the legend to Fig. 2.

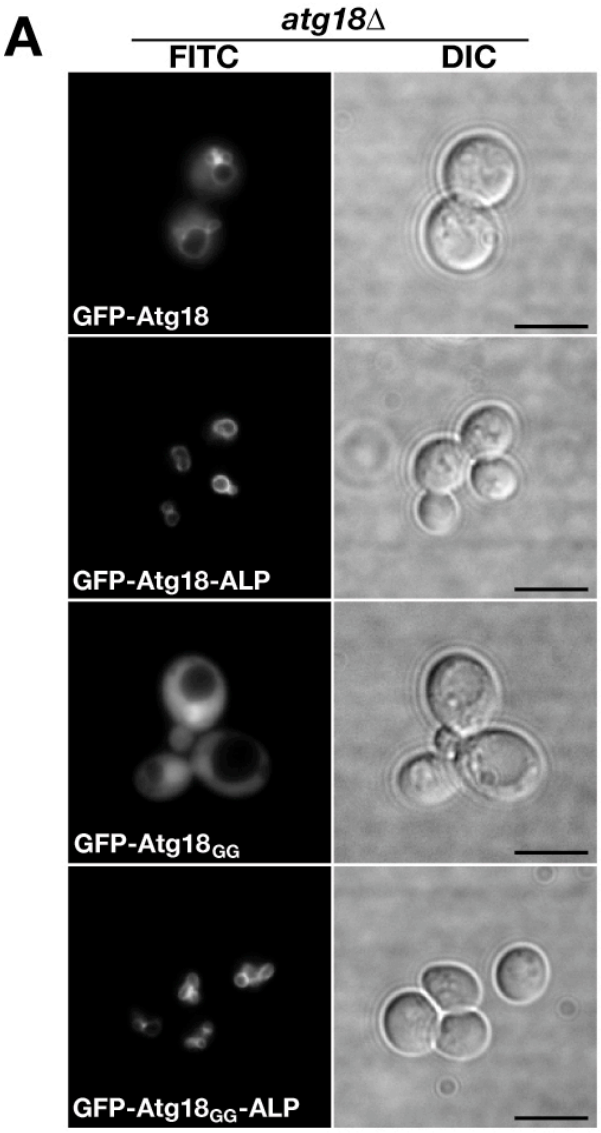
A
atg18Δ
FITC
DIC
GFP-Atg18
GFP-Atg18-ALP
GFP-Atg18GG
GFP-Atg18GG-ALP

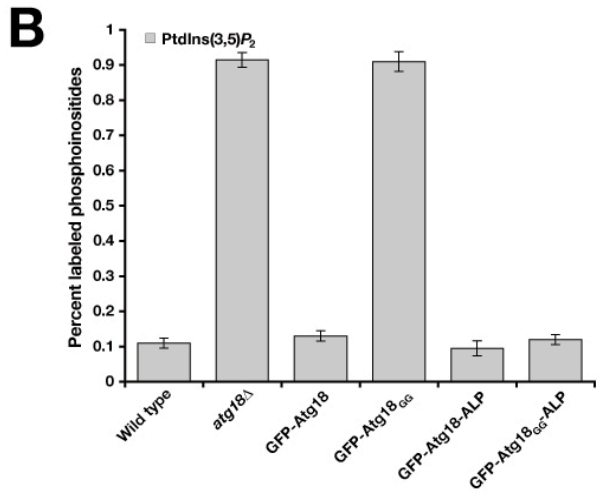
B
PtdIns(3,5)P2
Percent labeled phosphoinositides
1
0.9
0.8
0.7
0.6
0.5
0.4
0.3
0.2
0.1
0
Wild type
atg18Δ
GFP-Atg18
GFP-Atg18GG
GFP-Atg18-ALP
GFP-Atg18GG-ALP

Figure 4.5 GFP-2xAtg18 can bind to the vacuole membrane in the absence of PtdIns(3,5)P_2, but requires Vac7p for membrane localization. *Atg18Δ*, *vac14Δ*, *fab1Δ*, and *vac7Δ* cells expressing GFP-2xAtg18 were labeled with the fluorescent dye FM4-64 to highlight vacuoles. Coincidence of the GFP signal with the vacuole membrane was quantified as described in the legend to Fig.1. Bars, 4 mm.

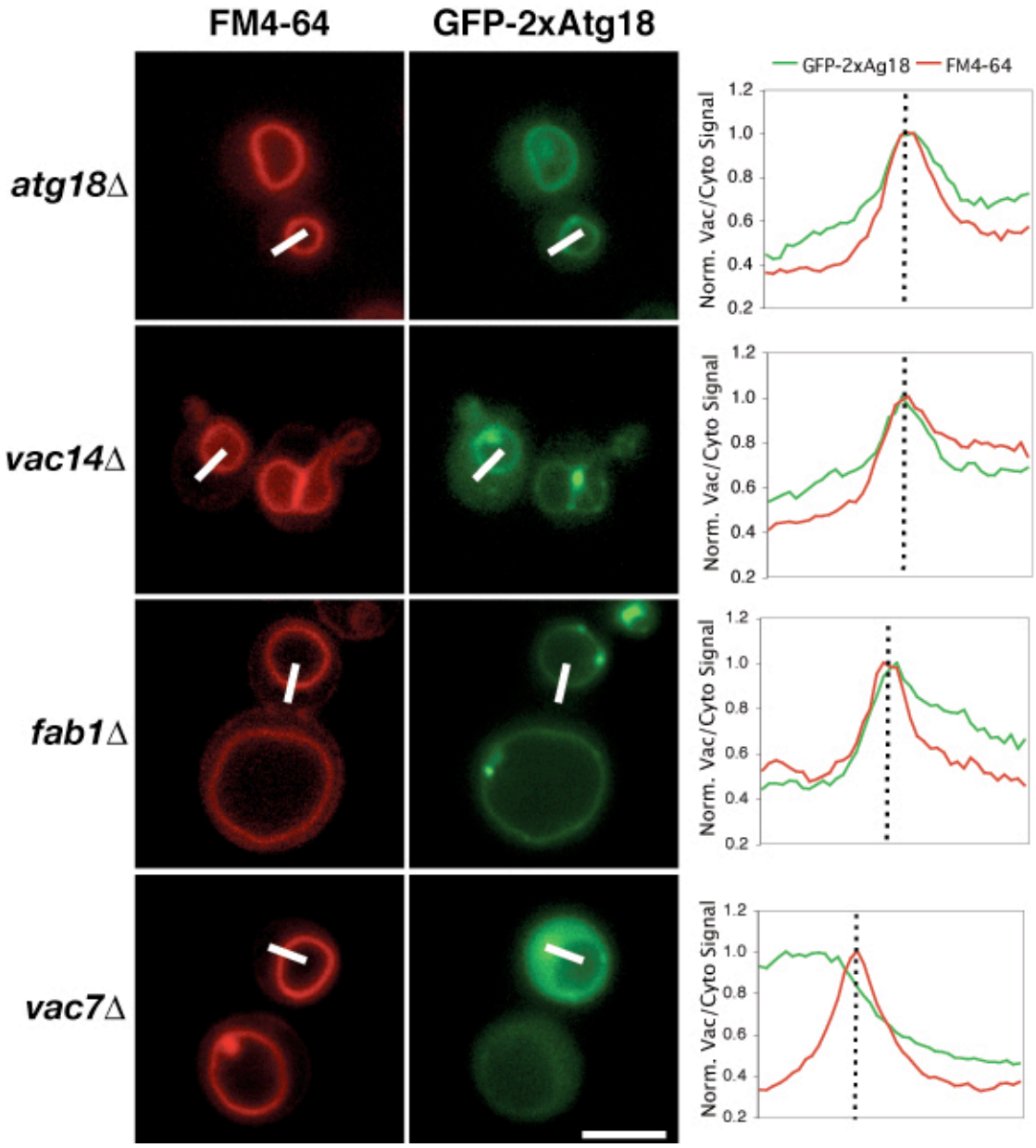
FM4-64
GFP-2xAtg18
atg18Δ
vac14Δ
fab1Δ
vac7Δ
GFP-2xAg18
FM4-64
Norm. Vac/Cyto Signal
1.2
1.0
0.8
0.6
0.4
0.2

Figure 4.6 Atg18p interacts with Vac17p *in vivo*. (A) Osmotic lysates from cells metabolically labeled with ^{35}S-methionine for one hour were cross-linked with DSP for 30 minutes and Atg18-HA was immunoprecipitated as described in MATERIALS AND METHODS. Following cleavage of the cross-linker, associated proteins were visualized by SDS-PAGE and subsequent autoradiography. (B) 20 OD_{600} units of the indicated strains were spheroplasted and osmotically lysed. Atg18-FLAG was immunoprecipitated from detergent-treated (0.2% Tween-20) whole cell lysates and association with GFP-Vac17 was determined by SDS-PAGE.

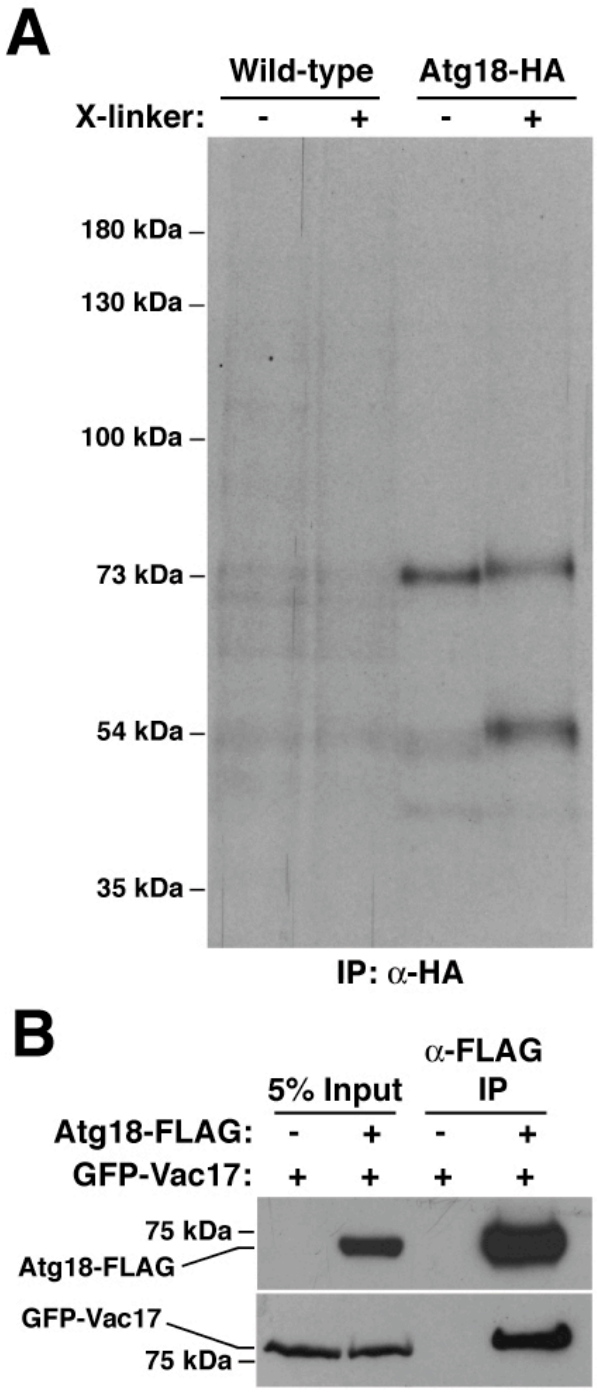
A
Wild-type
Atg18-HA
X-linker:
-
+
-
+
180 kDa
130 kDa
100 kDa
73 kDa
54 kDa
35 kDa
IP: α-HA
B
α-FLAG
IP
5% Input
Atg18-FLAG:
-
+
-
+
GFP-Vac17:
+
+
+
+
75 kDa
Atg18-FLAG
GFP-Vac17
75 kDa

Figure 4.7 Model of vacuole size regulation by PtdIns(3,5)P_2 and Atg18p. (A) PtdIns(3)*P* and PtdIns(3,5)P_2 most likely recruit Atg18 to two distinct membrane compartments, where it is required for autophagy (PAS) and regulation of organelle morphology (vacuole), respectively. On the vacuole, we envision Atg18 acting as a "sensor" of PtdIns(3,5)P_2, continually cycling between the cytosol (Atg18^{CYTO}) and the limiting membrane (Atg18^{VAC}) in response to changes in phosphoinositide levels. One function of Atg18 on the membrane is to inhibit the Fab1 kinase, thus establishing a negative feedback loop. This circuit forms the integral part of an elegant system that allows dynamic control of vacuole morphology. (B) Model for Atg18 function as it cycles on and off the vacuole membrane. During/following recruitment by the phospholipid PtdIns(3,5)P_2, Atg18 also associates with Vac7 and Vac17. Atg18 may indirectly regulate activity of the Fab1 kinase by sequestering Vac7. Vac17 most likely functions as a myosin-specific adapter for Atg18, thus enabling retrograde membrane transport from the vacuole along actin tracks. Membrane deformation could be directly or indirectly – e.g. via recruitment of an as of yet unidentified fission factor – mediated by Atg18.

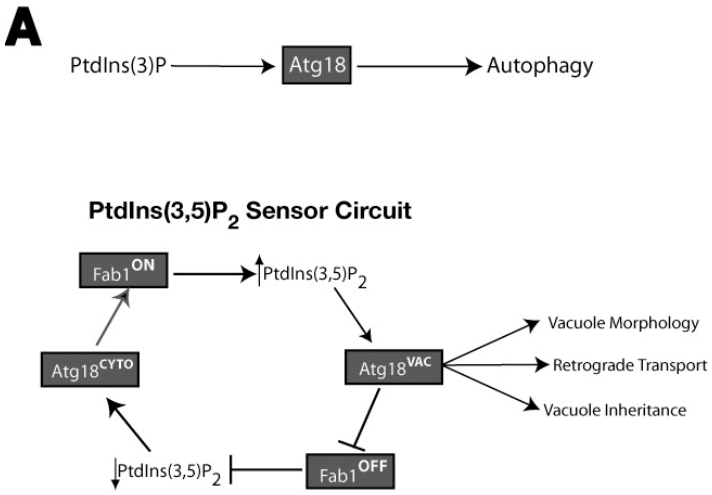
A
PtdIns(3)P
Atg18
Autophagy
PtdIns(3,5)P2 Sensor Circuit
Fab1ON
PtdIns(3,5)P2
Vacuole Morphology
Retrograde Transport
Vacuole Inheritance
Atg18CYTO
Atg18VAC
PtdIns(3,5)P2
Fab1OFF

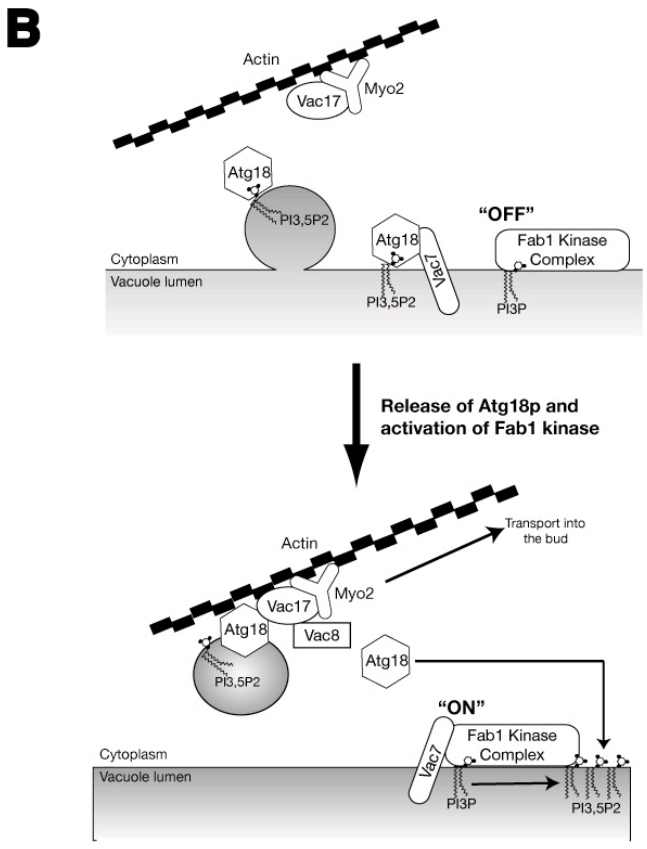
B
Actin
Vac17
Myo2
Atg18
PI3,5P2
"OFF"
Atg18
Vac7
Fab1 Kinase Complex
Cytoplasm
Vacuole lumen
PI3,5P2
PI3P
Release of Atg18p and activation of Fab1 kinase
Transport into the bud
Actin
Myo2
Vac17
Atg18
Vac8
PI3,5P2
Atg18
"ON"
Fab1 Kinase Complex
Vac7
Cytoplasm
Vacuole lumen
PI3P
PI3,5P2

ACKNOWLEDGEMENTS

We would like to thank Dr. Simon Rudge for his contributions in the early stages of the project as well as helpful discussions throughout. This work was supported in part by a fellowship from the Canadian Institutes of Health Research to R.J.B. S.D.E is an investigator of the Howard Hughes Medical Institute.

This chapter, in full, has been submitted for publication of the material as it appears in Molecular Biology of the Cell, 2007. Efe, J.A., Botelho, R.J., and S.D. Emr. Atg18p interacts with the Fab1 kinase activator Vac7p and regulates vacuole morphology independent of PtdIns(3,5)P_2. The dissertation author was the primary investigator and author of this paper.

CHAPTER 5

CONCLUSION: SUMMARY AND FUTURE DIRECTIONS

The processes of anterograde and retrograde membrane trafficking, osmoregulation, and vacuole inheritance are all linked to vacuole size regulation. While the major pathways governing these processes have been identified, a complete picture has yet to emerge. The research presented here was conducted with the goal of furthering our knowledge of how the individual pathways opertate, while at the same time maintaining a holistic view emphasizing continuity and interdependence.

Mon2p Is Required for Vacuolar Homeostasis and Cytoplasm-to-vacuole Transport

We have shown that Mon2p predominantly localizes to Golgi membranes, where it appears to play key roles in regulating endomembrane traffic. Not only do vacuoles fragment in the absence of Mon2p, but anterograde trafficking of ALP and retrograde traffic to the Golgi are also affected to varying degrees. Even though it has been proposed that Mon2p might be acting as a GEF for Arl1p, the absence of an actual catalytic domain in Mon2p raises questions about this hypothesis (Jochum *et al.*, 2002a).

Rather, recent research indicates that Mon2p most likely plays a scaffolding role, recruiting proteins critical to endomembrane homeostasis (Gillingham *et al.*, 2006). Furthermore, it likely has this function on multiple membrane compartments: two of the known interactors of Mon2p (Dop1p and Neo1) are thought to function on and ensure the integrity of endoplasmic reticulum membranes as well (Hua and Graham, 2003; Gillingham *et al.*, 2006). These observations might help explain why the deletion of *MON2*, unlike that of other genes encoding regulators of anterograde membrane traffic at the Golgi, has such a profound effect on the overall health of yeast cells. Perturbances in ER structure observed upon inactivation of Dop1p and Neo1p are presumably responsible for the lethal nature of their deletion (Gillingham and Munro, 2003; Hua and Graham, 2003). In the absence of Mon2p, a barely sufficient number of complexes might be forming on ER and Golgi membranes, allowing cells to stay alive.

Regarding the role of Mon2p in Cvt transport, it is unlikely that the defect observed in *mon2Δ* cells is an indirect result of vacuolar fragmentation or loss of the fusion machinery on target membranes, since macroautophagy (which uses most of same machinery) is unaffected in the deletion mutant. Deletion of critical fusion factors such as *MON1* and *CCZ1* adversely affects all types of vacuolar fusion reactions (Wang *et al.*, 2003). At this point, a more plausible hypothesis is that transport of a key Cvt protein from the Golgi is

impaired in the *mon2Δ* mutant. In fact, it might be the unavailability of Golgi membranes in general for Cvt vesicle formation that ultimately leads to the observed block. While the source of Cvt vesicle membranes is at present unclear, the Golgi has been implicated by others as well (Reggiori *et al.*, 2004b).

Future work on Mon2p will require a multi-pronged approach: first, the role of Arl1p in Golgi functions needs to be clarified. Most recent evidence suggest that a Mon2p-Arl1p-Neo1p complex plays a key role in Golgi/endosome homeostasis, but a clear function or mechanism is still lacking (Wicky *et al.*, 2004). Arl1p is also known to recruit the GRIP domain protein Imh1 to the Golgi, a function now linked to Gas1p transport to the plasma membrane (Liu *et al.*, 2006), but Mon2p has not been linked to this function. Second, possible functions for Mon2p at the ER need to be explored, especially in the context of Neo1p and Dop1p function; not much is currently known about the latter. The nuclear abnormalities observed in the *mon2Δ* strain could potentially stem from a defect in this compartment. Third, a closer look needs to be taken at the Cvt defects in the deletion strain: at exactly which stage is the process arrested, and are any of the other known Cvt proteins mislocalized in the absence of Mon2p?

Providing answers to these questions will undoubtedly represent an important advancement of our knowledge in the area of membrane trafficking,

especially given the high degree of conservation observed for Mon2p and the newly characterized Dop1p.

A Yeast Genetic Screen Identifies *L. pneumophila* Proteins that May Inhibit Endosomal/Vacuolar maturation

Due to the high degree of conservation in membrane trafficking pathways from yeast to humans, the former has been utilized to study the mode of action of certain pathogenic factors from bacteria (Valdivia, 2004). While the data obtained from such experiments may not be immediately relevant and follow-up studies in higher eukaryotic systems are required, the relative ease of conducting genetic studies in yeast can dramatically shorten the time needed to make an important initial discovery.

Here we have taken this approach one step further, using a yeast genetic screening method (PEPSY) to identify novel *L. pneumophila* proteins capable of inhibiting endosomal/vacuolar maturation. This inhibition is a hallmark of the infectious process, enabling rapid multiplication of the pathogen in a non-acidified, protective pre-vacuolar compartment resembling rough ER (Kagan and Roy, 2002). We reasoned that proteins causing membrane trafficking defects when overexpressed in yeast would be likely candidates for secretion into the host cytosol during a *Legionella* infection. Indeed, by transforming a *Legionella* genomic library into yeast and using a

colorimetric screening process, we were able to identify multiple proteins that perturbed endosomal maturation to varying extents. All were found to be substrates for the Legionella Icm/Dot translocation apparatus. These Vip proteins have now been added to the list of Icm/Dot effector proteins awaiting to be functionally characterized.

Unfortunately, the recognizable domains contained in the Vip proteins provide only very general information regarding their functions. Follow-up studies will focus on interactors of these proteins, with the goal of expressly identifying the pathways they perturb. For example, preliminary data suggest that VipD may interact with actin (our unpublished results). Moreover, it is important to note that yeast genetics provides another opportunity at this juncture: suppressor screens could be done to identify host genes that counter the effects of Vip overexpression. As the various functions of the Vip proteins become clearer, pathogen-host interactions will most likely provide novel insight into the regulation of endomembrane traffic near or at the eukaryotic lysosome/vacuole. For example, PtdIns4*P* has been implicated in the recruitment of virulence factors to the vacuolar limiting membrane upon *Legionella* infection (Weber *et al.*, 2006).

In the meantime, the PEPSY technique has also been succesfully used to identify novel *Chlamydia trachomatis* proteins relevant to pathogenesis (Sisko *et al.*, 2006).

Atg18 is the Effector that links PtdIns(3,5)P_2 Metabolism to Vacuole Morphology

It has been known for a number of years that cellular PtdIns(3,5)P_2 levels and vacuole size are inversely correlated (Gary *et al.*, 1998). Identification of the upstream activators of the Fab1 kinase, Vac7p and Vac14p, as well as the phosphatase Fig4 greatly enhanced our understanding of how PtdIns(3,5)P_2 synthesis and turnover are regulated, but the crucial link to vacuole size was not understood until Atg18p was observed to localize to the vacuole in a PtdIns(3,5)P_2-dependent manner (Bonangelino *et al.*, 2002b; Gary *et al.*, 2002; Dove *et al.*, 2004; Rudge *et al.*, 2004). We have now shown that Atg18 is a bona fide effector of PtdIns(3,5)P_2, both necessary and sufficient for remodeling the membranes of yeast vacuoles. The data presented implicate Vac7p as the link between Atg18p and the PtdIns(3,5)P_2 synthesis machinery. We have hypothesized that Vac7p not only constitutes the protein component of Atg18p recruitment to the vacuole, but also allows Atg18p to inhibit Fab1 kinase function by sequestering Vac7p, its major upstream activator. Intriguingly, the PtdIns(3,5)P_2 binding site identified by Dove *et al.* (2004) appears only to be required for recruitment and not for membrane remodeling or kinase inhibition by Atg18p. Finally, a possible role for Atg18p in vacuole inheritance and/or retrograde membrane traffic from the

vacuole is suggested, based on (a) the observation of a vesicular structure enhanced in Atg18-GFP budding from the vacuole membrane and (b) a strong physical interaction with the inheritance protein Vac17p.

Ultimately, a complete understanding of vacuole size control in yeast requires elucidating the molecular basis of the process. As the next step, it will be critical to find out whether Atg18 is capable of remodeling membranes on its own, or whether an effector must be separately recruited for this process. Furthermore, it is just as important to clarify whether a direct interaction between Atg18p and Vac7p can be demonstrated. Regardless of whether this turns out to be the case, preliminary evidence suggest that there could also be other ways in which Atg18p physically interacts with the PtdIns(3,5)P_2 production machinery (our unpublished results). Once these relationships are better understood, it may be easier to discern what constitutes the molecular switch between the autphagic and vacuole size control roles of Atg18 and how are these dual roles balanced. Finally, the Atg18p-Vac17p complex will need to be probed further to understand how it fits into the larger picture.

In the long run, identifying other novel effectors will be just as critical in solving the complex regulation of PtdIns(3,5)P_2 metabolism at the vacuole. Importantly, the high degree of conservation between the yeast (Fab1p) and mammalian (PIKfyve) pathways suggests that insights from yeast will be

important in a broader context as well (Sbrissa *et al.*, 2004; Sbrissa and Shisheva, 2005; Chow *et al.*, 2007; Ikonomov *et al.*, 2007; Sbrissa *et al.*, 2007). While significant progress has been made in the context of homotypic vacuole fusion, several key questions regarding membrane recycling and vacuole/vesicle fission remain unanswered: what are the components of the machinery driving fragmentation of the vacuole and how are they linked to Atg18p and PtdIns(3,5)P_2 metabolism? To what extent does the fission apparatus contribute to vacuolar membrane recycling via retrograde transport or microautophagy? Are there any endogenous proteins (e.g. a v-SNARE) that could be used reliably in assays probing retrograde transport? Through which effector(s) does PtdIns(3,5)P_2 regulate MVB sorting? Providing answers to these and other questions will be critical to understanding the mechanisms for regulating the size, shape, and number of this interesting organelle.

ACKNOWLEDGEMENTS

This chapter includes, in part, material as it appears in *Current Opinion in Cell Biology* 17(4):402-8, 2005. Efe, J.A., Botelho, R.J., and S.D. Emr. The Fab1 phosphatidylinositol kinase pathway in the regulation of vacuole morphology. The dissertation author was the primary investigator and author of this paper.

REFERENCES

1. Altschul, S.F., Madden, T.L., Schaffer, A.A., Zhang, J., Zhang, Z., Miller, W., and Lipman, D.J. (1997). Gapped BLAST and PSI-BLAST: a new generation of protein database search programs. Nucleic Acids Res *25*, 3389-3402.

2. Avaro, S., Belgareh-Touze, N., Sibella-Arguelles, C., Volland, C., and Haguenauer-Tsapis, R. (2002). Mutants defective in secretory/vacuolar pathways in the EUROFAN collection of yeast disruptants. Yeast *19*, 351-371.

3. Babst, M., Odorizzi, G., Estepa, E.J., and Emr, S.D. (2000). Mammalian tumor susceptibility gene 101 (TSG101) and the yeast homologue, Vps23p, both function in late endosomal trafficking. Traffic *1*, 248-258.

4. Babst, M., Wendland, B., Estepa, E.J., and Emr, S.D. (1998). The Vps4p AAA ATPase regulates membrane association of a Vps protein complex required for normal endosome function. Embo J *17*, 2982-2993.

5. Balasubramanian, K., and Schroit, A.J. (2003). Aminophospholipid asymmetry: A matter of life and death. Annu Rev Physiol *65*, 701-734.

6. Balla, T. (2005). Inositol-lipid binding motifs: signal integrators through protein-lipid and protein-protein interactions. J Cell Sci *118*, 2093-2104.

7. Bankaitis, V.A., Johnson, L.M., and Emr, S.D. (1986a). Isolation of yeast mutants defective in protein targeting to the vacuole. Proc Natl Acad Sci U S A *83*, 9075-9079.

8. Banta, L.M., Robinson, J.S., Klionsky, D.J., and Emr, S.D. (1988). Organelle assembly in yeast: characterization of yeast mutants defective in vacuolar biogenesis and protein sorting. J Cell Biol *107*, 1369-1383.

9. Barr, F.A., and Short, B. (2003). Golgins in the structure and dynamics of the Golgi apparatus. Curr Opin Cell Biol *15*, 405-413.

10. Barth, H., Meiling-Wesse, K., Epple, U.D., and Thumm, M. (2001). Autophagy and the cytoplasm to vacuole targeting pathway both require Aut10p. FEBS Lett *508*, 23-28.

11. Behnia, R., and Munro, S. (2005). Organelle identity and the signposts for membrane traffic. Nature *438*, 597-604.

12. Bonangelino, C.J., Catlett, N.L., and Weisman, L.S. (1997). Vac7p, a novel vacuolar protein, is required for normal vacuole inheritance and morphology. Mol Cell Biol *17*, 6847-6858.

13. Bonangelino, C.J., Chavez, E.M., and Bonifacino, J.S. (2002a). Genomic screen for vacuolar protein sorting genes in Saccharomyces cerevisiae. Mol Biol Cell *13*, 2486-2501.

14. Bonangelino, C.J., Nau, J.J., Duex, J.E., Brinkman, M., Wurmser, A.E., Gary, J.D., Emr, S.D., and Weisman, L.S. (2002b). Osmotic stress-induced increase of phosphatidylinositol 3,5-bisphosphate requires Vac14p, an activator of the lipid kinase Fab1p. J Cell Biol *156*, 1015-1028.

15. Bryant, N.J., Piper, R.C., Weisman, L.S., and Stevens, T.H. (1998). Retrograde traffic out of the yeast vacuole to the TGN occurs via the prevacuolar/endosomal compartment. J Cell Biol *142*, 651-663.

16. Bryant, N.J., and Stevens, T.H. (1998a). Vacuole biogenesis in Saccharomyces cerevisiae: protein transport pathways to the yeast vacuole. Microbiol Mol Biol Rev *62*, 230-247.

17. Bucher, P., Karplus, K., Moeri, N., and Hofmann, K. (1996). A flexible motif search technique based on generalized profiles. Comput Chem *20*, 3-23.

18. Burd, C.G., and Emr, S.D. (1998). Phosphatidylinositol(3)-phosphate signaling mediated by specific binding to RING FYVE domains. Mol Cell *2*, 157-162.

19. Burkhard, P., Stetefeld, J., and Strelkov, S.V. (2001). Coiled coils: a highly versatile protein folding motif. Trends Cell Biol *11*, 82-88.

20. Catlett, N.L., and Weisman, L.S. (1998). The terminal tail region of a yeast myosin-V mediates its attachment to vacuole membranes and sites of polarized growth. Proc Natl Acad Sci U S A *95*, 14799-14804.

21. Chardin, P., Paris, S., Antonny, B., Robineau, S., Beraud-Dufour, S., Jackson, C.L., and Chabre, M. (1996). A human exchange factor for ARF contains Sec7- and pleckstrin-homology domains. Nature *384*, 481-484.

22. Chen, J., Suwwan de Felipe, K., Clarke, M., Lu, H., Anderson, O.R., Segal, G., and Shuman, H.A. (2004). Legionella Effectors That Promote Nonlytic Release from Protozoa. Science *303*, 1358-1361.

23. Chen, J.Y., Brunauer, L.S., Chu, F.C., Helsel, C.M., Gedde, M.M., and Huestis, W.H. (2003). Selective amphipathic nature of chlorpromazine binding to plasma membrane bilayers. Biochim Biophys Acta *1616*, 95-105.

24. Cherfils, J., Menetrey, J., Mathieu, M., Le Bras, G., Robineau, S., Beraud-Dufour, S., Antonny, B., and Chardin, P. (1998). Structure of the Sec7 domain of the Arf exchange factor ARNO. Nature *392*, 101-105.

25. Chien, M., Morozova, I., Shi, S., Sheng, H., Chen, J., Gomez, S.M., Asamani, G., Hill, K., Nuara, J., Feder, M., Rineer, J., Greenberg, J.J., Steshenko, V., Park, S.H., Zhao, B., Teplitskaya, E., Edwards, J.R., Pampou, S., Georghiou, A., Chou, I.C., Iannuccilli, W., Ulz, M.E., Kim, D.H., Geringer-Sameth, A., Goldsberry, C., Morozov, P., Fischer, S.G., Segal, G., Qu, X., Rzhetsky, A., Zhang, P., Cayanis, E., De Jong, P.J., Ju, J., Kalachikov, S., Shuman, H.A., and Russo, J.J. (2004). The genomic sequence of the accidental pathogen Legionella pneumophila. Science *305*, 1966-1968.

26. Chow, C.Y., Zhang, Y., Dowling, J.J., Jin, N., Adamska, M., Shiga, K., Szigeti, K., Shy, M.E., Li, J., Zhang, X., Lupski, J.R., Weisman, L.S., and Meisler, M.H. (2007). Mutation of FIG4 causes neurodegeneration in the pale tremor mouse and patients with CMT4J. Nature *448*, 68-72.

27. Cianciotto, N.P. (2001). Pathogenicity of Legionella pneumophila. Int J Med Microbiol *291*, 331-343.

28. Clague, M.J., Jones, A.T., Mills, I.G., Walker, D.M., and Urbe, S. (1999). Regulation of early-endosome dynamics by phosphatidylinositol 3-phosphate binding proteins. Biochem Soc Trans *27*, 662-666.

29. Conover, G.M., Derre, I., Vogel, J.P., and Isberg, R.R. (2003). The *Legionella pneumophila* LidA protein: a translocated substrate of the Dot/Icm system associated with maintenance of bacterial integrity. Mol Microbiol *48*, 305-321.

30. Cooke, F.T., Dove, S.K., McEwen, R.K., Painter, G., Holmes, A.B., Hall, M.N., Michell, R.H., and Parker, P.J. (1998). The stress-activated phosphatidylinositol 3-phosphate 5-kinase Fab1p is essential for vacuole function in S. cerevisiae. Curr Biol *8*, 1219-1222.

31. Coppolecchia, R., Buser, P., Stotz, A., and Linder, P. (1993). A new yeast translation initiation factor suppresses a mutation in the eIF-4A RNA helicase. Embo J *12*, 4005-4011.

32. Darsow, T., Odorizzi, G., and Emr, S.D. (2000). Invertase fusion proteins for analysis of protein trafficking in yeast. Methods Enzymol *327*, 95-106.

33. Darsow, T., Rieder, S.E., and Emr, S.D. (1997). A multispecificity syntaxin homologue, Vam3p, essential for autophagic and biosynthetic protein transport to the vacuole. J Cell Biol *138*, 517-529.

34. de Figueiredo, P., Doody, A., Polizotto, R.S., Drecktrah, D., Wood, S., Banta, M., Strang, M.S., and Brown, W.J. (2001). Inhibition of transferrin recycling and endosome tubulation by phospholipase A2 antagonists. J Biol Chem *276*, 47361-47370.

35. Deloche, O., de la Cruz, J., Kressler, D., Doere, M., and Linder, P. (2004). A membrane transport defect leads to a rapid attenuation of translation initiation in Saccharomyces cerevisiae. Mol Cell *13*, 357-366.

36. Di Paolo, G., and De Camilli, P. (2006). Phosphoinositides in cell regulation and membrane dynamics. Nature *443*, 651-657.

37. Dove, S.K., Cooke, F.T., Douglas, M.R., Sayers, L.G., Parker, P.J., and Michell, R.H. (1997). Osmotic stress activates phosphatidylinositol-3,5-bisphosphate synthesis. Nature *390*, 187-192.

38. Dove, S.K., McEwen, R.K., Mayes, A., Hughes, D.C., Beggs, J.D., and Michell, R.H. (2002). Vac14 controls PtdIns(3,5)P(2) synthesis and Fab1-dependent protein trafficking to the multivesicular body. Curr Biol *12*, 885-893.

39. Dove, S.K., Piper, R.C., McEwen, R.K., Yu, J.W., King, M.C., Hughes, D.C., Thuring, J., Holmes, A.B., Cooke, F.T., Michell, R.H., Parker, P.J., and Lemmon, M.A. (2004). Svp1p defines a family of phosphatidylinositol 3,5-bisphosphate effectors. Embo J *23*, 1922-1933.

40. Duex, J.E., Nau, J.J., Kauffman, E.J., and Weisman, L.S. (2006a). Phosphoinositide 5-phosphatase Fig 4p is required for both acute rise and subsequent fall in stress-induced phosphatidylinositol 3,5-bisphosphate levels. Eukaryot Cell *5*, 723-731.

41. Duex, J.E., Tang, F., and Weisman, L.S. (2006b). The Vac14p-Fig4p complex acts independently of Vac7p and couples PI3,5P2 synthesis and turnover. J Cell Biol *172*, 693-704.

42. Efe, J.A., Botelho, R.J., and Emr, S.D. (2005). The Fab1 phosphatidylinositol kinase pathway in the regulation of vacuole morphology. Curr Opin Cell Biol *17*, 402-408.

43. Eugster, A., Pecheur, E.I., Michel, F., Winsor, B., Letourneur, F., and Friant, S. (2004). Ent5p is required with Ent3p and Vps27p for ubiquitin-dependent protein sorting into the multivesicular body. Mol Biol Cell *15*, 3031-3041.

44. Fratti, R.A., Backer, J.M., Gruenberg, J., Corvera, S., and Deretic, V. (2001). Role of phosphatidylinositol 3-kinase and Rab5 effectors in phagosomal biogenesis and mycobacterial phagosome maturation arrest. J Cell Biol *154*, 631-644.

45. Fratti, R.A., Jun, Y., Merz, A.J., Margolis, N., and Wickner, W. (2004). Interdependent assembly of specific regulatory lipids and membrane fusion proteins into the vertex ring domain of docked vacuoles. J Cell Biol *167*, 1087-1098.

46. Friant, S., Pecheur, E.I., Eugster, A., Michel, F., Lefkir, Y., Nourrisson, D., and Letourneur, F. (2003). Ent3p Is a PtdIns(3,5)P2 effector required for protein sorting to the multivesicular body. Dev Cell *5*, 499-511.

47. Fuller, R.S., Sterne, R.E., and Thorner, J. (1988). Enzymes required for yeast prohormone processing. Annu Rev Physiol *50*, 345-362.

48. Gary, J.D., Sato, T.K., Stefan, C.J., Bonangelino, C.J., Weisman, L.S., and Emr, S.D. (2002). Regulation of Fab1 phosphatidylinositol 3-phosphate 5-kinase pathway by Vac7 protein and Fig4, a polyphosphoinositide phosphatase family member. Mol Biol Cell *13*, 1238-1251.

49. Gary, J.D., Wurmser, A.E., Bonangelino, C.J., Weisman, L.S., and Emr, S.D. (1998). Fab1p is essential for PtdIns(3)P 5-kinase activity and the maintenance of vacuolar size and membrane homeostasis. J Cell Biol *143*, 65-79.

50. Gaynor, E.C., te Heesen, S., Graham, T.R., Aebi, M., and Emr, S.D. (1994). Signal-mediated retrieval of a membrane protein from the Golgi to the ER in yeast. J Cell Biol *127*, 653-665.

51. Georgakopoulos, T., Koutroubas, G., Vakonakis, I., Tzermia, M., Prokova, V., Voutsina, A., and Alexandraki, D. (2001). Functional analysis of the Saccharomyces cerevisiae YFR021w/YGR223c/YPL100w ORF family suggests relations to mitochondrial/peroxisomal functions and amino acid signalling pathways. Yeast *18*, 1155-1171.

52. Gillingham, A.K., and Munro, S. (2003). Long coiled-coil proteins and membrane traffic. Biochim Biophys Acta *1641*, 71-85.

53. Gillingham, A.K., Whyte, J.R., Panic, B., and Munro, S. (2006). Mon2, a relative of large Arf exchange factors, recruits Dop1 to the Golgi apparatus. J Biol Chem *281*, 2273-2280.

54. Gillooly, D.J., Morrow, I.C., Lindsay, M., Gould, R., Bryant, N.J., Gaullier, J.M., Parton, R.G., and Stenmark, H. (2000). Localization of phosphatidylinositol 3-phosphate in yeast and mammalian cells. Embo J *19*, 4577-4588.

55. Girotti, M., Evans, J.H., Burke, D., and Leslie, C.C. (2004). Cytosolic phospholipase A2 translocates to forming phagosomes during phagocytosis of zymosan in macrophages. J Biol Chem *279*, 19113-19121.

56. Gomes De Mesquita, D.S., Shaw, J., Grimbergen, J.A., Buys, M.A., Dewi, L., and Woldringh, C.L. (1997). Vacuole segregation in the Saccharomyces cerevisiae vac2-1 mutant: structural and biochemical quantification of the segregation defect and formation of new vacuoles. Yeast *13*, 999-1008.

57. Gomes de Mesquita, D.S., ten Hoopen, R., and Woldringh, C.L. (1991). Vacuolar segregation to the bud of Saccharomyces cerevisiae: an analysis of morphology and timing in the cell cycle. J Gen Microbiol *137*, 2447-2454.

58. Gruenberg, J., and Stenmark, H. (2004). The biogenesis of multivesicular endosomes. Nat Rev Mol Cell Biol *5*, 317-323.

59. Guan, J., Stromhaug, P.E., George, M.D., Habibzadegah-Tari, P., Bevan, A., Dunn, W.A., Jr., and Klionsky, D.J. (2001). Cvt18/Gsa12 is

required for cytoplasm-to-vacuole transport, pexophagy, and autophagy in Saccharomyces cerevisiae and Pichia pastoris. Mol Biol Cell *12*, 3821-3838.

60. Haas, A., Scheglmann, D., Lazar, T., Gallwitz, D., and Wickner, W. (1995). The GTPase Ypt7p of Saccharomyces cerevisiae is required on both partner vacuoles for the homotypic fusion step of vacuole inheritance. Embo J *14*, 5258-5270.

61. Han, B.K., Aramayo, R., and Polymenis, M. (2003). The G1 cyclin Cln3p controls vacuolar biogenesis in Saccharomyces cerevisiae. Genetics *165*, 467-476.

62. Harsay, E., and Bretscher, A. (1995). Parallel secretory pathways to the cell surface in yeast. J Cell Biol *131*, 297-310.

63. Herskowitz, I., and Jensen, R.E. (1991). Putting the HO gene to work: practical uses for mating-type switching. Methods Enzymol *194*, 132-146.

64. Hilgemann, D.W., Feng, S., and Nasuhoglu, C. (2001). The complex and intriguing lives of PIP2 with ion channels and transporters. Sci STKE *2001*, RE19.

65. Hoffman, C.S., and Winston, F. (1987). A ten-minute DNA preparation from yeast efficiently releases autonomous plasmids for transformation of Escherichia coli. Gene *57*, 267-272.

66. Horazdovsky, B.F., Busch, G.R., and Emr, S.D. (1994). VPS21 encodes a rab5-like GTP binding protein that is required for the sorting of yeast vacuolar proteins. Embo J *13*, 1297-1309.

67. Horwitz, M.A., and Maxfield, F.R. (1984). *Legionella pneumophila* inhibits acidification of its phagosome in human monocytes. J Cell Biol *99*, 1936-1943.

68. Horwitz, M.A., and Silverstein, S.C. (1983). Intracellular multiplication of Legionnaires' disease bacteria (Legionella pneumophila) in human monocytes is reversibly inhibited by erythromycin and rifampin. J Clin Invest *71*, 15-26.

69. Hua, Z., and Graham, T.R. (2003). Requirement for neo1p in retrograde transport from the Golgi complex to the endoplasmic reticulum. Mol Biol Cell *14*, 4971-4983.

70. Ikonomov, O.C., Sbrissa, D., Dondapati, R., and Shisheva, A. (2007). ArPIKfyve-PIKfyve interaction and role in insulin-regulated GLUT4 translocation and glucose transport in 3T3-L1 adipocytes. Exp Cell Res *313*, 2404-2416.

71. Ikonomov, O.C., Sbrissa, D., Mlak, K., Kanzaki, M., Pessin, J., and Shisheva, A. (2002). Functional dissection of lipid and protein kinase signals of PIKfyve reveals the role of PtdIns 3,5-P2 production for endomembrane integrity. J Biol Chem *277*, 9206-9211.

72. Ikonomov, O.C., Sbrissa, D., and Shisheva, A. (2001). Mammalian cell morphology and endocytic membrane homeostasis require enzymatically active phosphoinositide 5-kinase PIKfyve. J Biol Chem *276*, 26141-26147.

73. Ishikawa, K., Catlett, N.L., Novak, J.L., Tang, F., Nau, J.J., and Weisman, L.S. (2003). Identification of an organelle-specific myosin V receptor. J Cell Biol *160*, 887-897.

74. Ito, H., Fukuda, Y., Murata, K., and Kimura, A. (1983). Transformation of intact yeast cells treated with alkali cations. J Bacteriol *153*, 163-168.

75. Jackson, C.L., and Casanova, J.E. (2000). Turning on ARF: the Sec7 family of guanine-nucleotide-exchange factors. Trends Cell Biol *10*, 60-67.

76. Jeffries, T.R., Dove, S.K., Michell, R.H., and Parker, P.J. (2004). PtdIns-specific MPR pathway association of a novel WD40 repeat protein, WIPI49. Mol Biol Cell *15*, 2652-2663.

77. Jochum, A., Jackson, D., Schwarz, H., Pipkorn, R., and Singer-Kruger, B. (2002a). Yeast Ysl2p, homologous to Sec7 domain guanine nucleotide exchange factors, functions in endocytosis and maintenance of vacuole integrity and interacts with the Arf-Like small GTPase Arl1p. Mol Cell Biol *22*, 4914-4928.

78. Jordens, I., Marsman, M., Kuijl, C., and Neefjes, J. (2005). Rab proteins, connecting transport and vesicle fusion. Traffic *6*, 1070-1077.

79. Jun, Y., Fratti, R.A., and Wickner, W. (2004). Diacylglycerol and its formation by phospholipase C regulate Rab- and SNARE-dependent yeast vacuole fusion. J Biol Chem *279*, 53186-53195.

80. Jutila, A., Soderlund, T., Pakkanen, A.L., Huttunen, M., and Kinnunen, P.K. (2001). Comparison of the effects of clozapine, chlorpromazine, and haloperidol on membrane lateral heterogeneity. Chem Phys Lipids *112*, 151-163.

81. Kagan, J.C., and Roy, C.R. (2002). Legionella phagosomes intercept vesicular traffic from endoplasmic reticulum exit sites. Nat Cell Biol *4*, 945-954.

82. Kaiser, C.A., and Schekman, R. (1990). Distinct sets of SEC genes govern transport vesicle formation and fusion early in the secretory pathway. Cell *61*, 723-733.

83. Katzmann, D.J., Odorizzi, G., and Emr, S.D. (2002). Receptor downregulation and multivesicular-body sorting. Nat Rev Mol Cell Biol *3*, 893-905.

84. Katzmann, D.J., Sarkar, S., Chu, T., Audhya, A., and Emr, S.D. (2004). Multivesicular body sorting: ubiquitin ligase Rsp5 is required for the modification and sorting of carboxypeptidase S. Mol Biol Cell *15*, 468-480.

85. Kihara, A., Noda, T., Ishihara, N., and Ohsumi, Y. (2001). Two distinct Vps34 phosphatidylinositol 3-kinase complexes function in autophagy and carboxypeptidase Y sorting in Saccharomyces cerevisiae. J Cell Biol *152*, 519-530.

86. Kim, Y., Chattopadhyay, S., Locke, S., and Pearce, D.A. (2005). Interaction among Btn1p, Btn2p, and Ist2p Reveals Potential Interplay among the Vacuole, Amino Acid Levels, and Ion Homeostasis in the Yeast Saccharomyces cerevisiae. Eukaryot Cell *4*, 281-288.

87. Klionsky, D.J., Banta, L.M., and Emr, S.D. (1988). Intracellular sorting and processing of a yeast vacuolar hydrolase: proteinase A propeptide contains vacuolar targeting information. Mol Cell Biol *8*, 2105-2116.

88. Klionsky, D.J., and Emr, S.D. (1989). Membrane protein sorting: biosynthesis, transport and processing of yeast vacuolar alkaline phosphatase. Embo J *8*, 2241-2250.

89. Klionsky, D.J., Herman, P.K., and Emr, S.D. (1990). The fungal vacuole: composition, function, and biogenesis. Microbiol Rev *54*, 266-292.

90. Krick, R., Tolstrup, J., Appelles, A., Henke, S., and Thumm, M. (2006). The relevance of the phosphatidylinositolphosphat-binding motif FRRGT of Atg18 and Atg21 for the Cvt pathway and autophagy. FEBS Lett *580*, 4632-4638.

91. Kuroiwa, N., Nakamura, M., Tagaya, M., and Takatsuki, A. (2001). Arachidonyltrifluoromethy ketone, a phospholipase A(2) antagonist, induces dispersal of both Golgi stack- and trans Golgi network-resident proteins throughout the cytoplasm. Biochem Biophys Res Commun *281*, 582-588.

92. Ladant, D., and Ullmann, A. (1999). Bordatella pertussis adenylate cyclase: a toxin with multiple talents. Trends Microbiol *7*, 172-176.

93. Lagrassa, T.J., and Ungermann, C. (2005). The vacuolar kinase Yck3 maintains organelle fragmentation by regulating the HOPS tethering complex. J Cell Biol *168*, 401-414.

94. Latterich, M., and Watson, M.D. (1993). Evidence for a dual osmoregulatory mechanism in the yeast Saccharomyces cerevisiae. Biochem Biophys Res Commun *191*, 1111-1117.

95. Lawe, D.C., Patki, V., Heller-Harrison, R., Lambright, D., and Corvera, S. (2000). The FYVE domain of early endosome antigen 1 is required for both phosphatidylinositol 3-phosphate and Rab5 binding. Critical role of this dual interaction for endosomal localization. J Biol Chem *275*, 3699-3705.

96. Lemmon, M.A. (2003). Phosphoinositide recognition domains. Traffic *4*, 201-213.

97. Lesser, C.F., and Miller, S.I. (2001). Expression of microbial virulence proteins in Saccharomyces cerevisiae models mammalian infection. Embo J *20*, 1840-1849.

98. Liu, Y.W., Lee, S.W., and Lee, F.J. (2006). Arl1p is involved in transport of the GPI-anchored protein Gas1p from the late Golgi to the plasma membrane. J Cell Sci *119*, 3845-3855.

99. Longtine, M.S., McKenzie, A., 3rd, Demarini, D.J., Shah, N.G., Wach, A., Brachat, A., Philippsen, P., and Pringle, J.R. (1998). Additional modules for versatile and economical PCR-based gene deletion and modification in Saccharomyces cerevisiae. Yeast *14*, 953-961.

100. Lu, L., and Hong, W. (2003). Interaction of Arl1-GTP with GRIP domains recruits autoantigens Golgin-97 and Golgin-245/p230 onto the Golgi. Mol Biol Cell *14*, 3767-3781.

101. Lu, L., Horstmann, H., Ng, C., and Hong, W. (2001). Regulation of Golgi structure and function by ARF-like protein 1 (Arl1). J Cell Sci *114*, 4543-4555.

102. Luo, Z.Q., and Isberg, R.R. (2004). Multiple substrates of the Legionella pneumophila Dot/Icm system identified by interbacterial protein transfer. Proceedings of the National Academy of Sciences of the United States of America *101*, 841-846.

103. Maniatis, T., Fritsch, E.F., and Sambrook, J. (1992). Molecular Cloning: A Laboratory Manual. Cold Spring Harbor Laboratory Press: Cold Spring Harbor, NY.

104. Mansour, S.J., Skaug, J., Zhao, X.H., Giordano, J., Scherer, S.W., and Melancon, P. (1999). p200 ARF-GEP1: a Golgi-localized guanine nucleotide exchange protein whose Sec7 domain is targeted by the drug brefeldin A. Proc Natl Acad Sci U S A *96*, 7968-7973.

105. Morinaga, N., Moss, J., and Vaughan, M. (1997). Cloning and expression of a cDNA encoding a bovine brain brefeldin A-sensitive guanine nucleotide-exchange protein for ADP-ribosylation factor. Proc Natl Acad Sci U S A *94*, 12926-12931.

106. Mouratou, B., Biou, V., Joubert, A., Cohen, J., Shields, D.J., Geldner, N., Jurgens, G., Melancon, P., and Cherfils, J. (2005). The domain architecture of large guanine nucleotide exchange factors for the small GTP-binding protein Arf. BMC Genomics *6*, 20.

107. Muller, O., Sattler, T., Flotenmeyer, M., Schwarz, H., Plattner, H., and Mayer, A. (2000). Autophagic tubes: vacuolar invaginations involved in lateral membrane sorting and inverse vesicle budding. J Cell Biol *151*, 519-528.

108. Munro, S. (2002). Organelle identity and the targeting of peripheral membrane proteins. Curr Opin Cell Biol *14*, 506-514.

109. Munro, S. (2004). Organelle identity and the organization of membrane traffic. Nat Cell Biol *6*, 469-472.

110. Muren, E., Oyen, M., Barmark, G., and Ronne, H. (2001). Identification of yeast deletion strains that are hypersensitive to brefeldin A or monensin, two drugs that affect intracellular transport. Yeast *18*, 163-172.

111. Nagai, H., Kagan, J.C., Zhu, X., Kahn, R.A., and Roy, C.R. (2002). A bacterial guanine nucleotide exchange factor activates ARF on Legionella phagosomes. Science *295*, 679-682.

112. Nair, U., and Klionsky, D.J. (2005). Molecular mechanisms and regulation of specific and nonspecific autophagy pathways in yeast. J Biol Chem *280*, 41785-41788.

113. Natarajan, P., Wang, J., Hua, Z., and Graham, T.R. (2004). Drs2p-coupled aminophospholipid translocase activity in yeast Golgi membranes and relationship to in vivo function. Proc Natl Acad Sci U S A *101*, 10614-10619.

114. Nie, Z., Hirsch, D.S., and Randazzo, P.A. (2003). Arf and its many interactors. Curr Opin Cell Biol *15*, 396-404.

115. Odorizzi, G., Babst, M., and Emr, S.D. (1998). Fab1p PtdIns(3)P 5-kinase function essential for protein sorting in the multivesicular body. Cell *95*, 847-858.

116. Odorizzi, G., Babst, M., and Emr, S.D. (2000). Phosphoinositide signaling and the regulation of membrane trafficking in yeast. Trends Biochem Sci *25*, 229-235.

117. Odorizzi, G., Cowles, C.R., and Emr, S.D. (1998). The AP-3 complex: a coat of many colours. Trends Cell Biol *8*, 282-288.

118. Onishi, M., Nakamura, Y., Koga, T., Takegawa, K., and Fukui, Y. (2003). Isolation of suppressor mutants of phosphatidylinositol 3-phosphate 5-kinase deficient cells in Schizosaccharomyces pombe. Biosci Biotechnol Biochem *67*, 1772-1779.

119. Panic, B., Perisic, O., Veprintsev, D.B., Williams, R.L., and Munro, S. (2003a). Structural basis for Arl1-dependent targeting of homodimeric GRIP domains to the Golgi apparatus. Mol Cell *12*, 863-874.

120. Panic, B., Whyte, J.R., and Munro, S. (2003b). The ARF-like GTPases Arl1p and Arl3p Act in a Pathway that Interacts with Vesicle-Tethering Factors at the Golgi Apparatus. Curr Biol *13*, 405-410.

121. Pascon, R.C., and Miller, B.L. (2000). Morphogenesis in Aspergillus nidulans requires Dopey (DopA), a member of a novel family of leucine zipper-like proteins conserved from yeast to humans. Mol Microbiol *36*, 1250-1264.

122. Pasqualato, S., Renault, L., and Cherfils, J. (2002). Arf, Arl, Arp and Sar proteins: a family of GTP-binding proteins with a structural device for 'front-back' communication. EMBO Rep *3*, 1035-1041.

123. Payne, G.S., and Schekman, R. (1989). Clathrin: a role in the intracellular retention of a Golgi membrane protein. Science *245*, 1358-1365.

124. Peplowska, K., and Ungermann, C. (2005). Expanding dynamin: from fission to fusion. Nat Cell Biol *7*, 103-104.

125. Peters, C., Baars, T.L., Buhler, S., and Mayer, A. (2004). Mutual control of membrane fission and fusion proteins. Cell *119*, 667-678.

126. Peterson, M.R., and Emr, S.D. (2001). The class C Vps complex functions at multiple stages of the vacuolar transport pathway. Traffic *2*, 476-486.

127. Phillips, R.M., Six, D.A., Dennis, E.A., and Ghosh, P. (2003). In vivo phospholipase activity of the Pseudomonas aeruginosa cytotoxin ExoU and protection of mammalian cells with phospholipase A2 inhibitors. J Biol Chem *278*, 41326-41332.

128. Piper, R.C., Bryant, N.J., and Stevens, T.H. (1997). The membrane protein alkaline phosphatase is delivered to the vacuole by a route that is distinct from the VPS-dependent pathway. J Cell Biol *138*, 531-545.

129. Poupon, V., Stewart, A., Gray, S.R., Piper, R.C., and Luzio, J.P. (2003). The role of mVps18p in clustering, fusion, and intracellular localization of late endocytic organelles. Mol Biol Cell *14*, 4015-4027.

130. Prezant, T.R., Chaltraw, W.E., Jr., and Fischel-Ghodsian, N. (1996). Identification of an overexpressed yeast gene which prevents aminoglycoside toxicity. Microbiology *142 (Pt 12)*, 3407-3414.

131. Proft, M., and Struhl, K. (2004). MAP kinase-mediated stress relief that precedes and regulates the timing of transcriptional induction. Cell *118*, 351-361.

132. Pruyne, D., and Bretscher, A. (2000). Polarization of cell growth in yeast. J Cell Sci *113 (Pt 4)*, 571-585.

133. Rabin, S.D., and Hauser, A.R. (2003). Pseudomonas aeruginosa ExoU, a toxin transported by the type III secretion system, kills Saccharomyces cerevisiae. Infect Immun *71*, 4144-4150.

134. Rabin, S.D., and Hauser, A.R. (2005). Functional regions of the Pseudomonas aeruginosa cytotoxin ExoU. Infect Immun *73*, 573-582.

135. Raymond, C.K., Howald-Stevenson, I., Vater, C.A., and Stevens, T.H. (1992). Morphological classification of the yeast vacuolar protein sorting mutants: evidence for a prevacuolar compartment in class E vps mutants. Mol Biol Cell *3*, 1389-1402.

136. Reggiori, F., Shintani, T., Nair, U., and Klionsky, D.J. (2005). Atg9 cycles between mitochondria and the pre-autophagosomal structure in yeasts. Autophagy *1*, 101-109.

137. Reggiori, F., Tucker, K.A., Stromhaug, P.E., and Klionsky, D.J. (2004a). The Atg1-Atg13 complex regulates Atg9 and Atg23 retrieval transport from the pre-autophagosomal structure. Dev Cell *6*, 79-90.

138. Reggiori, F., Wang, C.W., Nair, U., Shintani, T., Abeliovich, H., and Klionsky, D.J. (2004b). Early stages of the secretory pathway, but not endosomes, are required for Cvt vesicle and autophagosome assembly in Saccharomyces cerevisiae. Mol Biol Cell *15*, 2189-2204.

139. Reggiori, F., Wang, C.W., Stromhaug, P.E., Shintani, T., and Klionsky, D.J. (2003). Vps51 is part of the yeast Vps fifty-three tethering complex essential for retrograde traffic from the early endosome and Cvt vesicle completion. J Biol Chem *278*, 5009-5020.

140. Rieder, S.E., Banta, L.M., Kohrer, K., McCaffery, J.M., and Emr, S.D. (1996). Multilamellar endosome-like compartment accumulates in the yeast vps28 vacuolar protein sorting mutant. Mol Biol Cell *7*, 985-999.

141. Rieder, S.E., and Emr, S.D. (1997). A novel RING finger protein complex essential for a late step in protein transport to the yeast vacuole. Mol Biol Cell *8*, 2307-2327.

142. Robinson, J.S., Klionsky, D.J., Banta, L.M., and Emr, S.D. (1988a). Protein sorting in Saccharomyces cerevisiae: isolation of mutants

defective in the delivery and processing of multiple vacuolar hydrolases. Mol Cell Biol *8*, 4936-4948.

143. Robinson, J.S., Klionsky, D.J., Banta, L.M., and Emr, S.D. (1988b). Protein sorting in Saccharomyces cerevisiae: isolation of mutants defective in the delivery and processing of multiple vacuolar hydrolases. Mol Cell Biol *8*, 4936-4948.

144. Rose, M.D., Winston, F., and Hieter, P. (1990). Methods in Yeast Genetics. A Laboratory Course Manual. Cold Spring Harbor Laboratory Press: Cold Spring Harbor, NY.

145. Rosenwald, A.G., Rhodes, M.A., Van Valkenburgh, H., Palanivel, V., Chapman, G., Boman, A., Zhang, C.J., and Kahn, R.A. (2002). ARL1 and membrane traffic in Saccharomyces cerevisiae. Yeast *19*, 1039-1056.

146. Rost, B. (1996). PHD: predicting one-dimensional protein structure by profile-based neural networks. Methods Enzymol *266*, 525-539.

147. Rudge, S.A., Anderson, D.M., and Emr, S.D. (2004). Vacuole size control: regulation of PtdIns(3,5)P2 levels by the vacuole-associated Vac14-Fig4 complex, a PtdIns(3,5)P2-specific phosphatase. Mol Biol Cell *15*, 24-36.

148. Sato, H., and Frank, D.W. (2004). ExoU is a potent intracellular phospholipase. Mol Microbiol *53*, 1279-1290.

149. Sato, H., Frank, D.W., Hillard, C.J., Feix, J.B., Pankhaniya, R.R., Moriyama, K., Finck-Barbancon, V., Buchaklian, A., Lei, M., Long, R.M., Wiener-Kronish, J., and Sawa, T. (2003). The mechanism of action of the Pseudomonas aeruginosa-encoded type III cytotoxin, ExoU. Embo J *22*, 2959-2969.

150. Sato, T.K., Rehling, P., Peterson, M.R., and Emr, S.D. (2000). Class C Vps protein complex regulates vacuolar SNARE pairing and is required for vesicle docking/fusion. Mol Cell *6*, 661-671.

151. Sbrissa, D., Ikonomov, O.C., Fu, Z., Ijuin, T., Gruenberg, J., Takenawa, T., and Shisheva, A. (2007). Core Protein Machinery for Mammalian Phosphatidylinositol 3,5-Bisphosphate Synthesis and Turnover That Regulates the Progression of Endosomal Transport: NOVEL SAC PHOSPHATASE JOINS THE ArPIKfyve-PIKfyve COMPLEX. J Biol Chem *282*, 23878-23891.

152. Sbrissa, D., Ikonomov, O.C., and Shisheva, A. (1999). PIKfyve, a mammalian ortholog of yeast Fab1p lipid kinase, synthesizes 5-phosphoinositides. Effect of insulin. J Biol Chem *274*, 21589-21597.

153. Sbrissa, D., Ikonomov, O.C., Strakova, J., Dondapati, R., Mlak, K., Deeb, R., Silver, R., and Shisheva, A. (2004). A mammalian ortholog of Saccharomyces cerevisiae Vac14 that associates with and up-regulates PIKfyve phosphoinositide 5-kinase activity. Mol Cell Biol *24*, 10437-10447.

154. Sbrissa, D., and Shisheva, A. (2005). Acquisition of Unprecedented Phosphatidylinositol 3,5-Bisphosphate Rise in Hyperosmotically Stressed 3T3-L1 Adipocytes, Mediated by ArPIKfyve-PIKfyve Pathway. J Biol Chem *280*, 7883-7889.

155. Schu, P.V., Takegawa, K., Fry, M.J., Stack, J.H., Waterfield, M.D., and Emr, S.D. (1993). Phosphatidylinositol 3-kinase encoded by yeast VPS34 gene essential for protein sorting. Science *260*, 88-91.

156. Segal, G., Purcell, M., and Shuman, H.A. (1998). Host cell killing and bacterial conjugation require overlapping sets of genes within a 22-kb region of the Legionella pneumophila genome. Proc Natl Acad Sci U S A *95*, 1669-1674.

157. Setty, S.R., Shin, M.E., Yoshino, A., Marks, M.S., and Burd, C.G. (2003). Golgi recruitment of GRIP domain proteins by Arf-like GTPase 1 is regulated by Arf-like GTPase 3. Curr Biol *13*, 401-404.

158. Sherman, F. (1991). Getting started with yeast. Methods Enzymol. *194*, 2-21.

159. Siddhanta, U., McIlroy, J., Shah, A., Zhang, Y., and Backer, J.M. (1998). Distinct roles for the p110alpha and hVPS34 phosphatidylinositol 3'-kinases in vesicular trafficking, regulation of the actin cytoskeleton, and mitogenesis. J Cell Biol *143*, 1647-1659.

160. Sikorski, R.S., and Hieter, P. (1989). A system of shuttle vectors and yeast host strains designed for efficient manipulation of DNA in Saccharomyces cerevisiae. Genetics *122*, 19-27.

161. Simonsen, A., Lippe, R., Christoforidis, S., Gaullier, J.M., Brech, A., Callaghan, J., Toh, B.H., Murphy, C., Zerial, M., and Stenmark, H. (1998). EEA1 links PI(3)K function to Rab5 regulation of endosome fusion. Nature *394*, 494-498.

162. Singer-Kruger, B., and Ferro-Novick, S. (1997). Use of a synthetic lethal screen to identify yeast mutants impaired in endocytosis, vacuolar protein sorting and the organization of the cytoskeleton. Eur J Cell Biol *74*, 365-375.

163. Sisko, J.L., Spaeth, K., Kumar, Y., and Valdivia, R.H. (2006). Multifunctional analysis of Chlamydia-specific genes in a yeast expression system. Mol Microbiol *60*, 51-66.

164. Starai, V.J., Thorngren, N., Fratti, R.A., and Wickner, W. (2005). Ion regulation of homotypic vacuole fusion in Saccharomyces cerevisiae. J Biol Chem.

165. Stefan, C.J., Audhya, A., and Emr, S.D. (2002). The yeast synaptojanin-like proteins control the cellular distribution of phosphatidylinositol (4,5)-bisphosphate. Mol Biol Cell *13*, 542-557.

166. Stepp, J.D., Huang, K., and Lemmon, S.K. (1997). The yeast adaptor protein complex, AP-3, is essential for the efficient delivery of alkaline phosphatase by the alternate pathway to the vacuole. J Cell Biol *139*, 1761-1774.

167. Stromhaug, P.E., Reggiori, F., Guan, J., Wang, C.W., and Klionsky, D.J. (2004). Atg21 is a phosphoinositide binding protein required for efficient lipidation and localization of Atg8 during uptake of aminopeptidase I by selective autophagy. Mol Biol Cell *15*, 3553-3566.

168. Takenawa, T., and Itoh, T. (2006). Membrane targeting and remodeling through phosphoinositide-binding domains. IUBMB Life *58*, 296-303.

169. Tamas, M.J., and Hohmann, S. (2003). The osmotic stress response of Saccharomyces cerevisiae. Topics in Current Genetics *1*, 121-200.

170. Tang, F., Kauffman, E.J., Novak, J.L., Nau, J.J., Catlett, N.L., and Weisman, L.S. (2003). Regulated degradation of a class V myosin receptor directs movement of the yeast vacuole. Nature *422*, 87-92.

171. Togawa, A., Morinaga, N., Ogasawara, M., Moss, J., and Vaughan, M. (1999). Purification and cloning of a brefeldin A-inhibited guanine nucleotide-exchange protein for ADP-ribosylation factors. J Biol Chem *274*, 12308-12315.

172. Valdivia, R.H. (2004). Modeling the function of bacterial virulence factors in Saccharomyces cerevisiae. Eukaryot Cell *3*, 827-834.

173. Vetter, I.R., and Wittinghofer, A. (2001). The guanine nucleotide-binding switch in three dimensions. Science *294*, 1299-1304.

174. Vida, T.A., and Emr, S.D. (1995). A new vital stain for visualizing vacuolar membrane dynamics and endocytosis in yeast. J Cell Biol *128*, 779-792.

175. Vogel, J.P., Andrews, H.L., Wong, S.K., and Isberg, R.R. (1998). Conjugative transfer by the virulence system of Legionella pneumophila. Science *279*, 873-876.

176. Wang, C.W., Stromhaug, P.E., Kauffman, E.J., Weisman, L.S., and Klionsky, D.J. (2003). Yeast homotypic vacuole fusion requires the Ccz1-Mon1 complex during the tethering/docking stage. J Cell Biol *163*, 973-985.

177. Weber, S.S., Ragaz, C., Reus, K., Nyfeler, Y., and Hilbi, H. (2006). Legionella pneumophila exploits PI(4)P to anchor secreted effector proteins to the replicative vacuole. PLoS Pathog *2*, e46.

178. Weisman, L.S. (2003). Yeast vacuole inheritance and dynamics. Annu Rev Genet *37*, 435-460.

179. Whitley, P., Reaves, B.J., Hashimoto, M., Riley, A.M., Potter, B.V., and Holman, G.D. (2003). Identification of mammalian Vps24p as an effector of phosphatidylinositol 3,5-bisphosphate-dependent endosome compartmentalization. J Biol Chem *278*, 38786-38795.

180. Wickner, W. (2002). Yeast vacuoles and membrane fusion pathways. Embo J *21*, 1241-1247.

181. Wicky, S., Schwarz, H., and Singer-Kruger, B. (2004). Molecular interactions of yeast Neo1p, an essential member of the Drs2 family of aminophospholipid translocases, and its role in membrane trafficking within the endomembrane system. Mol Cell Biol *24*, 7402-7418.

182. Wiederkehr, A., Meier, K.D., and Riezman, H. (2001). Identification and characterization of Saccharomyces cerevisiae mutants defective in fluid-phase endocytosis. Yeast *18*, 759-773.

183. Wilcox, C.A., and Fuller, R.S. (1991). Posttranslational processing of the prohormone-cleaving Kex2 protease in the Saccharomyces cerevisiae secretory pathway. J Cell Biol *115*, 297-307.

184. Wilsbach, K., and Payne, G.S. (1993). Dynamic retention of TGN membrane proteins in Saccharomyces cerevisiae. Trends Cell Biol *3*, 426-432.

185. Winter, D.C., Choe, E.Y., and Li, R. (1999). Genetic dissection of the budding yeast Arp2/3 complex: a comparison of the in vivo and structural roles of individual subunits. Proc Natl Acad Sci U S A *96*, 7288-7293.

186. Wurmser, A.E., Sato, T.K., and Emr, S.D. (2000). New component of the vacuolar class C-Vps complex couples nucleotide exchange on the Ypt7 GTPase to SNARE-dependent docking and fusion. J Cell Biol *151*, 551-562.

187. Yamaji, R., Adamik, R., Takeda, K., Togawa, A., Pacheco-Rodriguez, G., Ferrans, V.J., Moss, J., and Vaughan, M. (2000). Identification and localization of two brefeldin A-inhibited guanine nucleotide-exchange proteins for ADP-ribosylation factors in a macromolecular complex. Proc Natl Acad Sci U S A *97*, 2567-2572.

188. Yamamoto, A., DeWald, D.B., Boronenkov, I.V., Anderson, R.A., Emr, S.D., and Koshland, D. (1995). Novel PI(4)P 5-kinase homologue, Fab1p, essential for normal vacuole function and morphology in yeast. Mol Biol Cell *6*, 525-539.

189. Yoshimori, T., Yamagata, F., Yamamoto, A., Mizushima, N., Kabeya, Y., Nara, A., Miwako, I., Ohashi, M., Ohsumi, M., and Ohsumi, Y. (2000). The mouse SKD1, a homologue of yeast Vps4p, is required for normal endosomal trafficking and morphology in mammalian cells. Mol Biol Cell *11*, 747-763.